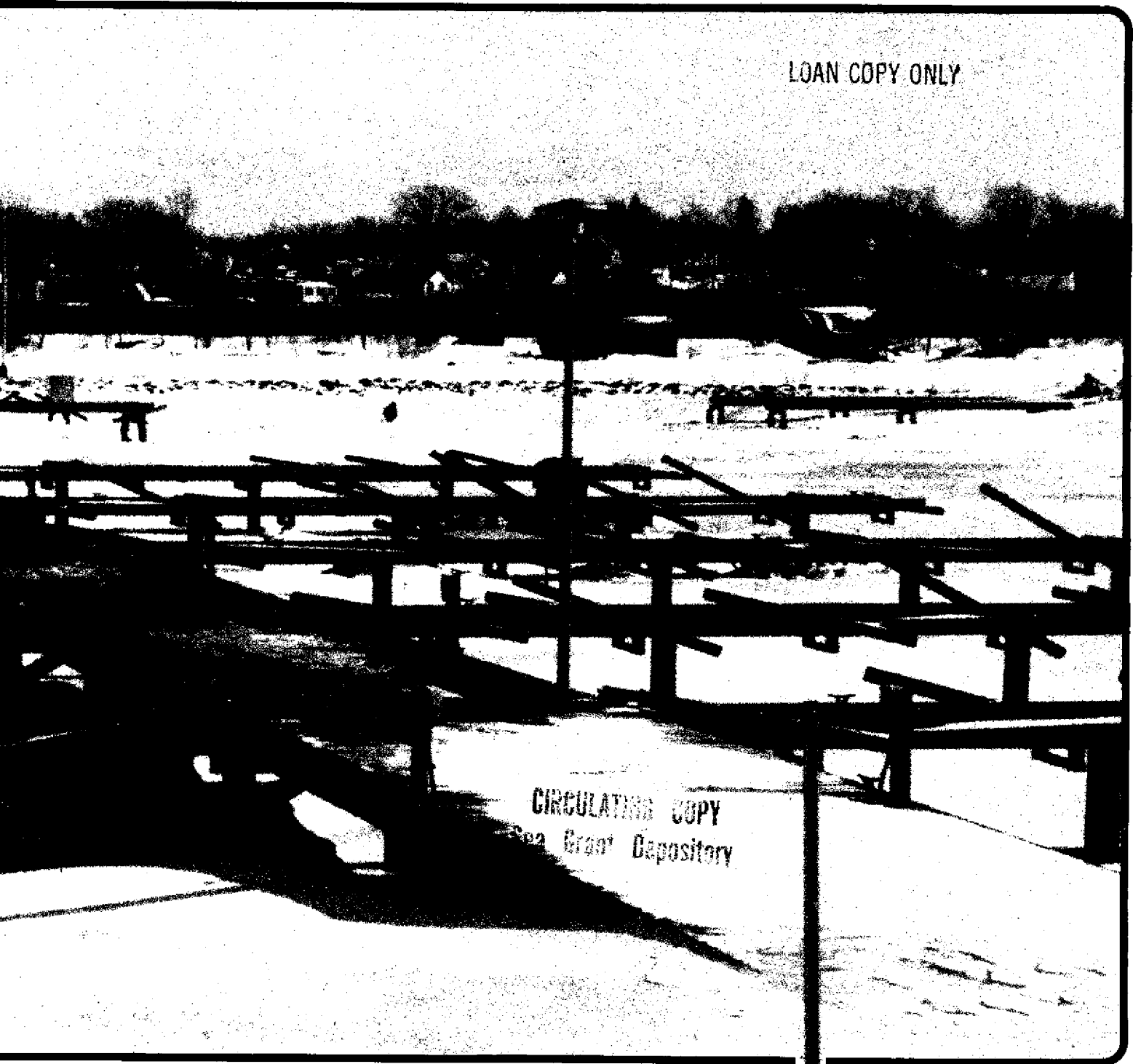


LOAN COPY ONLY



Ice Engineering Guide for Design and Construction of Small Craft Harbors

C. Allen Wortley

LOAN COPY ONLY

ICE ENGINEERING GUIDE
FOR
DESIGN AND CONSTRUCTION
OF
SMALL CRAFT HARBORS

NATIONAL SEA GRANT DEPOSITORY
PELL LIBRARY BUILDING
URI, NARRAGANSETT BAY CAMPUS
NARRAGANSETT, RI 02882

C. Allen Wortley

Department of Engineering and Applied Science
University of Wisconsin-Extension
Madison, Wisconsin

University of Wisconsin Sea Grant College Program

This work was funded (in part) by the University of Wisconsin Sea Grant College Program under a grant from the Office of Sea Grant, National Oceanic and Atmospheric Administration, U.S. Department of Commerce and by the State of Wisconsin.

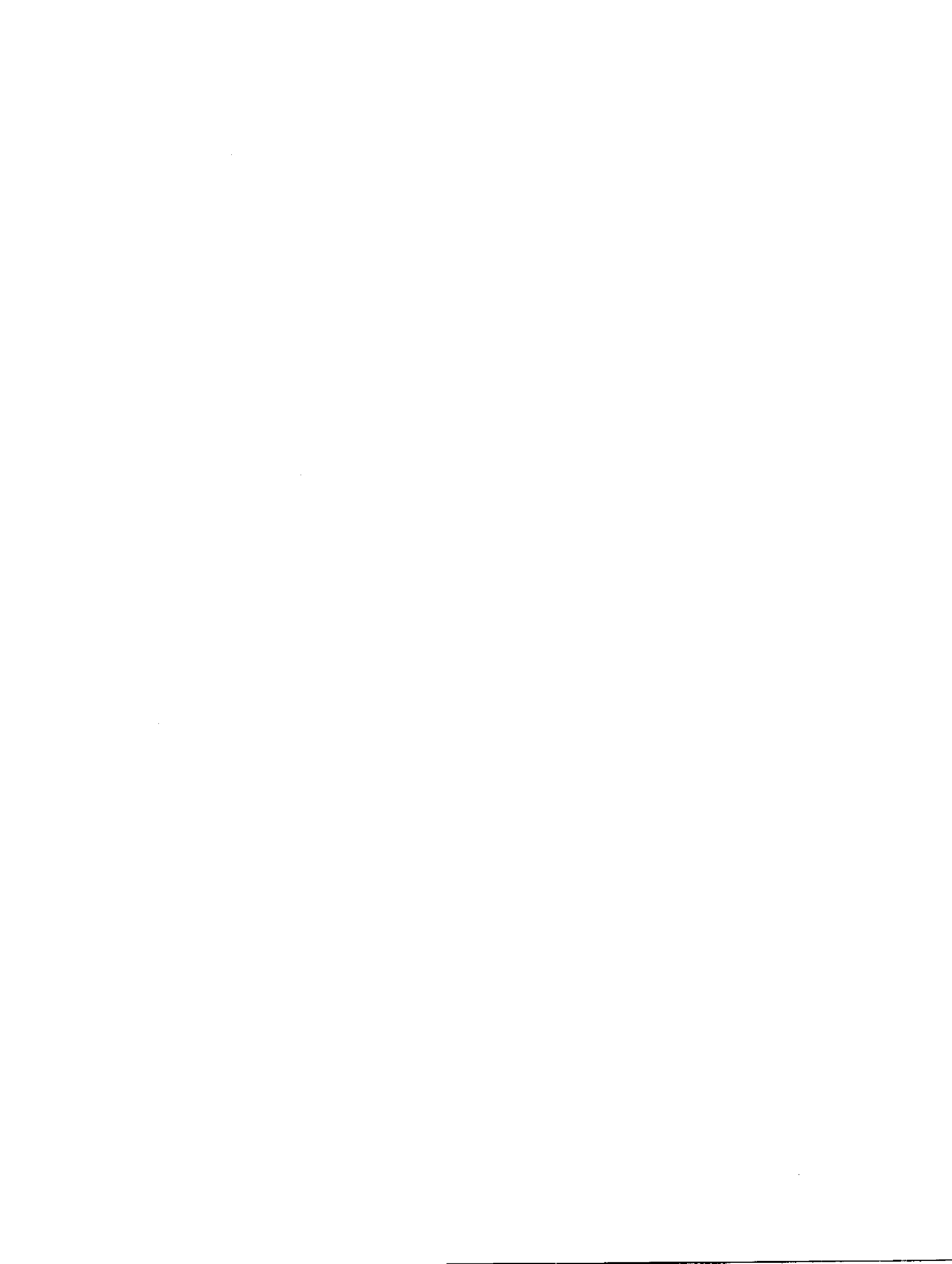
*Advisory Report #WIS-SG-78-417
May 1978*

*University of Wisconsin
Sea Grant Communications Office
1800 University Avenue
Madison, WI 53706*

608/263-3259

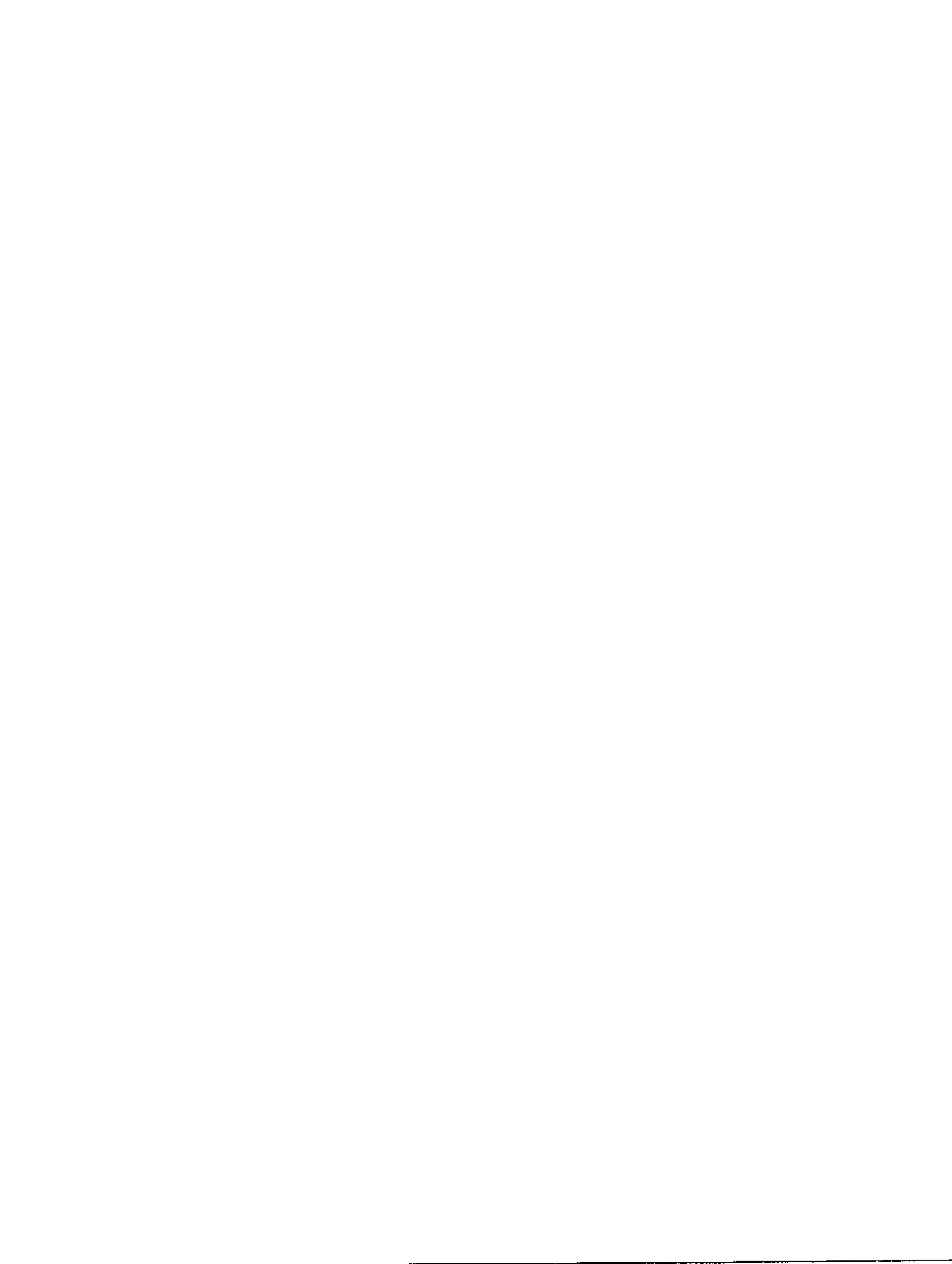
ABSTRACT

This ice engineering guide is an aid to designers and builders of small craft harbors in northern climates. In these areas ice does great damage to structures. The guide has been prepared from a review of the technical literature, consultation with knowledgeable engineers, contractors, and scientists, and field observations. It is applicable to lake ice in protected harbors. Information on the behavior and properties of ice and ice covers is presented. Descriptions of ice pressures of thermal origin and estimated thrusts on structures are given. The operation and design of compressed air suppression systems are explained. Safe bearing loads on ice sheets are estimated, as well as ice uplift loads for design. The information presented answers many questions about ice behavior and serves as a basis for innovative and economical small craft harbor design.



CONTENTS

ABSTRACT	<i>iii</i>
PREFACE	<i>ix</i>
ACKNOWLEDGEMENTS	<i>xi</i>
INTRODUCTION	<i>xv</i>
UNITS	<i>xix</i>
PART I--ICE AND ICE COVERS	1
Crystal Structure of Ice	2
Polycrystalline Ice	2
Nucleation and Growth of Ice Crystals	3
Freeze-Up and Break-Up of Fresh Water Lakes	6
Anecdotal Behavior of Natural Ice Covers	9
Thicknesses of Great Lakes Ice	12
Deformation and Strength Behavior of Polycrystalline Ice	14
PART II--ICE PRESSURES OF THERMAL ORIGIN	17
Introduction	18
Thermal Properties of Ice	18
Heat Transfer in Ice Sheets	20



Climatological Data	21
Rheological Aspects	22
Laboratory Test Results, Ice Thrusts	23
Biaxial Restraint	25
Effects of Cracks and Snow on Ice Thrusts	26
Ice Thrust on Individual Piers	29
Closure	29
PART III--ICE SUPPRESSION AND WEAKENING	31
Principles of Bubbler System Operation	32
Ice Suppression Bubbler Systems Design	33
Other Ways to Suppress or Weaken Ice	41
PART IV--BEARING CAPACITY OF ICE	43
Flexural Rigidity Length	44
Bearing Capacity of Ice Sheets	46
Safe Loads on Ice Sheets	50
Thickening and Strengthening Ice Covers	54
PART V--VERTICAL ICE FORCES AND OTHER FORCES	57
Water Level Fluctuations	58
Minimum Ice Sheet Uplift Loads	59
Reducing Ice Sheet Uplift Loads	65
Other Ice Forces and Actions	67
APPENDIX I--LITERATURE CITED	71
APPENDIX II--DEFORMATION AND STRENGTH OF ICE, LAVROV	75
APPENDIX III--SAFE LOADS COMPUTED WITH A POCKET CALCULATOR, NEVEL	79
APPENDIX IV--TABLES OF KELVIN FUNCTIONS AND THEIR DERIVATIVES, NEVEL	97



PREFACE

More than a hundred years ago Dumble (1858) stated,

"I may add, that the ignorance, or want of proper appreciation, of the properties of ice, evinced in the construction of numerous wharves, piers, and bridges on the inland lakes and rivers of Canada and the northern States, has proved a source of infinite annoyance and of immense expense".

Dumble was an engineer with the Cobourg and Peterborough Railway. Today, most designers of small craft harbors in northern climates have an appreciation of the behavior of ice. However, the level of relative ignorance about ice behavior is still high.

The successful design and construction of small craft harbor structures (such as docks, piers, and piles) subjected to ice forces and motions continues to be an uncertain science. The four methods currently being used are: (1) Predict the ice forces and motions, both horizontal and vertical, and design the marina structures to withstand them, (2) Predict the ice prevention or suppression capabilities of various systems to remove the adverse effects of ice or render them ineffective, (3) Estimate the relative scope of structure required by local comparative studies of successful and unsuccessful constructions and build accordingly, and (4) Remove the dockage by either beaching floating docks or retracting fixed piers.

Designers and builders should continue innovations and improvements in the state of the art of small craft harbor construction in northern climates. This publication endeavors to aid them and serve as a guide. It is a first step. It is incomplete. And likely will never be totally complete due to the uncertainty existing in the field of ice engineering. It is hoped the U.S. Cold Regions Research and Engineering Laboratory (US CRREL) will subsequently expand and update ice information necessary to construct small craft harbors in ice conditions.

Madison, Wisconsin
January, 1978

C. Allen Wortley
Principal Investigator



ACKNOWLEDGEMENTS

This work was funded by the University of Wisconsin Sea Grant College Program under a grant from the Office of Sea Grant, National Oceanic and Atmospheric Administration, U.S. Department of Commerce and by the State of Wisconsin.

The U.S. Government is authorized to produce and distribute reprints for governmental purposes notwithstanding any copyright notation that may appear hereon.

The project has been undertaken with the assistance of an Advisory Committee. Members were

<u>Name</u>	<u>Affiliation</u>
Guenther E. Frankenstein	U.S. Army Cold Regions Research and Engineering Laboratory, Hanover, New Hampshire
Theodore Green	Departments of Civil and Environmental Engineering and Meteorology, University of Wisconsin-Madison
John P. Klus	Department of Engineering, University of Wisconsin-Extension, Madison
Raymond G. Lawrence	Waterways Division, Michigan Department of Natural Resources, Lansing, Michigan
J. Robert McCullough	Aeration Division, Schramm, Inc. West Chester, Pennsylvania
James E. Muschell	United Marine Associates, Cheboygan, Michigan
Harry Nelson	Madeline Island Ferry Lines, Inc. La Pointe, Wisconsin



Raymond F. Pesch	Roen Salvage Company Sturgeon Bay, Wisconsin
Max Pollack	Architectural-Engineering Division Milwaukee County Department of Public Works, Milwaukee, Wisconsin
A. R. Striegl	Civil Engineer Milwaukee, Wisconsin
John P. Zarling	Mechanical Engineering Department, University of Alaska College, Alaska
R. C. Zirbel	Edward E. Gillen Company Marine Engineers and Contractors, Milwaukee, Wisconsin

The project was commenced in 1973. In addition to the present principal investigator the following co-investigators also contributed to the work: Profs. John P. Klus and Lawrence A. Soltis of the University of Wisconsin-Extension Department of Engineering, and Prof. John P. Zarling, formerly with the University of Wisconsin-Parkside and currently with the Mechanical Engineering Department at the University of Alaska.

The principal investigator is especially grateful for the suggestions and assistance received from Messrs. G. D. Ashton, G. E. Frankenstein, and D. E. Nevel, all of the US CRREL.



INTRODUCTION

This publication is a guide for designers and builders of small craft harbors in northern climates, where ice forces and motions do great damage to man's works.

It has been prepared from a review of the literature, consultation with knowledgeable engineers, contractors and scientists, and the experiences and observations of the principal investigator and members of an Advisory Committee.

Zarling (1974) prepared an annotated bibliography entitled "Ice Engineering in Small Craft Marinas". This work served as the starting point for reviewing the literature. Additional and more recent publications were examined as well as many of those noted in the bibliography. There is a large amount of information in the overall field of ice engineering and ice physics. However, very little is easily applied by the small craft harbor designer or builder because of its research-technical nature. Also much of the information doesn't relate directly to the problems of designers and builders, or is of such orders of magnitude as to render it useless for safe and economical design.

However it is from the more useful, more current, and more applied information in the literature that much of this guide has been prepared. The literature has been freely cited. No additional laboratory experimental work has been undertaken. Field observations and measurements have been made and have influenced the recommendations derived from the information in the literature.

Ice for purposes of this guide is primarily stationary lake ice. River ice, ice floes and sea ice are not specifically dealt with. They can and do present different problems. Small craft harbors are customarily built in sheltered areas, away from dynamic ice forces.

The guide is divided into five parts. Part I presents information on the characteristics, behavior and properties of ice and ice covers. It presents as much specific quantitative information as is available. The other information presented is of a general nature but useful in understanding ice and its behavior.



Part II deals with ice pressures of thermal origin. It is derived largely from current laboratory research on thrusts on hydraulic structures. Certain information however is applicable to small craft harbors.

Part III presents recommendations for design and construction of compressed air ice suppression systems and other information on weakening ice. These suppression systems are effective in small craft harbors.

Part IV discusses the bearing capacity of ice and presents recommended maximum short term construction loadings.

Part V gives minimum and expected maximum values for ice uplift forces. Information about other ice forces is also presented.

As stated initially this is a guide for designers and builders of marinas in northern climates. It by no means answers all the pertinent questions, nor does it present all the "how to's". This is beyond our present scope and our present abilities.

It is hoped that the reader will review all Parts of this guide and form an overall understanding of ice behavior. Successful, innovative and economical design of small craft harbor structures is our goal.



UNITS

Conversion Factors: U.S. Customary to SI Metric Units

Measurements in this guide are shown in customary U.S. units with SI metric equivalents. Specific quantities are converted accurately, but where the measurements are general the conversion is approximate only. As much of the source data was in the metric system and not the U.S. customary or the SI systems, some data appear to have "odd" values. For example, pressures in kilograms per square centimeter (kg/cm^2) have been converted to pounds per square inch (psi) and kilonewtons per square meter (kN/m^2). The SI unit for pressure is pascal (Pa). One Pa is equal to one N/m^2 . Because we are dealing with forces, and forces per unit length, as well as pressures, we have elected to leave pressures in force-length units rather than the derived pressure unit Pa.

Some U.S. Customary to SI Metric conversion factors are given below. The ASTM E380-76 Standard for Metric Practice gives additional conversion factors.

<u>To Convert</u>	<u>To</u>	<u>Multiply By</u>
inches (in)	millimeters (mm)	25.40
inches (in)	centimeters (cm)	2.540
feet (ft)	meters (m)	0.3048
yards (yd)	meters (m)	0.9144
miles (mi)	kilometers (km)	1.609
inches per yard (in/yd)	millimeters per meter (mm/m)	27.78
square inches (sq in)	square centimeters (cm^2)	6.45
square feet (sq ft)	square meters (m^2)	0.093
cubic inches (cu in)	cubic centimeters (cm^3)	16.39
cubic feet (cu ft)	cubic meters (m^3)	0.0283
pounds (lb)	kilograms (kg)	0.453
tons (ton)	kilograms (kg)	907.185
tons (ton)	metric tons (mt)	0.907



<u>To Convert</u>	<u>To</u>	<u>Multiply By</u>
one pound force (lb)	newtons (N)	4.448
one kip (kip)	kilonewtons (kN)	4.448
one kilogram force (kg)	newtons (N)	9.806
kips per foot (kips/ft)	kilonewtons per meter (kN/m)	14.59
pounds per square foot (psf)	newtons per square meter (N/m ²)	47.88
pounds per square inch (psi)	kilonewtons per square meter (kN/m ²)	6.89
pounds per square inch (psi)	meganewtons per square meter (MN/m ²)	0.00689
pounds per square inch (psi)	kilograms per square centimeter (kg/cm ²)*	0.07031
kips per square inch (ksi)	meganewtons per square meter (MN/m ²)	6.89
pounds per cubic foot (pcf)	kilograms per cubic meter (kg/m ³)*	16.02
Degree Fahrenheit (F)	Degree Celsius (C)*	0.555
Temperature Fahrenheit (F)	Temperature Celsius (C)*	(F-32)/1.8
square feet per minute (ft ² /min)	square meters per second (m ² /sec)	0.001548
square feet per hour (ft ² /hr)	square centimeters per second (cm ² /hr)	929.03
Btu per hour per square foot (Btu hr ⁻¹ ft ⁻²)	watts per square meter (W m ⁻²)	3.152
Btu per pound per degree Fahrenheit (Btu lb ⁻¹ F ⁻¹)	joule per kilogram per degree Celsius (J kg ⁻¹ C ⁻¹)*	4186.8
Btu per hour per square foot per degree Fahrenheit (Btu hr ⁻¹ ft ⁻² F ⁻¹)	watts per square meter per degree Celsius (W m ⁻² C ⁻¹)	5.678
Btu inch per hour per square foot per degree Fahrenheit (Btu in hr ⁻¹ ft ⁻² F ⁻¹)	watts per meter per degree Celsius (W m ⁻¹ C ⁻¹)*	0.1442
miles per hour (mph)	meters per second	0.4470

*not an SI unit

PART I

ICE AND ICE COVERS

This section of the guide contains information on the crystal structure of ice, the polycrystalline forms of ice, the nucleation and growth of ice, the freeze-up and break-up processes on fresh-water lakes, the thicknesses and behavior of ice covers and some introductory material on the deformation and strength of polycrystalline ice, a viscoelastic material.

Some of the material is pertinent to present design techniques for small craft harbors and some is only of general background interest. The general information may be useful in developing new design techniques, explaining behavior of ice covers, understanding other ice research papers and monographs that readers may come in contact with, and in other ways in the future. The material should answer some of the readers' questions about ice and confirm some of their observations in the field.

Simply stated, ice is not well understood. At the present time straight-forward and proven design approaches for small craft harbors are not available. Therefore the best approach for design is to begin with an understanding of the present state of knowledge about ice, especially in the context of small craft harbors, and go from there.

Those wishing more detailed technical and theoretical information on the physics and mechanics of ice should consult references such as the two monographs by Glen (1974, 1975) and textbooks by Pounder (1965) and Hobbs (1974).

Crystal Structure of Ice

Ice is a solid consisting of a crystallographic arrangement of water molecules. Each molecule has an oxygen atom with chemical bonds with two hydrogen atoms.

Although several forms of ice can exist, we shall be concerned only with the ordinary form of ice. It is the form with which most people are familiar. This form is hexagonal in crystal symmetry. The symmetry is clearly demonstrated in the symmetry of many snow crystals.

Each crystal of ice is made up of water molecules arranged in a regular geometric pattern forming hexagon prisms. The axis of the prism is known as the optic axis and the surface perpendicular to this axis is called the basal plane. Crystallographic terminology labels planes and directions. In the hexagonal system, there are three directions in the basal plane that are crystallographically equivalent. These directions are called a, b and d (sometimes a_1 , a_2 , and a_3) and the axis perpendicular to the basal plane is called the c-axis (i.e. the optic axis).

Runnels (1966) suggests that at the molecular level the seemingly rigid perfection of the ice crystal is disrupted by an astonishingly busy traffic of molecules and migrating lattice faults. There is a good deal of empty space between molecules and hence ice has a rather open structure. Because of this fact, water, in contrast to almost all other substances, is less dense in the solid state than in the liquid state. This results in ice floating on water. The density of pure ice is given by Pounder (1965) as 57.2 pcf (916.8 kg/m^3).

Ice encountered in nature, such as on a lake, is in a high temperature state. It is floating on its own melt with its bottom surface at a temperature equal to its melting point and the upper surface varying with ambient conditions. Predicting the properties and behavior of a material in such a state is quite difficult.

Polycrystalline Ice

Most bulk ice in nature consists of polycrystalline ice, that is, ice composed of a large number of single crystals in different orientations. Polycrystalline ice behaves differently from single crystals of ice because of the existence of grain boundaries and the fact that single crystals are anisotropic. A single crystal of ice has physical properties that are different in directions parallel and perpendicular to its c-axis. If the constituent crystals of polycrystalline ice are randomly oriented, then the bulk properties will be some kind of average of the properties of the single crystals of which it is composed. For some properties such as elasticity, this averaging is fairly straightforward, but for others, such as plastic deformation, there is such a radical difference in the behavior of ice crystals in different directions that the physical properties of the polycrystal are quite different from that of the single crystal.

Moreover, the grain size as well as the crystal orientation of polycrystalline ice has an effect on the strength and behavior of an ice sheet. Fortunately, from a design point of view, those effects may be minor for cold polycrystalline ice, the type that normally would present the most severe forces on structures placed in ice. This may not always be true for all kinds of polycrystalline ice encountered in lakes and rivers. The kind of ice which forms depends upon its genesis.

Nucleation and Growth of Ice Crystals

Ice in the absence of very great supercoolings or supersaturations will only form if some nucleus is present on which it can grow. This can be ice itself, and if an ice seed is present, ice will normally develop and grow. It may also be a nucleus consisting of some other material.

Once an ice nucleus is present, ice can grow from the surrounding water provided the temperature remains favorable. How ice will grow will depend on whether the water surface is supercooled, and also on the amount of impurities it contains.

Michel and Ramseier (1969) have classified river and lake ice based upon its genesis, structure and texture. An ice sheet or ice cover is divided into three basic ice formations: primary ice, secondary ice, and snow ice.

Primary ice is the first type of ice of uniform structure and texture which forms on a water body. On a calm water body the primary ice is in the form of an ice skim which grows horizontally in the supercooled layer and is about a hundredth of an inch (a few tenths of a mm) thick. Usually when water freezes a little plate-like disc forms. It may rapidly develop dendritic extensions depending on the amount of supercooling and the rate of heat loss. Since the planar structure will naturally float with its plane parallel to the surface, the ice which forms when water freezes often has its surface crystals oriented with their c-axes vertical, i.e. perpendicular to the free surface. These initial crystals spread over the surface until they interact and form a layer over the whole surface of the water. The subsequent growth of this layer downwards into the water is not usually dendritic.

In rough and turbulent water the primary ice consists of congealed frazil slush which can be an inch (several centimeters) thick. Frazil slush is a floating agglomerate of loosely packed individual ice crystals having the form of small discoids or spicules which are formed in supercooled turbulent water. If the nucleation occurred by snow, the resulting congealed snow slush (i.e. a loosely packed agglomerate of floating snow particles) would also be part of the primary ice.

Secondary ice forms parallel to the heat flow which is perpendicular to the primary ice. As the ice grows down into the water under conditions of calm formation and growth the grain boundaries are almost perpendicular to the surface. The result is a columnar-grained structure with the c-axes

vertical in the long direction of the grains. This type of secondary ice is referred to as type S1. The crystal size increases with depth, because unfavorably oriented crystals disappear. S1 ice is found in lakes, reservoirs and in rivers with low flow velocities.

S2 columnar ice is a secondary ice form with the c-axes horizontal. It forms under similar conditions to S1 ice but where the primary ice has a random or preferred vertical orientation superimposed on a random orientation. As the ice grows down into the water, the c-axes vertical preferred orientation gives way to one in which the c-axes are horizontal. Some crystals are wedged out at the expense of others. This type of ice is found in lakes, reservoirs, shores and rivers.

Another type of secondary ice, but granular rather than columnar in form, is S4 Congealed Frazil Slush. Its crystal boundaries are irregular and the grains highly angular and randomly oriented. Frazil is found in rivers where it is taken downstream and deposited upwards under the secondary ice overlying more slowly moving water. S4 ice is found in rivers and reservoirs, and lakes fed by turbulent waters. An entire ice cover can consist of S4 ice or it can be found layered between columnar forms of ice.

An interesting ice form, anchor ice, results when frazil is being formed in supercooled water. The frazil particles stick and grow on bottom weeds and stones. After a night of frazil formation the morning sun can cause anchor ice on stones and other objects to float to the surface and be carried downstream.

Snow ice is the third basic formation of ice. This type of ice always forms on top of the primary ice due to snow deposits which lie on the ice cover. Snow ice may form due to variations in discharge of water, by melt or rain, or by the depression of the ice cover due to a heavy snow load. In general snow ice is formed from any imaginable kind of water source. T1 is the designation for Snow Ice and its grains are round to angular and randomly oriented. Being granular it is similar in appearance to the S4 Congealed Frazil Slush ice found usually under the secondary ice layer.

The crystal size of ice depends greatly on meteorological parameters. If the water surface is calm and the temperature gradient is not too steep extra large crystals will develop. Their diameters can be greater than 0.8 inches (20 mm). If the temperature gradient becomes larger then the crystal size will decrease. If snow causes the nucleation, crystals will be of the 0.2 inches (5 mm) size and smaller. Extra large and giant size crystals can form under extremely calm conditions such as in a pool during the formation of the primary ice layer. Crystal dimensions in yards (meters) are possible.

During the evolution of an ice cover the crystal size will change. In lake ice it is possible to go from fine sized to extra large sized crystals in a columnar layer if nucleation has occurred by snow.

Gow and Langston (1977) describe the growth history of lake ice in relation to its stratigraphic, crystalline and mechanical structure. They have

successfully correlated specific increments of ice growth with major weather events. This was accomplished by diagnosing bubble layering observed in stratigraphic samples of lake ice. The ice covers of the two New Hampshire lakes used in their studies contained two major components: lake ice formed solely from the freezing of lake water and snow ice formed from the freezing of water-saturated snow. The lake ice component consisted of predominately fibrous-textured crystals with a vertical c-axis orientation. Columnar crystals elongated in the vertical but with horizontal c-axes fabrics, were observed only in the top 4 to 6 inches (10 to 15 cm) of ice that fringed the shores of both lakes. These fabrics had reverted entirely to a vertical c-axis condition at 6 inches (15 cm) depth. The reason for this reversal in orientation texture has not clearly been established. However, indications are that the temperature gradient in the water may be a significant factor in initially controlling the growth textures, since continued growth of ice near shore resulted in rapid elimination of the horizontal c-axis in favor of crystals with vertical c-axes.

Several variants of snow ice were distinguished, depending upon the source of infiltrating water. Both ice types were readily distinguished on the basis of differences in their stratigraphic and crystalline structure.

Michel and Ramseier (1969) have also found that studying ice profiles from lakes and rivers enables one to determine what some of the meteorological conditions were upon formation of the primary ice. Similar analyses can be obtained from snow ice and overlying snow. They believe that in the future it may even be possible to predict directly the texture at a particular site from meteorological and hydrodynamic data.

The predominant inclusion in ice is air. During solidification the air is rejected at the ice-water interface and is supplemented by gases arising from biochemical processes which take place in a natural body of water. Air can also be incorporated from the atmosphere through cracks, drained snow ice or an agitated water surface. If the growth is slow most of the air will be rejected and the ice will be transparent like glass. This transparent ice is sometimes called black ice. (The term blue ice is sometimes used in connection with glacial ice, but not transparent lake ice.)

If the solidification process proceeds rapidly air in the form of bubbles will be distributed throughout some parts of the ice cover. If air is being emitted continuously, the bubbles take on a cylindrical shape. It is the air entrapped in ice that causes it to appear white. This type of ice is sometimes called white ice. Snow ice is an example of white ice because of entrapped air. Grain size does not determine the color of ice. Frozen frazil ice can appear transparent in spite of its granular texture.

Freeze-Up and Break-Up of Fresh Water Lakes

Water, in the temperature range of 39°F to 32°F (4°C to 0°C), increases in volume with decreasing temperature. This is contrary to the behavior of most substances. In this temperature range the coefficient of expansion of water is negative, that is, water expands as it becomes cooler. Since the volume of a given mass of water is smallest at 39°F (4°C), it has its maximum density at this temperature. The negative coefficient of expansion of water in this range is one of nature's anomalies. This explains why lakes first freeze at their surfaces and why somewhat warmer (and denser) water is found near the bottom.

Williams (1966) has prepared a detailed and comprehensive description of how fresh water lakes freeze and thaw. Michel (1971) also describes the winter regime of rivers and lakes in a monograph. It too is comprehensive and contains information on rivers as well as lakes. For our purposes we will recite the lake ice processes described by Williams (1966).

His descriptions are applicable to sheet ice, the type that forms on relatively still lakes, slow-moving rivers, and sheltered harbors. Williams designates three distinct periods in the life of sheet ice: the freeze-up period, the ice-growth period, and the ice-melting period. These periods roughly correspond with the fall, winter and spring seasons.

During the fall, or early winter, smaller lakes freeze over. A solid ice sheet forms. In larger lakes the sheet may only cover harbors and the area near the shoreline, but is generally extensive. The Great Lakes rarely completely freeze over, at least for any extended period of time.

The formation of an ice cover on a lake is a function of the water's heat exchange with the atmosphere, the initial amount of heat stored in the water body, and the amount of inflow of warm water (heat) to the site. The amount of heat lost to the atmosphere is a function of the air temperature, the wind velocity, and solar radiation. The amount of heat that can be stored in a water body is a function of depth. Usually, the deeper the lake, the deeper the convective mixing and the slower the rate of water cooling for a given surface heat loss. (In a man-made harbor, depths are usually shallow and hence significant thermal reserves because of depth are not present.) Inflow of heat by currents from warmer water in rivers or from deep reservoirs can prevent or delay sheet ice formation at certain sites.

The cooling of a fresh water lake occurs in two stages: gradual cooling until all the water is at a temperature of about 39°F (4°C), and cooling of the surface water from the time the water is isothermal (i.e. the same temperature, top to bottom) at 39°F (4°C) until sheet ice forms.

First the warm lake surface water cools down (even steams or mists when giving up its heat to the cool atmosphere) and thereby contracts and becomes more dense. This water sinks in the less dense lake and forces up the lower less dense, warmer water to in turn be cooled. This process is repeated until the lake is isothermal at 39°F (4°C). The lake has then "turned over".

From this point on the lighter, cooler surface water continues to cool down until it freezes as sheet ice. (A thin layer of ice first forms along the edges of the lake. A convective air motion from land toward rising warm air over the lake cools the lake edges more rapidly than the center.) Since the density of ice is even less than that of freezing water, the ice floats on the water below it, and further freezing can only result from heat flow upward by conduction.

The mid-winter period, when the permanent ice cover on lakes gradually increases to a maximum thickness late in the winter, is a period of interest to harbor engineers concerned with ice pressures, ice uplifts, and bearing capacities.

When the ice cover is thin, and the air very cold, there will be a relatively large heat flow from the water, through the ice, to the atmosphere. This will cause a rapid increase in ice thickness at the interface between the ice and the water. As the ice cover thickens, an insulating effect occurs, and ice grows at a slower rate. A snow cover on the initial ice formation can effectively prevent any further ice growth.

Ice normally grows downward into the water, but not always. The upper surface of ice can be submerged below the water level due to the weight of a snow cover. Snow ice then forms and freezes on top of the ice sheet. Sometimes this causes rapid increases in the total thickness.

A frozen snow covered lake can be highly variable in its underlying stratigraphy. The snow cover can conceal slush and weak layers of ice, as well as strong sound ice.

The clearing of ice from bodies of water at break-up is affected by heat gain from the atmosphere, snow and ice conditions, wind and currents, and inflow or runoff of warm water to a site. The heat gained from the atmosphere weakens and melts the ice. The amount of solar radiation absorbed is determined by the reflectivity of the snow or ice surface. The properties of the ice cover determine the depth solar radiation will penetrate, causing internal melting. The thickness of the snow and ice is a measure of the amount of ice to be melted. The mechanical action of wind and currents is of great importance in breaking up the ice after it has been weakened by surface and internal melting.

At the beginning of break-up, snow melt runoff from surrounding land areas may flood onto part of the lake surface. At the same time the snow cover on the ice densifies and begins to melt. The runoff usually accumulates near the mouths of streams draining into the lakes and along the shoreline, producing dark-looking slush on the ice surface. At this stage the darkened ice cover surface absorbs a large proportion of the incoming solar radiation.

The ice around the shoreline tends to melt first, partly because of the darkened surface layers but also because the ice thickness is often less close to the shore, where it can only grow as thick as the depth of the water. Eventually the ice cover completely melts around the shoreline, leaving the main body of ice floating free. This body of ice can still have considerable strength.

During melting, drainage holes can develop in the ice sheet. In the early stages of melt these holes develop near the shore often where runoff flows into old thermal cracks. The flow is due to difference in level between the lake water supporting the ice and the melt water on the ice surface. Such drainage holes can enlarge rapidly, sometimes developing into holes one to two feet (0.3 to 0.6 m) in diameter.

Later on during melting, the main body of ice, floating free, melts at the surface. This melt water flows along the surface of the ice and eventually creates surface drainage patterns. It can drain to the open water adjacent to the shoreline, or down the holes that appear to develop preferentially along old thermal cracks. If the surface melt water can drain away, the surface of the ice becomes a porous, crumbly white structure which reflects solar radiation readily, thus retarding melting by solar radiation. As the melt season progresses, penetrating solar radiation causes internal melting in the ice sheet. At this time the ice sheet may consist of a shallow, porous surface layer several inches (several cm) thick, a layer of water-logged ice also several inches (several cm) thick, and then solid unmelted ice (whose lower surface is melting in the lake water).

In the final stages of break-up the underlying entrapped water layers result in darkened surface ice and most of the incoming solar radiation is absorbed. The ice is now ripe for breaking by wind and currents and is unsafe for over-ice transportation. The current created by strong winds will break up the ice cover and induce circulation that brings the warmer subsurface water to the surface. This can cause rapid melting of ice from a lake. Indeed the final disappearance of ice covers has occurred so quickly at times that early observers believed that the ice actually sank.

The term rotten ice is sometimes used to refer to disintegrating ice at break-up time. If the ice has a columnar structure it becomes candled and is referred to as candle ice. Melting is concentrated at the boundaries of the columnar prisms leaving a weak candle-like structure.

Williams (1966) and Michel (1971), as well as others, have proposed methods to estimate the date of freeze-up, maximum ice thickness, and the date of break-up of fresh water lake ice. The method of doing this is approached in two ways: develop formulas based on physical principles, and make an analysis of past records to give statistical limits within which maximum ice thickness or freeze-up or break-up can be expected to occur.

The operational use of formulas is usually limited because of difficulties in making dependable forecasts of such variables as air temperature and snow depth. It is also difficult to allow for natural variability, as the rate at which ice forms, grows, and melts varies not only from lake to lake but on an individual lake.

The statistical climatological approach also has limitations. The required long-term records are only available for some lakes and it is difficult to use the records collected to estimate freeze-up or break-up for other lakes with different sites and thermal regimes. In addition, even for lakes where some long-term records are available, the statistical

approach will only define upper and lower limits within which freeze-up or break-up will occur.

We believe direct on-site observations by the small craft harbor designer coupled with any information from local residents is the best approach to predicting freeze-up or break-up. Ice thickness determination can be handled in the same manner but of course modified by recommended design criteria for minimum thicknesses and strengths.

The U.S. Great Lakes Environmental Research Laboratories (GLERL) in cooperation with Canadian and other agencies are involved in efforts to understand and forecast behavior of ice formations on the Great Lakes. Samples and measurements of ice thicknesses from many places on the Great Lakes are underway. This information together with other published measurements and observations will be useful to marina designers.

Anecdotal Behavior of Natural Ice Covers

Many anecdotal accounts of the behavior of ice covers are contained in the literature. Some of the explanations about its behavior have since been proven wrong. Some have been substantiated with research and additional observations. During the nineteenth century Dumble (1858), who was an engineer with a railway company, published accounts of his observations on inland lakes and rivers in the northern states and Canada. A few of his observations are repeated below together with some of our parenthetical comments.

The most violent shoves of ice occur previous to rainstorms. (This would be associated with warm winter weather and thermal expansion.)

Contraction generally occurs at night, and is accompanied by sharp reports. (This would be associated with cooling nighttime weather and thermal contraction cracking.)

A coating of snow of any depth over six inches (15 cm) effectively prevents any motion of ice. (Snow is a very effective insulator and prevents thermal motion of ice.)

It is but reasonable to suppose that any solid, equally dense throughout its dimensions, and susceptible of expansion, would, when equally acted upon by the active agent or moving cause, expand from its center towards its circumference. This is the effect produced on any large field of ice of equal thickness and density, when acted upon uniformly by either the mid-day sun or warm winds. It is a fact, however, that it moves from other directions than from the center of the lake. Shoves are sometimes witnessed from the east and sometimes from the west, to the north and to the south.

Ice owing to the peculiar circumstances under which it sometimes forms, is not found to be equally pure or dense, neither is it of uniform thickness. This ice irregularly acted upon by warm winds, or by the slanting rays of the sun at different altitudes, shoves, or expands from various directions other than from the center of the lake.

Shoving is from the stronger and most susceptible ice toward the weaker and less expansive.

Ice on any large and irregular sheet of water studded with islands must naturally be of unequal thickness and density. There is therefore no doubt whatever, that the phenomenon of ice expanding and shoving from various directions is caused by the unequal thickness, density and glare of the ice and likewise by the manner in which the heated atmosphere strikes it.

(Ice sheets and covers are variable in their composition and frequently expand, contract and move in erratic ways.)

It is observed, that when a large extent of field ice expands towards the shore it does not shove into deep bays but fractures from point to point in a zig-zag manner, across the chord at the mouth. A thrust of the main field must find less resistance across this chord than around the area of the bay. (Crack patterns can now easily be observed from the air and indicate where ice has failed as it moved into or by some shore configuration such as a bay.)

Much more recently Striegl (1952) described the formation of ice in the Great Lakes, and particularly in Lake Michigan.

Ice normally starts to form along the shores of the southern part of Lake Michigan about the middle of December. By the early part of January the initial ice sheet may reach a thickness of 6 to 8 inches (15 to 20 cm) and extend off shore distance of one to five miles (1.6 km to 8.0 km) depending on the continuity of cold weather and the strength of the winds. Frequently during this initial ice period the thin ice cover may be broken up by the wind and wave action. If the wind is toward shore, one of a series of windrows may develop where the drifting cake of ice will pile up on or under the sheet of ice until it may reach a depth of many feet (meters) above and below water, and may ultimately pack to the bottom where shallower water is reached. If the ice along the shore is weak the windrow may be pushed ashore until a large part of it is above the water level. If the wind is off shore the fields of floating ice are driven out into the lake where they may drift for long periods or pile up in ice windrows or along shore in another part of the lake, depending on the continuity and direction of the wind.

Engineering structures built in the lakes for harbor protection or other purposes must be designed to support enormous ice loads due to the ice build up on the structure by continued freezing of wave wash and spray or by loose ice piled on top of the structure by ice jams and then consolidated by continued freezing action. Those ice loads may pile up to 20 to 25 feet (6 to 8 m) above the top of the structures. Usually this load, does little damage to overloading individual structural members because of the extra support and bridging effect of the ice itself. However, it may cause considerable damage in other ways. Stones or concrete may be broken, through freezing and thawing action to such sizes that they will later be displaced by wave action. Also large breakwater stones, up to several tons each, may be carried bodily from the structure when encased in large ice

blocks. Such stones have been carried by ice floes miles from structures and dropped in navigable channels where they have become obstructions to navigation. Smaller rocks have been found in the channels of harbors which were picked up by the ice on the beach or from the structures and floated with the ice to areas where they were dropped on melting or breaking of the ice.

In Chicago in January 1948, a strong easterly wind storm, accompanied by sleet, snow and low temperatures, piled ice in a solid mass along the entire Illinois shoreline. The ice was as much as 15 feet (5 m) above the water surface and extended 50 to 100 feet (15 to 30 m) behind sea walls and bulkheads in Chicago, and from 100 to 300 feet (30 to 90 m) in front of the beaches and natural shoreline and other points.

The section of this guide dealing with pressures of thermal origin exerted by ice sheets on structures will give additional and current information on the behavior of ice covers.

Thicknesses of Great Lakes Ice

Striegl (1952), Aune, Beaudin, and Borrowman (1957), and others have reported observations on natural ice thicknesses on the Great Lakes. Because of the wide geographic extent of the lakes area, as well as the differences in the characteristics of individual lakes, the ice season varies considerably. Climatic conditions obviously are the major factors in the amount and rapidity of ice formation and disintegration.

The following typical cases indicate the range in temperatures and the differences in length of the cold season which are primary factors in connection with the formation of ice. As these figures are based on normal daily mean temperatures published by the U.S. Weather Bureau it is obvious that there will be wide variations from these means depending on the general character of the season. Please refer to Table 1.

<u>Locality</u>	<u>Normal Length of Freezing Season</u>		<u>Total Days</u>	<u>Ave. Temp. During Freezing Season</u>	<u>Freezing Index* F°-(C°) Degree Days of Freezing</u>
	<u>From</u>	<u>To</u>			
Duluth	Nov. 12	Apr. 2	142	16.73°F (-8.48°C)	2168 (1204)
Sault Ste. Marie	Nov. 16	Apr. 4	140	18.76°F (-7.36°C)	1854 (1030)
Milwaukee	Nov. 28	Mar. 15	108	24.22°F (-4.32°C)	840 (467)
Port Huron	Dec. 1	Mar. 20	110	24.98°F (-3.90°C)	772 (429)
Buffalo	Dec. 8	Mar. 19	102	26.35°F (-3.14°C)	576 (320)

Table 1
(Striegl--1952)

It will be noted that these figures indicate 3.76 times as much of the air temperature condition which, when in contact with undisturbed water, causes the formation of ice at Duluth as at Buffalo. Naturally one would expect the formation of more ice at Duluth, and the northerly areas of the Great Lakes, than in the southern areas. Other conditions such as sunshine, winds, volume of the body of water, etc., of course, modify the relationship between temperature and ice formation so there is no direct relationship that may be determined for natural conditions.

*Freezing Index is the total number of Degree Days using the freezing temperature as the reference. A Degree Day is defined as the departure of the daily mean temperature from the freezing temperature.

Aune, Beaudin, and Borrowman (1957) indicate maximum thicknesses of solid lake ice observed in locations from 1899 through 1951 and average daily temperatures for the month of January for a period of 20 years. They described solid lake ice as occurring in protected harbors, bays, and channels of low velocity current. Ice of this type begins to form in November and continues to increase in thickness throughout the winter occasionally obtaining a depth of three and one half feet (1.1 meters) with depths of two feet (0.6 meters) being quite ordinary in northern localities. Solid lake ice conditions usually prevail to the later part of March or early April at which time the ice begins to honeycomb and break up. Their data is presented in Table 2.

<u>Location</u>	<u>North Latitude</u>	<u>Average Daily January Temperature</u>	<u>Maximum Thickness of Ice</u>
Duluth, Minnesota	47°	10° F (-12° C)	38 in (97 cm)
Marquette, Michigan	46°	15° F (- 9° C)	27 in (69 cm)
Escanaba, Michigan	46°	15° F (- 9° C)	35 in (89 cm)
Green Bay, Wisconsin	44°	17° F (- 8° C)	36 in (91 cm)
Milwaukee, Wisconsin	43°	22° F (- 6° C)	-----
Chicago, Illinois	42°	25° F (- 4° C)	-----
Mackinaw City, Michigan	46°	17° F (- 8° C)	-----
Saginaw Bay, Michigan	43°	22° F (- 6° C)	35 in (89 cm)
Detroit, Michigan	42°	26° F (- 3° C)	-----
Cleveland, Ohio	41°	27° F (- 3° C)	17 in (43 cm)
Buffalo, New York	43°	25° F (- 4° C)	24 in (61 cm)
Oswego, New York	43°	23° F (- 5° C)	25 in (64 cm)
Ogdensburg, New York	45°	17° F (- 8° C)	30 in (76 cm)
Kingston, Ontario	44°	23° F (- 5° C)	25 in (64 cm)
Sault Ste. Marie, Michigan	46°	-----	27 in (69 cm)
Port Arthur, Ontario	48°	10° F (-12° C)	41 in (104 cm)

Table 2
(Aune, Beaudin and Borrowman--1957)

Freshwater lakes and rivers lying between 35°F (2°C) and 30°F (-1°C) January isothermals will freeze on rare occasions of extremely cold temperatures (about 0°F or -18°C) which are usually of only several day's duration.

Between 30°F (-1°C) and 25°F (-4°C) isothermals some ice normally less than 4 inches (10 cm) in thickness can be expected almost every winter. Northward of the 25°F (-4°C) isothermal ice can be expected every winter. The thickness will vary from 6 inches (15 cm) to 12 inches (30 cm) in the vicinity of 25°F (-4°C) isothermal to 36 inches (91 cm) near the 10°F (-12°C) isothermal.

During January and February 1977 we made ice thickness measurements in harbors on Lakes Superior, Michigan and Huron. This was an unusually cold winter in the western Great Lakes area. Many thicknesses in the range of 30 to 39 inches (75 to 100 cm) were observed between 42° and 47° North latitudes. At 42° North latitude on Lake Michigan, 35 inches (90 cm) was measured. There seems little doubt but that three feet (one meter) of ice is probable in the western Great Lakes. Also, as was previously mentioned, the U.S. Great Lakes Environmental Research Laboratories is measuring and recording ice thickness in the Great Lakes.

Deformation and Strength Behavior of Polycrystalline Ice

Polycrystalline ice is a viscoelastic material. A comprehensive description of a complete linear viscoelastic model representing the stress-strain behavior is given by Nevel (1976).

For our purposes we will review deformation behavior by describing a laboratory unconfined uniaxial compressive strength test of ice. The test is run at a constant stress, i.e. a single load is placed on the sample. As it remains on the sample, the sample will compress or deform. The amount of deformation divided by the sample length is the strain.

The longer the load is left on the sample, the more the sample will deform. Strain is therefore a function of time. This is termed creep behavior. (Strain is also a function of other variables, e.g. the magnitude of the stress.)

The total creep occurring before the sample breaks is described by three creep periods. These periods are termed primary, secondary, and tertiary.

When the load is first placed on the ice, the ice has an instantaneous elastic response which can be thought of as an elastic compression in a spring. If the load is too great, the sample may break before creep can take place. Assuming however that the load is moderate, the ice will next exhibit a delayed elastic response. This response can be thought of as the travel in a dashpot, i.e. a plunger moving in a viscous fluid. Together these two responses make up the creep period called primary creep.

During secondary creep the strain increases with time and if the ice behaves as a linear viscoelastic material this strain increase is linear.

At some point in time the strain will accelerate. This increasing straining is the tertiary creep. The sample compresses at a faster and faster rate until it fails. At lower stresses ice may not exhibit tertiary creep, but may fail during secondary creep.

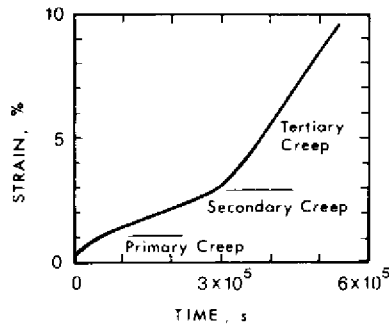


Figure 1
Creep Curve for Granular Ice
(Gold, 1973)

Figure 1 is a creep curve for granular ice reported by Gold (1973). The ice was stressed at 145 psi (1 MN/m^2). Its temperature was 14°F (-10°C). The primary creep represents about one percent strain. Secondary creep occurred until three and one-half days (3×10^5 s) had elapsed. The strain increased to an increasing rate and at the end of about six days had deformed ten percent of its original length.

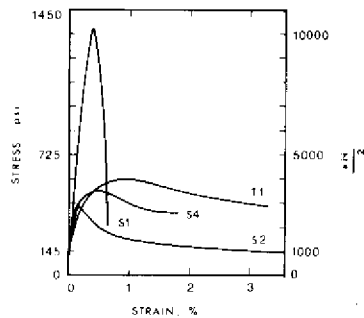


Figure 2
Strain Dependence on Stress
(Gold, 1973)

If now instead of applying a constant stress to the sample we apply a constant rate of strain we can obtain stress-strain curves like those in Figure 2 by Gold (1973). Some ice engineering problems involve conditions approaching constant strain. S1 and S2 are columnar ice and were tested with the load perpendicular to the long direction of the grains. T1 is granular ice and S4 is frazil ice. The temperature of the ice was 15°F (-9.4°C). The strain rate $1.67 \times 10^{-5} \text{ s}^{-1}$, i.e. 0.0000167 per second. (The time to reach one percent strain was ten minutes and the time to reach three percent was one-half hour.) For the given strain rate and ice temperature the influence of ice's structure is clearly seen: columnar-grained, type S-1 ice, is appreciably more brittle in its behavior than the other three, and granular, type T1 ice, more ductile.

To adequately describe the deformation and strength behavior of ice many things must be considered. These include the type of ice, the temperature, the type of load (compression, tension, etc.), load direction with respect to ice structure, the strain rate, and the stress level. Furthermore, to analyze ice in an engineering context it is necessary to establish failure criteria in either ductile or brittle modes of behavior under a variety of boundary conditions. There is much that is not presently understood about ice behavior.

Use of published laboratory strength test data from ice specimens (or simulated ice specimens) must be done with care as the values determined by such testing may not be representative of conditions in the field. For example, uniaxial laboratory strength tests may not represent biaxial and triaxial conditions encountered in the field, because of influence of shear stress in the deformation and failure behavior of ice. Also, small samples generally do not adequately represent conditions in large, sometimes irregular, cracked sheets of ice containing various impurities.

Appended to this guide is an abbreviated summary of a comprehensive monograph entitled, "Deformation and Strength of Ice", by Lavrov (1969). For the reader wishing to delve more into ice strength and behavior it will be of interest. Also the previously mentioned viscoelastic ice model by Nevel (1976) will be very useful.

In subsequent sections of this guide we will introduce strength parameters and design criteria we believe applicable to ice engineering problems in small craft harbors.

PART II

ICE PRESSURES OF THERMAL ORIGIN

Drouin and Michel (1974), working in the Laval University Ice Mechanics Laboratory have prepared a comprehensive work entitled, "Pressures of Thermal Origin Exerted by Ice Sheets Upon Hydraulic Structures". This work, undertaken by Drouin for a doctoral thesis, we believe is the most comprehensive and recent treatment of thermally induced ice forces on structures.

Prior to this work, Michel (1970) prepared a monograph entitled, "Ice Pressure on Engineering Structures". With respect to thermal forces, the later work should be used as it corrects some previous assumptions now proven erroneous.

The material that follows in this section of the guide is largely based on Drouin and Michel (1974). It is recognized that it was originally prepared in the context of reservoir ice forces that affect dams, and that it is a laboratory study. Nevertheless, understanding this work and the ranges of thermally produced loads that can be predicted for dams, will give the harbor designer a feel for the problem he faces. With flexible harbor structures, the forces will be less. Also with real field ice, the forces will be less because of faults, cracks, discontinuities, etc. Laboratory samples test stronger than field ice.

Introduction

Thermally induced ice pressures on dams and other hydraulic structures are significant, and may even be the controlling design load for some structures. In the past these thermal thrusts have been calculated for the condition of ice failing by crushing at stresses like 400 psi (2756 kN/m²). This resulted in thermal loads now known to be too high, e.g. 50 kips per foot (730 kN/m). Now values of $\frac{1}{4}$ to $\frac{1}{2}$ these are normally used. Flexible structures experience even smaller loads than rigid structures, but ways to accurately determine ice loadings on flexible structures have not been developed. The loads would however be expected to be less than those predicted in this section.

During the past fifty years, engineers and scientists, e.g. Royen, Brown and Clarke, Rose, Monfore, Lofquist, and Lindgren researched and estimated thermally induced ice pressures. None of them took into account the crystallographic characteristics of the types of ice and actual strain rates that exist in nature in the regime of thermal expansion of ice sheets. Also the initial temperature of the ice was not considered in some of the previous work, and some research was based on too few tests. The composite picture of past studies is one with ambiguities and many deficiencies. Therefore we won't review this previous work, but instead will present the recent work of Drouin and Michel (1974) who have, however, comprehensively analyzed the work of those before them.

To estimate ice pressures, we must first consider the thermal properties of ice, heat transfer in ice sheets, types of naturally occurring air temperature rises, and the deformation characteristics of several types of ice strained slowly. With a laboratory testing program supported by theoretical rheological mathematical models, Drouin and Michel (1974) have developed estimates for thermally induced ice thrusts.

Thermal Properties of Ice

Conductivity, specific heat, diffusivity and expansion are all properties of ice important to estimating thermal forces. Like most properties of ice their values are still imprecise. Drouin and Michel (1974) estimate the most probable values of thermal properties from the works of others. Table 3 presents their estimated values.

Temperature °F (°C)	Thermal Conductivity Btu in hr ⁻¹ ft ⁻² °F ⁻¹ (W m ⁻¹ °C ⁻¹)	Specific Heat Btu lb ⁻¹ °F ⁻¹ (J kg ⁻¹ °C ⁻¹)	Thermal Diffusivity ft ² hr ⁻¹ (cm ² hr ⁻¹)	Thermal Expansion °F ⁻¹ (°C ⁻¹)
32° (0°)	15.6 (2.25)	.506 (2117)	.0449 (41.7)	30.0 × 10 ⁻⁶ (54.0 × 10 ⁻⁶)
14° (-10°)	16.1 (2.32)	.487 (2039)	.0481 (44.7)	29.0 × 10 ⁻⁶ (52.2 × 10 ⁻⁶)
-4° (-20°)	16.8 (2.42)	.468 (1961)	.0522 (48.5)	28.0 × 10 ⁻⁶ (50.4 × 10 ⁻⁶)
-22° (-30°)	17.6 (2.54)	.450 (1883)	.0570 (53.0)	27.0 × 10 ⁻⁶ (48.6 × 10 ⁻⁶)
-40° (-40°)	18.6 (2.68)	.431 (1805)	.0629 (58.4)	26.0 × 10 ⁻⁶ (46.8 × 10 ⁻⁶)

Table 3 Thermal Properties
(after Drouin and Michel, 1974)

In the above table, the thermal diffusivity (equal to the conductivity divided by the factor density times the specific heat) was computed assuming an ice density of 57.2 pcf (916 kg/m³). Ice containing air bubbles may easily have a lower density, say as low as 49 pcf (785 kg/m³).

Heat transfer through a porous medium, like bubbly ice, will be less because the air cells offer greater resistance to heat transfer than does the solid ice. The value for thermal conductivity becomes less as the amount of entrapped air increases.

Notwithstanding the inherent variations in the thermal properties of ice, we can adequately proceed, within the range of design accuracies, to make engineering estimates of ice thrusts.

Heat Transfer in Ice Sheets

The studies and solutions by Drouin and Michel (1974) do not take into account any thermal boundary layers (air-ice and air-snow) or any solar radiation on the ice. However, they believe their pressures calculated on the basis of heat transfer solely by conduction are of the proper order of magnitude, and perhaps greater than the pressure calculated with the air-ice boundary layer and absorption of solar radiation taken into consideration.

Air-ice or air-snow boundary layers can contribute to increasing the initial temperature of the surface of an ice sheet. Absorption of solar radiation by the ice adds to the heat transferred by conduction. The rates of temperature increase at various levels in the ice would then be higher than those computed on the basis of conduction alone. Increasing the initial surface temperature results in a decrease in the stresses throughout the ice sheet. Increasing the heat transferred by convection (because of solar radiation) results in an increase in stresses in the upper portions of the ice sheet and in shorter times to reach maximum stress levels which thereafter diminish rapidly. However, an increase in the average rate of temperature increase of the surface of an ice sheet implies a decrease in the maximum pressure. Hence their pressures are thought to be conservative, i.e. greater than necessary for design of conditions actually present in the field.

In the foregoing explanation it should be noted that an increase in the rate of temperature increase in the surface of the ice sheet results in a decrease in the maximum pressure. Drouin and Michel (1974) found, contrary to many other published theories and results, that the pressure in an ice sheet was highest for small rates of temperature increase at the surface of the ice. From a physical standpoint, they explain this by the deeper penetration into the ice sheet of the temperature variations at the time when the stress at the surface attains its maximum. It is in the top zone of an ice sheet where the stressed condition related to the maximum pressure exerted by thick ice sheets develops. Attenuation of temperature variation in the interior of an ice sheet is very rapid.

The stress in an ice sheet is determined by the temperature distribution in the ice sheet as a function of the variation of air temperature. Drouin and Michel (1974) use a sinusoidal air temperature variation, rather than a linear variation or step function. The use of sinusoidal variation produces larger stresses and fits well with natural temperature variations (in Canada).

The sinusoidal variation used is one where the temperature increases at an increasing rate until it has achieved one half of its total rise. This occurs when one half of the time to achieve its total rise has passed. The temperature continues to rise but at a decreasing rate until the total temperature rise has occurred for the period.

Other factors that affect the temperature variation in an ice sheet include the presence of snow on the ice sheet, the thickness of the ice sheet, increase of thickness in the ice sheet as a function of time, solar radiation absorbed, and variable thermal properties of ice. (These vary primarily with temperature.)

Analytic methods are available to describe temperature distribution in a mass as a function of the variation in temperature of an ambient medium. To solve the equations developed by these analyses requires simplifying assumptions. For example, Drouin and Michel (1974) had to assume that the thickness of the ice remained constant during the period of ambient temperature increase. This would not be the case for thin ice but would be reasonable for sheets thicker than 16 inches (40 cm).

Climatological Data

In order to compute the pressures from thermal ice expansion we need to know the total temperature rise and the time required to obtain that rise. Also we should know if the temperature rise is linear or varies somehow, such as sinusoidally. Drouin and Michel (1974) present climatological data for Quebec City from 1944 to 1967, inclusive. Quebec City is at 46°48'N latitude and 71°23'W longitude. Climatological data from Quebec City will not be applicable at most other sites, but by presenting them here we will be able to subsequently demonstrate a design methodology. The designer of a small craft harbor at another location would of course investigate climatological conditions there.

Table 4 presents a statistical analysis of data for 23 winters at Quebec City. For that city it was calculated that 90 percent of the air temperature increases had durations of less than 20 hours. About two-thirds of the time the duration was less than 10 hours. The most frequent temperature spread was 17°F (9.5°C) with a duration of 7 hours, which is an average rate of air temperature increase of 2.4 F/hr (1.3 C/hr). Sinusoidal variation in temperature rise was generally present.

<u>Period of Recurrence (years)</u>	<u>Duration of Temperature Increase (hrs)</u>		
	<u>5</u>	<u>10</u>	<u>20</u>
12.5	4.4 (2.4)	3.1 (1.7)	1.6 (0.9)
25	4.7 (2.6)	3.3 (1.8)	1.7 (0.9)
50	5.2 (2.9)	3.5 (1.9)	1.8 (1.0)
100	5.6 (3.1)	3.7 (2.1)	1.9 (1.1)

Table 4 Rates of Increase, F/hr (C/hr), for Linear Air Temperature Increases as a Function of the Period of Recurrence and Duration of the Increase (Quebec, December 1, 1944--March 31, 1967)

(after Drouin and Michel, 1974)

Rheological Aspects

When an ice specimen, mechanically fixed at its ends, is heated it will try to expand. However, since the ends are fixed a thermal stress will be produced. The strain from this thermal stress offsets that due to the temperature rise. Thus, even though the specimen undergoes no apparent change in length, it is subjected to mechanical strain equal to the thermal deformation that would have resulted if it had been unrestrained. Maintaining a constant length and measuring the forces (stresses) that occur at different temperatures is one way of carrying out laboratory tests on ice.

The laboratory procedure used by Drouin and Michel (1974) used a somewhat different approach, one that avoids errors caused by the metal parts of the testing machine expanding. The tests were performed, at different temperatures, on ice specimens at constant strain rates. The tests determined by means of the experimental curves obtained, the stresses and thrusts induced by the effects of temperature variation.

Ice in nature responds to thermal changes in a ductile manner. The strain rates are quite small and hence ice exhibits ductile behavior. The small strain rates accompanying thermal behavior can be shown with the following calculation.

Assume a temperature rise of 5 F/hr (2.8 C/hr) and a coefficient of thermal expansion of $28 \times 10^{-6} \text{ F}^{-1}$ ($50.4 \times 10^{-6} \text{ C}^{-1}$)

Strain Rate = Coefficient of Expansion x Rate of Temperature Rise

$$\begin{aligned} &= \frac{(28 \times 10^{-6} \text{ F}^{-1}) (5 \text{ F/hr})}{(3600 \text{ s/hr})} \\ &= 3.89 \times 10^{-8} \text{ s}^{-1} \end{aligned}$$

The thermal strain is also quite small.

Assume a rise in temperature from -30°F (-34°C) to 32°F (0°C) at the above rate. The strain rate is $3.89 \times 10^{-8} \text{ s}^{-1}$ for a coefficient of thermal expansion of $28 \times 10^{-6} \text{ F}^{-1}$ ($50.4 \times 10^{-6} \text{ C}^{-1}$)

$$\begin{aligned} \text{Strain} &= \frac{(62 \text{ F}) (3600 \text{ s/hr}) (3.89 \times 10^{-8} \text{ s}^{-1})}{(5 \text{ F/hr})} \\ &= 0.00174 \\ &= 0.174\% \end{aligned}$$

The total strain is less than one quarter of one percent. However, if for this strain the ice were unrestrained, it would expand nearly 10 feet (3 m) in a mile (1.6 km)

To deform laboratory specimens by a factor of one percent at constant rates of 10^{-7} , 10^{-8} , and 10^{-9} per second, test durations of 28, 280, and 2800 hours are necessary. These long periods explain why few tests in the range of strain rates that accompany thermal expansion in the field are cited in the literature. At very low strain rates even small temperature variations in the ambient medium impair the validity of a test. Also, the deformation of a measuring element of a load cell, is not negligible in comparison with the actual deformation of the specimen. The laboratory testing program undertaken by Drouin and Michel (1974) overcame many difficulties of this nature.

Laboratory Test Results, Ice Thrusts

Two types of ice were tested, S1 columnar ice loaded perpendicular to the c-axis (and parallel to the basal plane) and T1 snowpack ice. Samples were generally columns 1 inch (2.54 cm) in diameter and 3 inches (7.62 cm) long. As they were compressed, at strain rates ranging between 10^{-7} , and 10^{-8} per second and at different temperatures ranging between freezing and about -20°F (-29°C), the deformations and loads were measured.

In the snowpack ice the maximum loads occurred after the stress had increased at a constant rate for some time. The stress, after having attained its maximum, usually remained constant or nearly so. The average deformation to reach maximum stress was 0.15 percent.

In the columnar ice the stress increased at a constant rate for a long time. Following that, the rate of increase of stress gradually diminished until it was nil. The maximum stress was reached when the specimen had been deformed between 0.08 and 0.20 percent. The stress, after reaching its maximum value, fell very rapidly and then stabilized at a near constant value.

At the low strain rates the sample behavior is plastic, i.e. the sample doesn't break or shatter, but yields as time proceeds.

The maximum thrusts for columnar and snowpack ice are given in Table 5. They have been computed from the laboratory test data and a sinusoidal varied ambient temperature rise from an initial linear steady temperature state in the ice (i.e. the initial ice temperature profile varies linearly from the ambient temperature at the surface to the melting point at the water-ice interface). With time the ice warms up and thereby exerts thermal stresses. These stresses reach maximums and the stress in the ice at various depths can be summed up to obtain the maximum ice thrust per unit length for a given ice thickness, total temperature rise, and duration of temperature rise.

Ice thrusts for ice thinner than indicated in the table will be less than the tabulated values. Also, the analysis of stresses indicates that the stresses in an ice sheet are particularly high in the first 8 to 12 inches (20 to 30 cm) of the thickness of a thermally stressed ice sheet. The bottom region of a thick ice sheet may consist of a different type of ice without appreciably altering the stressed conditions, the heat transfer being the same.

Ice Surface Temperature, F (C) and
Classification of Ice:

S1 = Columnar Ice and I1 = Snowpack Ice

<u>Ice Thickness and Duration of Temperature Increase (hrs)</u>	<u>14° F (-10° C)</u>		<u>-4° F (-20° C)</u>		<u>-22° F (-30° C)</u>	
	<u>S1</u>	<u>I1</u>	<u>S1</u>	<u>I1</u>	<u>S1</u>	<u>I1</u>
20 in (50 cm)						
t = 5 hrs	5 (73)	4 (58)	11 (160)	8 (117)	19 (277)	13 (190)
t = 10 hrs	6 (88)	5 (73)	14 (204)	11 (160)	23 (336)	16 (233)
t = 20 hrs	9 (131)	7 (102)	18 (263)	13 (190)	27 (394)	18 (263)
30 in (75 cm)						
t = 5 hrs	5 (73)	4 (58)	11 (160)	8 (117)	20 (292)	14 (204)
t = 10 hrs	7 (102)	5 (73)	15 (219)	11 (160)	24 (350)	18 (263)
t = 20 hrs	9 (131)	8 (117)	20 (292)	15 (219)	30 (438)	20 (292)
40 in (100 cm)						
t = 5 hrs	5 (73)	4 (58)	11 (160)	8 (117)	20 (292)	15 (219)
t = 10 hrs	7 (102)	5 (73)	15 (219)	12 (175)	25 (365)	19 (277)
t = 20 hrs	9 (131)	8 (117)	20 (292)	16 (233)	32 (467)	22 (321)

Table 5 Pressures of Thermal Origin by an
Ice Sheet Restrained in One Direction
kips/ft (kN/m)

(after Drouin and Michel, 1974)

Use of the table is illustrated by the following example. Given a 30 inch (75 cm) ice sheet with a surface temperature of -4°F (-20°C). The thrust exerted by a rise in temperature to 32°F (0°C) over a period of 10 hours (i.e. at a rate of 3.6°F/hr or 2.0°C/hr) would be 11 to 15 kips per foot (160 to 219 kN/m) depending on whether the ice was granular or columnar (loaded perpendicular to the c-axis).

Except for complete biaxial restraint, most factors encountered in nature tend to decrease calculated ice thrusts. Among the factors which reduce stresses of thermal origin are the insulating qualities of a snow cover on the ice and cracks in the surface of the ice.

Biaxial Restraint

Determining rheological behavior of ice deformed in two directions is a subject of current research. Drouin and Michel (1974) performed some biaxial tests on snowpack ice and concluded that snowpack ice deforms in the manner of an almost perfectly plastic material when the maximum biaxial stress of thermal origin is obtained. This maximum biaxial stress is about twice the maximum stress previously obtained in the uniaxial tests. Also they concluded that maximum stresses for S1 and S2 columnar ice having pressures of thermal origin and biaxially restrained can be adequately estimated by using the uniaxial test results for S1 ice.

They give no ice thrusts for the biaxial condition as such, but suggest using uniaxial thrusts for a dam and reservoir with the following example. Assume an ice sheet is totally restrained in a direction perpendicular to a dam crest. Stresses of great magnitude develop in the first 8 inches (20 cm) of the ice thickness. Under natural conditions, the crystallographic orientation of the grains of columnar ice in the top layer of an ice sheet can be considered random. In such case, the stresses developed are considerably lower than if all the columns have, for instance, a vertical crystallographic orientation. Experimentally the biaxial restraint of S1 or S2 columnar ice having some grains randomly oriented gives substantially the same maximum stress values as are obtained from S1 ice specimens restrained in only a single direction (deformed perpendicular to the c-axis). Also a reservoir with rocky vertical walls around the entire perimeter would be unusual. It would correspond to an ice sheet in a swimming pool (or a small-craft harbor completely surrounded by vertical sheet piling walls).

Within the present state of knowledge, Drouin and Michel (1974) recommend using thrusts in reservoirs on laboratory testing of ice under uniaxial loading.

Effects of Cracks and Snow on Ice Thrusts

Snow covered ice or cracked ice or both significantly reduce the thrust of an ice sheet.

The effect of cracks (either from thermal contractions or water level changes) is to mitigate the effect of a temperature rise or spread.

Metge (1976) has reported on a five year study and field observation on thermal cracks at Kingston, Ontario. The frequency of cracking tends to decrease as an ice cover becomes thicker. He categorizes thermal cracks into three groups. The first are dry cracks which absorb a significant amount of thermal ice movement. They are common and consist of cracks that extend from the top of the sheet down one-half to two-thirds of the ice thickness. These dry cracks open and close according to the ice temperature. The second and third groups are respectively, wet cracks which are relatively rare, and wide wet cracks which are just too wide to easily refreeze into sound ice. Wet cracks are narrow enough to refreeze rapidly and in so doing add material to the ice sheet. Since wet cracks are not prevalent, we are mainly concerned with the beneficial effects of the dry thermal cracks. The following example illustrates their effect on thermal thrusts.

Assume a coefficient of thermal expansion of $28 \times 10^{-6} \text{ F}^{-1}$
($50.4 \times 10^{-6} \text{ C}^{-1}$) and a total summation of
crack widths of 0.02 inches per yard (0.56 mm/m)

Strain (%) = (Coef. of Expansion) (Temp. Rise) (100)

$\frac{(0.02 \text{ in/yd}) (100)}{(36 \text{ in/yd})} = (28 \times 10^{-6} \text{ F}^{-1}) (100) (\text{Temp. Rise F})$

Temp. Rise = 20 F (11 C) = Equivalent Temperature Spread

In this example, the first 20 F (11 C) of a temperature rise would be taken up by the cracks. The remainder of the rise would produce thermal thrusts.

Table 6 gives temperature spreads for cracked ice.

Summation of Crack Widths per Unit of Length of an Ice Sheet		Total Deformation or Strain of the Ice	Equivalent Temperature Spread	
<u>in/yd</u>	<u>mm/m</u>	<u>%</u>	<u>F</u>	<u>C</u>
0.009	0.25	0.025	9	5
0.018	0.5	0.05	18	10
0.036	1.0	0.10	36	20
0.054	1.5	0.15	54	30
0.072	2.0	0.20	72	40

Table 6 Summation of Crack Widths Per Unit of Length of an Ice Sheet Expressed as Percent Thermal Deformation of the Ice and Equivalent Temperature Spreads (Coef. of Expansion = $28 \times 10^{-6} \text{ F}^{-1}$ or $50.4 \times 10^{-6} \text{ C}^{-1}$)

(after Drouin and Michel, 1974)

Snow accumulated on an ice sheet has a drastic effect on the temperature variations in the ice, and as a result the pressures of thermal origin are much less. A uniform fresh snow cover can drown an ice sheet causing no thrust until the ice reforms on the top. This can occur when a snow fall roughly equal to the ice thickness occurs.

Snow, a complex material which undergoes a continuous process of metamorphosis, can be converted to an equivalent thermal thickness of ice by proportioning through the coefficients of thermal conductivity for snow and for ice. However, the thermal conductivity of snow varies with density (as well as other things). Mellor (1964) gives snow conductivities as a function of density. Drouin and Michel (1974) report the average density of snow 20 to 40 inches (50 to 100 cm) thick on the ground to be 25 to 28 pcf (400 to 450 kg/m^3). Snow at this density will barely show a man's foot print. For snow layers of small thicknesses the density is much less--lower than 12 pcf (200 kg/m^3).

Table 7 gives equivalent ice thicknesses for snow densities.

Snow Density pcf (kg/m ³)	<u>Ratio of Thermal Equivalent Thicknesses of Ice to the Actual Thicknesses of Snow</u>
6.2 (100)	24.0
9.4 (150)	17.1
12.5 (200)	13.2
15.6 (250)	10.6
18.7 (300)	8.7
21.8 (350)	7.2
25.0 (400)	6.1
28.1 (450)	5.0

Table 7 Ratios of Thermally Equivalent
Thickness of Ice to Actual Thicknesses of Snow
(Drouin and Michel, 1974)

To illustrate the use of the above table, assume we have 6 inches (15 cm) of snow weighing 21.8 pcf (350 kg/m³) on top of a two foot (0.6 m) thick ice sheet. The ratio of equivalent thickness of ice to actual thickness of snow is 7.2; therefore, thermally the snow simulates an additional layer of 43.2 (110 cm) thick. The fictitious sheet is now 67 inches (170 cm) thick. The temperature variations to be taken into account in calculating the stresses of thermal origin are those which prevail 43 inches (110 cm) below the surface of the fictitious sheet. At this depth into an ice sheet the attenuation of temperature is complete and thus the pressure of thermal origin is very small or nil.

Ice Thrust on Individual Piers

Petrunichev (1954), cited by Korzhavin (1971), considers static horizontal pressure of ice on individual piers. The question is raised as to whether one should determine the pressure from an ice field by the width equalling half the sum of the adjacent spans or be limited to considering only the pier width.

The deformation of the part of the ice field lying between the piers would not occur separately. It exerts a partial effect on the amount of pressure on a pier. It would be increased. Petrunichev (1954) suggests that the total force on a pier should be equal to the thrust (force per unit length) times the sum of the width of the pier and one-third the half sum of the spans contiguous with the pier.

The suggestion for somehow increasing forces for 'bridging' action would be applicable for small craft harbors. For example, consider the case of a marina pier constructed with horizontal elements spanned across intermittent cribs. The total lateral force would exceed that computed from ice contact with the crib alone. In part, the ice would 'bridge' over and produce a larger horizontal force.

Closure

In this section we have reviewed the thermal ice pressures proposed by Drouin and Michel (1974) and presented some estimates of thrusts. Flexible marina structures and conditions existing in nature should result in forces smaller than those given.

The forces were computed for assumed temperature rises equal to the difference in the cold ice sheet surface temperatures and the melting point. Temperature rise is a function of the site's climatology. The highest pressure occurs for the smaller rates of temperature rise. Also the attenuation of temperature rise occurs very rapidly and it is the top zone of the ice sheet that experiences the thermal stresses. (Query, can one mitigate these stresses in this area somehow. If the ice were weakened or broken, or if made thin or warmer, or if separated from the structure with a pliable material, the force on the structure would be reduced.)

Strain rates in the regime of thermal expansion of ice sheets are very low (less than 10^{-7} s⁻¹) and the ice behaves in a ductile manner. Also forces produced from uniaxial testing can adequately represent some level of biaxial conditions that might be present at a particular site.

Each site where thermal pressures will exist should be separately studied. The climatology, characteristics of the ice sheet, bank configuration, and type of structure are all important.



PART III

ICE SUPPRESSION AND WEAKENING

Ashton (1974) has prepared a monograph on air bubbler systems to suppress ice. Analytical methods were used to develop a procedure for predicting the effectiveness of using bubbler systems to suppress ice formation under various field conditions. We believe air bubbling is an effective method to suppress ice. The material contained in this section is based largely on the procedures suggested by Ashton but simplified somewhat to fit our concern, namely, melting ice in a small-craft harbor (rather than in a lake shipping channel or a deep-water port). The resulting suppression predictions agree well with our field observations and experiences of air bubbler manufacturers.

Those wishing to examine air bubbler systems in more detail than what is presented here can refer to the original Ashton (1974) monograph, Ashton (1975) and Ashton (1977). The 1975 work is a laboratory experimental report on heat transfer coefficients associated with flow induced by a line source bubbler system. The 1977 work is a refinement of the monograph and a numerical simulation for a system. US CRREL has developed a computer program in BASIC language that simulates analyses of diffuser lines, plumes and heat transfer, ice melting, and thermal reserves. The simulation agrees satisfactorily with one example case for a winter in Duluth, Minnesota.

We will begin with a description of how a compressed air bubbler de-icing system works. This will be followed with a review of the suggested design method and practical considerations to achieve a successful installation. Also included are a few notes on other ways to suppress or weaken ice.

Principles of Bubbler System Operation

Figure 3 is a cross sectional view along the axis of an air diffuser pipe on a lake bottom. It is also representative of the action of a point source diffuser.

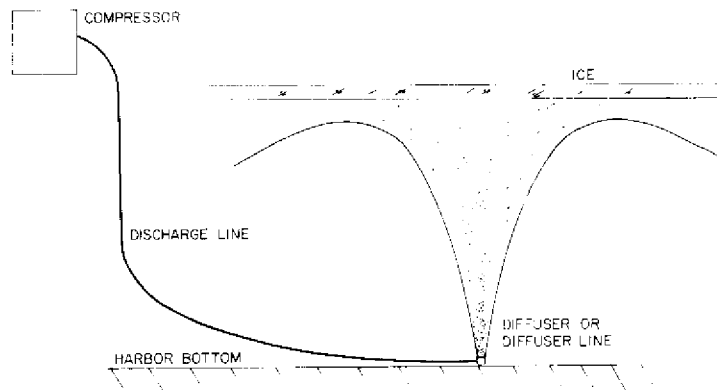


Figure 3
Bubbler System Schematic
(after Ashton, 1974)

Air is compressed by a compressor either located indoors or suitably protected and mounted on a marina pier. In an overall ice suppression system, several compressors may be used and interconnected through a discharge manifold piping system. Air travels through the discharge line to the diffuser or diffuser line on the lake bottom. The air has been warmed during compression but normally is cooled down to the ambient lake temperature by the time it reaches the diffuser. Here the air is discharged through an orifice. It must have enough pressure at the diffuser to overcome the depth of water hydrostatic pressure.

The discharging air is cooled as it expands going through the orifice. If it expands too quickly an icing condition can occur at the orifice. With proper air pressures this does not happen. The momentum of the air jet sets the bubbles in motion. The momentum quickly dissipates and bubble buoyancy takes over. As the bubbles rise they entrain water into the rising plume from the lateral direction. Many bubble sizes are present, but the tinier ones are more efficient as they move more water for the same volume of air. In fact, this principle explains why large air bubbles, like those produced by belcher devices, aren't as effective as a continuous stream of tiny bubbles. The ice melting that occurs on the underside of the sheet is the result of both temperature and volume of water being moved upwards from the warmer bottom water by the bubble plume.

At some point near the surface the buoyant plume spreads as it either impinges on the ice cover or encounters open water. If a free water surface is present, the bubbles will escape directly to the atmosphere. This results in a certain amount of heat being wasted. If a cover exists the bubbles will move laterally along the underside of the ice. As they do, melting primarily by convection occurs. This heat loss results in cooling of the flow whose velocity has also decreased as it spread out. Rapid decay in the heat transfer rate is the result.

Finally, the plume imposes a net circulation on the water and this allows more warm water to be drawn into the area from distant lateral directions. A bubbler system would not work in a swimming pool for example, because the amount of warm water is limited by the pool's volume and eventually it would all be cooled down. The pool would freeze to the bottom. Design of bubblers in sea water is complicated because salinity may vary with depth and theoretically the maximum density occurs at the freezing point. (There may be no "warm" dense bottom water.) Also rivers with currents tend to be isothermal and even super-cooled, and hence do not have enough heat. What heat there may be is already impinging on the river cover.

In a fresh water or brackish water marina, however, a bubbler system can work if lateral warm water recharge is present and it is designed and maintained properly.

Ice Suppression Bubbler Systems Design

The following design procedure is a trial-and-error procedure based upon Ashton (1974). For a given site and conditions the quantity of air required Q_a is estimated for a tolerated ice equilibrium thickness n_e . This thickness is a steady state thickness of an ice cover that will persist with a continual flow of heat to the cover's lower surface and a cooler atmosphere forming ice. At the equilibrium thickness, the ice is melting as fast as it forms.

The design of an ice suppression system requires the selection of this thickness. To reduce it to zero or near zero requires disproportionate amounts of heat, i.e. the air flows required become large. The ice itself is an insulator and a free water surface is heat wasteful. (However, the designer may wish to choose to obtain free water in order to better monitor the bubbler's operation throughout the winter.) In selecting a thickness to be tolerated, factors like the following must be considered: first cost and operating costs, resistance available to ice uplift through embedment of piles being protected, magnitude of lateral forces from thicknesses of ice, availability of manpower to chop ice during severe cold periods, temperature extremes existing at the site, and the amount of damage to be tolerated.

The quantity of air required Q_a is estimated from experience and local conditions. Table 8 gives heat transfer coefficients as a function of water depth H and air flow rates Q_a . (Q_a is in terms of volume per time per length of diffuser which reduces to area per time.) The depth of water

used is from the underside of the ice (nominally the top surface for suppressed ice) to the diffuser level (on the bottom generally).

<u>Water Depth</u>	<u>Air Flow Rate, Q_a, ft² min⁻¹ (m² s⁻¹)</u>						
	.01 (1.55)*	.02 (3.10)	.03 (4.64)	.04 (6.19)	.05 (7.74)	.06 (9.29)	.07 (10.8)
H, ft (m)							
6 (1.8)	151 (857)	169 (960)	180 (1022)	189 (1073)	195 (1107)	201 (1141)	206 (1170)
8 (2.4)	142 (806)	158 (897)	169 (960)	177 (1005)	184 (1045)	189 (1073)	194 (1102)
10 (3.0)	134 (761)	150 (852)	159 (903)	167 (948)	173 (982)	178 (1011)	183 (1039)
12 (3.7)	127 (721)	142 (806)	151 (857)	158 (897)	164 (931)	169 (960)	174 (988)
14 (4.3)	121 (687)	135 (767)	144 (818)	151 (857)	157 (891)	162 (920)	166 (943)
16 (4.9)	116 (659)	130 (738)	138 (784)	145 (823)	150 (852)	155 (880)	159 (903)

*Multiply values by 10^{-5}

Table 8 HEAT TRANSFER COEFFICIENTS, h_b
 Btu hr⁻¹ ft⁻² F⁻¹ (W m⁻² C⁻¹)
 (after Ashton, 1974)

The heat transfer rate q_w is obtained from

$$q_w = h_b (T_w - T_m)$$

where T_w is the water temperature

and T_m is the melting point temperature of ice

The water temperature can be measured at a given site or conservative estimates made for its value. We have made water temperature measurements in many western Great Lakes small craft harbors and found them to be isothermal and only slightly above the freezing temperature ($\frac{1}{2}$ F, 0.3 C, or cooler). Others have also reported very cold water. It is reasonable to assume that the water temperature is constant throughout its depth because being shallow and agitated by rising bubbles are conditions tending to destroy any thermal stratification.

Figure 4 gives the equilibrium thicknesses n_e for the calculated heat transfer rate q_w as functions of the ambient air temperatures T_a . It has been assumed that no snow cover is present and that the average wind speed is 10 mph (4.5 m s^{-1}). If snow is present the equilibrium thicknesses become smaller for a given q_w . Conversely, if windier conditions prevail the equilibrium thicknesses increase.

The average daily temperature during the period of the winter under consideration can, for most sites, be used for T_a . Ice once formed grows rather slowly during cold spells. During the day, warmer temperatures counteract cooler evening temperatures.

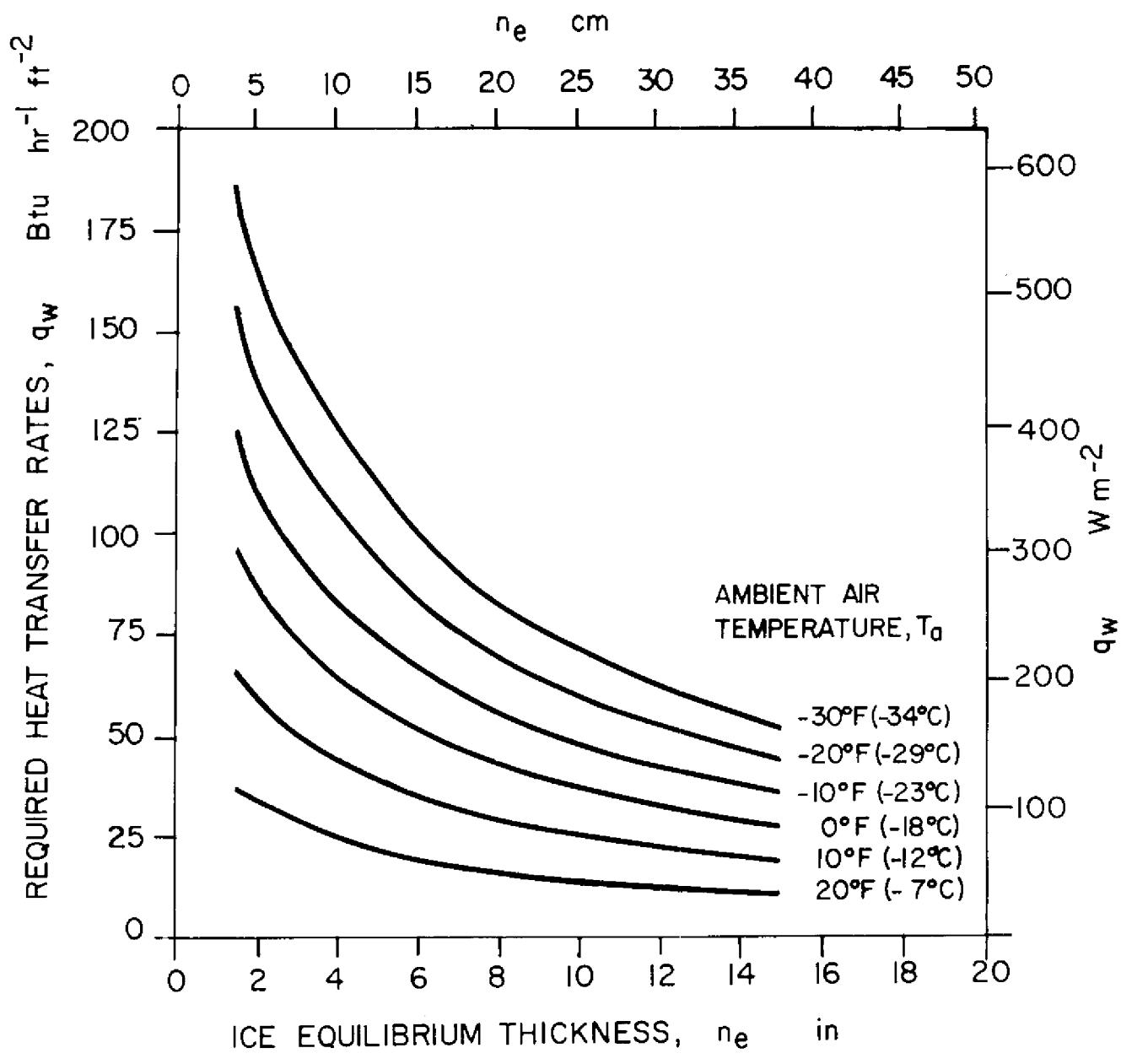


Figure 4. REQUIRED HEAT TRANSFER RATES TO ATTAIN EQUILIBRIUM THICKNESS AS FUNCTION OF AMBIENT AIR TEMPERATURE (after Ashton, 1974)

The use of Table 8 and Figure 4 is illustrated by the following example.

Assume $Q_a = 0.06 \text{ ft}^2 \text{ min}^{-1}$ ($9.29 \times 10^{-5} \text{ m}^2 \text{ s}^{-1}$) of air

$H = 10 \text{ ft}$ (3 m) water depth

$T_w = 32.5^\circ \text{F}$ (0.3°C) water temperature

$T_a = -10^\circ \text{F}$ (-23°C) ambient air temperature

From Table 8 at $Q_a = 0.06$ and $H = 10$ find the heat transfer coefficient h_b

$$h_b = 178 \text{ Btu hr}^{-1} \text{ ft}^{-2} \text{ F}^{-1} \\ (1011 \text{ W m}^{-2} \text{ C}^{-1})$$

Find q_w , the heat transfer rate from

$$q_w = h_b (T_w - T_m) \\ = 178 \text{ Btu hr}^{-1} \text{ ft}^{-2} \text{ F}^{-1} (32.5^\circ \text{F} - 32.0^\circ \text{F}) \\ = 89 \text{ Btu hr}^{-1} \text{ ft}^{-2} (281 \text{ W m}^{-2})$$

From Figure 4 at $T_a = -10^\circ \text{F}$ and $q_w = 89$ find

$$n_e = 4 \text{ inches (10 cm)}$$

Should the ambient temperature (approximately the average daily temperature) fall below -10°F (-23°C) say to -30°F (-34°C) for a few days, then the ice equilibrium thickness would increase to 7 inches (18 cm). Whether 7 inches (18 cm) of ice would be tolerable would depend on the site and what is being protected.

Now assume instead of $Q_a = 0.06 \text{ ft}^2 \text{ min}^{-1}$ ($9.29 \times 10^{-5} \text{ m}^2 \text{ s}^{-1}$) we use one-half as much air. From Table 8 at $Q_a = 0.03 \text{ ft}^2 \text{ min}^{-1}$ ($4.64 \times 10^{-5} \text{ m}^2 \text{ s}^{-1}$) $h_b = 159 \text{ Btu hr}^{-1} \text{ ft}^{-2} \text{ F}^{-1}$ ($903 \text{ W m}^{-2} \text{ C}^{-1}$). For $\frac{1}{2} \text{ F}$ (0.3 C), $q_w = 80 \text{ Btu hr}^{-1} \text{ ft}^{-2}$ (252 W m^{-2}). From Figure 4, at an air temperature of -10°F (-23°C) we find $n_e = 5$ inches (13 cm) and at -30°F (-34°C), $n_e = 9$ inches (23 cm). Changing the quantity of air does not have a linear effect on the ice thickness. If however, the water temperature is cooler (or warmer) than estimated, large changes in n_e occur.

Assume the water temperature is $32\frac{1}{4}^\circ \text{F}$ (0.1°C) instead of $32\frac{1}{2}^\circ \text{F}$ (0.3°C). For $Q_a = 0.06 \text{ ft}^2 \text{ min}^{-1}$ ($9.29 \times 10^{-5} \text{ m}^2 \text{ s}^{-1}$) $h_b = 178 \text{ Btu hr}^{-1} \text{ ft}^{-2} \text{ F}^{-1}$ ($1011 \text{ W m}^{-2} \text{ C}^{-1}$). The required heat transfer rate is $(\frac{1}{4}) (178) = 45 \text{ Btu hr}^{-1} \text{ ft}^{-2}$ (142 W m^{-2}). Corresponding equilibrium thicknesses at -10°F (-23°C) and -30°F (-34°C) would be 11 inches (28 cm) and more than 15 inches (38 cm). These ice conditions would probably be intolerable.

The above analysis is for a line source diffuser system. A solution to a point source diffuser is not presently available. It is estimated that a series of point sources (such as would exist in a bubbler system layout protecting individual piles spaced throughout a marina) would approximate the line source condition. This of course would be a function of how far apart the point sources become. But in general, adding up the air discharges at each point source and dividing by the distribution diffuser length would be a reasonable approximation for Q_a in a typical small craft harbor.

We can estimate the time required to melt out an ice cover if one is already in place. For thicker ice there is little tendency for it to thicken. The simplest analysis occurs when we assume there is no conduction through the cover and that it is melted by the warm water impinging on its lower surface.

For these conditions the melting rate can be calculated as follows:

$$\text{Melting Rate} = \frac{q_w}{\rho_i \lambda}$$

where q_w is the heat transfer rate in $\text{Btu hr}^{-1} \text{ft}^{-2}$ (W m^{-2})

ρ_i is the mass density of ice and equal to 57.2 lbs ft^{-3} (916 kg m^{-3})

λ is the heat fusion of ice and equal to $143.7 \text{ Btu lb}^{-1}$ ($3.34 \times 10^5 \text{ J kg}^{-1}$)

Find q_w to melt one inch (2.5 cm) in a day.

$$1 \text{ in da}^{-1} = \frac{(q_w \text{ Btu hr}^{-1} \text{ft}^{-2}) (12 \text{ in ft}^{-1}) (24 \text{ hr da}^{-1})}{(57.2 \text{ lbs ft}^{-3}) (143.7 \text{ Btu lb}^{-1})}$$

$$q_w = 28.5 \text{ Btu hr}^{-1} \text{ft}^{-2} (89.8 \text{ W m}^{-2})$$

Therefore with $100 \text{ Btu hr}^{-1} \text{ft}^{-2}$ (315 W m^{-2}) we can melt $3\frac{1}{2}$ inches (9 cm) of ice per day.

We can also make an estimate of the exhaustion of the thermal reserve in a closed body of water. The following computations show the absolute necessity of having a warm water recharge at any small craft harbor using air diffusers to suppress the ice.

We can compute the volume of warm water necessary to melt a given volume of ice as follows. Assume we have ice at the freezing point and warm water at 33°F (0.55°C). On a cubic foot (0.0283 m^3) basis then:

$$\text{Ratio of Volumes} = \frac{\text{Heat Required to Melt Ice}}{\text{Heat Content of Water}}$$

$$= \frac{\rho_i \lambda}{\rho_w c_p (T_w - T_m)}$$

where ρ_i and λ are defined above

ρ_w is the mass density of water and equal to
62.4 lbs ft⁻³ (1000 kg m⁻³)

c_p is the specific heat capacity of water and
equal to 1.0 Btu lb⁻¹ F⁻¹ (4187 J kg⁻¹ C⁻¹)

$(T_w - T_m)$ is the difference in the temperature
of the water and the melting point of ice

$$= \frac{(57.2 \text{ lbs ft}^{-3}) (143.7 \text{ Btu lb}^{-1})}{(62.4 \text{ lbs ft}^{-3}) (1.0 \text{ Btu lb}^{-1} \text{ F}^{-1}) (1^\circ \text{ F})}$$

$$= 132$$

It takes 132 cubic feet (3.74 m³) of water at 33°F (0.55°C) to melt 1 cubic foot (0.0283 m³) of ice at the freezing point.

Assume we have an air diffuser system installed in a closed body of water that is at a temperature of 33°F (0.55°C). Also assume a depth of water of 10 feet (3 m), diffuser lines spaced 30 feet (9 m) on centers, and that we want to use the diffuser lines to melt ice in a band 3 feet (1 m) wide.

$$\text{Suppressed Thickness} = \frac{(30 \text{ ft}) (10 \text{ ft}) (1 \text{ ft})}{(132) (3 \text{ ft}) (1 \text{ ft})}$$

$$= 0.76 \text{ ft or } 9 \text{ in (23 cm)}$$

Under these closed conditions the thermal reserve would be exhausted in a few days. If an ice cover grows rapidly a large amount of heat can be sealed in. However it would still not be enough to operate a suppression system throughout a winter. There must be a source of warm water. Also operating these systems in shallow water, say six feet (2 m) or less, is not recommended because of lack of enough warm water to melt an ice cover.

The detailed design and layout of an ice suppression bubbler system is outside the scope of this ice engineering guide. A few comments on the design of systems that are presently installed and are working are in order however.

Having determined the required amount of air (a function of water depth, water temperature, water body thermal reserves, atmospheric conditions, and thickness of ice to be tolerated) an air manifold distribution system together with branch diffuser lines would be designed in accordance with standard air flow design procedures. It is important that manifold and diffuser lines are large enough to reduce pressure losses and to make sure the air supply is not exhausted before the last diffuser is reached. Balancing air flows and pressures is quite important for a successful compression system.

The total air pressure required will be a function of the line and orifice losses and the hydrostatic head to be overcome at the diffuser. Where the harbor bottom is sloping, it is best to distribute the air in an uphill direction from the deep end; otherwise if the air is first emitted in shallow water, the deeper diffusers may be starved.

Spacing of orifices would normally be between 1/2 and 1/3 the water depth along a line diffuser. Pre-slit vinyl weighted bubbler hoses are available from component manufacturers. Fixed opening orifices are usually a nominal 3/64 inch (1 mm) size. The orifice diameter (or head differential) can be determined from a standard discharge equation given below.

$$Q_o = sQ_a = C_d \frac{\pi d^2}{4} \sqrt{2 \Delta p / \rho_a}$$

where Q_o = discharge from a single orifice

s = spacing of orifice

Q_a = air discharge per unit length

C_d = orifice loss coefficient (from fluid mechanics texts, etc.)

d = orifice diameter

Δp = pressure difference across orifice

ρ_a = mass density of air

Usually an air bubbler system is a low pressure, high volume design. This suggests the use of rotary blowers instead of piston compressors used previously. A disadvantage of a piston compressor is the presence of finely atomized oil in the air diffuser lines which has passed by the pistons. This causes clogging of the lines and orifices. Noise is a disadvantage of the rotary compressor system.

Standby power or other alternative procedures should be available at a marina in the event that power is lost during a storm or for other reasons.

A well designed air bubbler ice suppression system will rapidly prove inadequate if little attention is paid to its pre-season cleaning and balancing. It is essential to begin an icing season with clean, balanced and operable system components.

Other Ways to Suppress or Weaken Ice

At this time it appears that compressed air ice suppression systems are best for the small craft harbor. A few other methods are given below and they may have some applicability.

Velocity or propeller systems drive a propeller that churns warm water to the surface. A lot of water is moved with only a few percent of the volume contributing to melting ice where suppression is desired. Methods to analyze melting ice with these systems have not been published. The velocity system's chief applicability appears to be in keeping limited areas open, e.g. around a boat left in the ice.

US CRREL personnel have observed a field experiment where 57°F (14°C) warm water was emitted from a diffuser 19 feet (6 m) below the ice surface. The warm water rose until it cooled to 39°F (4°C); at which time it descended as it was denser than the surrounding water. It did not reach the surface to melt the cover. Warm water diffusers might work with shallow water, higher pressures for momentum and insulated manifold and diffuser lines.

Insulating ice is very effective in reducing its thickness and retarding its growth. A few trials have been made in river ice. They effectively reduced a normal cover of 12 inches (30 cm) to zero. Problems involved are installing, maintaining and removing the insulation material.

Snow is a good insulator and snow thrown by a snow-blower is reworked and tends to set up. In this form, a snow cover might provide satisfactory insulation during severe periods of a winter.

Dark substances will absorb heat and cause melting. However coal dusting and other techniques are one-time temporary measures. Such procedures as well as chemical applications for melting are not acceptable today.

Electrical resistance heating is more expensive than other suppression methods but is feasible and perhaps applicable. Frazil ice, which is quite sticky can be electrically melted from intake structures. Lake ice could also be melted with electrical heat. As the area of contact between the structure to be protected and the ice diminishes, the more favorable resistance heating becomes. (Query, could pilings whose diameters were made small at the ice line, an area not usually requiring a large pile section modulus, be incorporated in a dock system design with electric heating to suppress the ice.)

Finally, ice can be weakened and cracked by impacting, chopping, wave generation schemes and other mechanical means. These do not appear feasible for a small craft harbor however.



PART IV

BEARING CAPACITY OF ICE

This section of the guide contains information on the capacity of ice to support loads, especially construction loads resulting from using ice as a work platform for building small craft harbors. Winter construction has proven very successful in the Great Lakes. The ice easily handles men and small equipment with few accidents. Heavier loads have been moved and supported by ice also, including driving piling with light pile drivers and excavation dredging with regular construction cranes and draglines. Predicting safe allowable loads necessarily must be conservative. Ice strength must be assumed to be weaker than strengths which will be assigned in the next section for estimating the forces and uplifts due to ice.

This section begins with a discussion of ice parameters and bearing capacity theory. A figure is presented for maximum safe loads. The section concludes with some comments on thickening and strengthening ice.

Flexural Rigidity Length

Nevel (1976) introduced a term, flexural rigidity length, for a characteristic feature of all ice plate problems. The term in fact has been called characteristic length, or sometimes action radius. To derive the term, let us first consider the differential equation for a beam.

$$EI \frac{d^4w}{dx^4} = q$$

where w = deflection

x = distance

q = load

E = modulus of elasticity

I = moment of inertia

The term EI is a measure of how stiff the beam is. If now the beam rests on water the deflection increases the water pressure which reduces the load.

$$EI \frac{d^4w}{dx^4} = q - kw$$

where k = weight density of water

$$EI \frac{d^4w}{dx^4} + kw = q$$

$$\frac{EI}{k} \frac{d^4w}{dx^4} + w = \frac{q}{k}$$

The term $\frac{EI}{k}$ on a unit width basis has the dimensions of the length to the fourth power, so the fourth root of $\frac{EI}{k}$ is a length, i.e.

$$\frac{EI}{k} = \frac{FL^{-2} L^3}{F L^{-3}} = L^4$$

where F and L represent force and length units

$$\frac{EI}{k} = \frac{(E) (1/12) (h^3)}{k} = \frac{Eh^3}{12k}$$

where h is the plate thickness

Now for a plate instead of a beam the term $(1 - \nu^2)$ is introduced through strain compatibility relationships, where ν is Poisson's Ratio. The flexural rigidity length l for a plate is defined as follows:

$$l = \left[\frac{Eh^3}{12(1 - \nu^2)} \right]^{1/4}$$

The value of l is rather insensitive to E and ν , and sensitive to h , the plate thickness. This means that we need not know E and ν precisely, but do need to know the ice thickness to make good engineering estimates. The flexural rigidity lengths for various E 's and h 's for a Poisson's Ratio of $1/3$ are listed in Table 9. The values will be used in solving bearing capacity and other plate problems.

Ice Thickness, h inches (cm)	Modulus of Elasticity, E				
	500 (3445)	750 (5168)	1000 (6890)	1250 (8613)	1500 (10335)
6 (15)	10.8 (3.3)	11.9 (3.6)	12.8 (3.9)	13.6 (4.1)	14.2 (4.3)
12 (30)	18.1 (5.5)	20.1 (6.1)	21.6 (6.6)	22.8 (6.9)	23.9 (7.3)
18 (46)	24.6 (7.5)	27.2 (8.3)	29.2 (8.9)	30.9 (9.4)	32.3 (9.8)
24 (61)	30.5 (9.3)	33.8 (10.3)	36.3 (11.1)	38.3 (11.7)	40.1 (12.2)
30 (76)	36.1 (11.0)	39.9 (12.2)	42.9 (13.1)	45.3 (13.8)	47.5 (14.5)
36 (91)	41.3 (12.6)	45.7 (13.9)	49.2 (15.0)	52.0 (15.8)	54.4 (16.6)
42 (107)	46.4 (14.1)	52.4 (16.0)	55.2 (16.8)	58.4 (17.8)	61.1 (18.6)

TABLE 9 FLEXURAL RIGIDITY (CHARACTERISTIC) LENGTHS, l , Feet (m)
(Poisson's Ratio = $1/3$)

Bearing Capacity of Ice Sheets

Kerr (1976) has presented a critical survey of the literature on bearing capacity of floating ice plates subjected to static or quasi-static loads. The work contains discussions of general questions, analytical solutions, and field and laboratory results.

When using an ice sheet for supporting loads one question of obvious interest is what is the maximum load or the "breakthrough" load. Also the time at which this breakthrough occurs is of interest. Simple proven methods have not been developed to tell us the breakthrough load and when it will occur. It is a viscoelastic problem.

Field and laboratory observations indicate that indeed an ice sheet continues to carry a load after the first crack occurs. To solve analytically any plate problem requires limiting the problem, choosing an idealized model and formulating the proper equations from mechanics (statics and dynamics). Having formulated the problem, exact or approximate solutions are sought that agree with field and laboratory observations. However, if we limit the plate problem, for ease of analysis and conservatism, to an uncracked plate we then have a different problem after the first crack appears. More complex and different problem formulations are then necessary. We will however use the "first crack" analysis to determine our safe loads for construction on the ice.

If we place a uniform load on a circular area and increase the load, the ice will crack. There will be one or more radial cracks that extend out from the load. If we continue to add load a circumferential crack will form somewhat concentrically around the load but at a distance out from the load at the ends of the radial cracks. This forms wedges which usually number from four to eight or more. When this circumferential crack forms breakthrough can be expected shortly thereafter. On thick ice, even more load may be added due to side interaction between the wedges. However this possible support cannot be counted upon. In fact, it is reasonable to assume that when radial cracking begins the ice is sustaining a load that is no longer a safe load.

Nevel (1976) has formulated a mathematical creep model for ice which includes primary, secondary and tertiary creep. His equations show that at the load, the deflection increases with time while the stresses decrease, or relax. This means that the maximum tensile stress (which is usually the critical stress in an ice plate bearing problem) occurs at the moment the plate is loaded. A usual failure criterion is to limit the maximum tensile stress. Using this criterion means the sheet should fail at once or not at all as the stresses relax with increasing deflection. This however is contrary to observations on ice sheets under sustained loads. A possible explanation is that the tensile strength is somehow affected by the creep process.

Frankenstein (1966) describes the results of a number of large scale breakthrough field tests, for both concentrated loads and distributed loads placed on an Arctic lake cover. In the distributed load tests a

15-ft (4.6-m) diameter aluminum tank, with a height adjustable to 20 ft (6.1 m), was placed directly on the ice surface. Lake water was pumped into the tank at a more or less constant rate to load the ice. The concentrated load tests were conducted in the same manner as the distributed tests except that the tank was placed on a platform balanced on a 24 inch (61 cm) diameter wooden block.

For distributed load tests the first circumferential crack did not produce breakthrough. Additional cracking of the wedges occurred parallel to the first circumferential but closer to the load. Some side wedge interaction probably occurred before final breakthrough on the closer circumferential cracks, numbering one or two in addition to the first crack connecting the far ends of the radials.

The crack phenomenon for the concentrated tests differed greatly from that of the distributed tests. The distributed tests always yielded a circumferential crack but in some of the concentrated tests, no circumferential cracks were visible either during loading or after failure. The failure hole diameter for the concentrated tests was very close to the diameter of the bearing block.

Tables 10 and 11 present some of Frankenstein's load test data. Temperatures taken in the ice ranged between 30°F and 15°F (-1°C and -9 °C). The load contact pressures were computed on a nominal 15-ft (4.6-m) tank diameter and a 2-ft (0.6-m) block diameter. The punching shears for the concentrated load tests data were computed using the nominal block diameter, the ice thickness, and the collapse load.

Ice Thickness inches (cm)	Maximum Loads pounds (kN)	Time of Failure minutes	Maximum Deflection feet (m)	Ratio of Max. Load and Square of Ice Thickness lbs/in ² (N/cm ²)	Load Contact Pressure lbs/sf (kN/m ²)	Pressure per Ice Thickness lbs/sf/in (kN/m ² /cm)
6.3 (16.0)	23955 (107)	11.7	1.06 (0.32)	604 (416)	136 (6.5)	22 (0.41)
8.2 (20.8)	28550 (127)	12.2	0.77 (0.23)	424 (292)	162 (7.8)	20 (0.38)
9.5 (24.1)	36980 (164)	14.6	0.87 (0.27)	410 (283)	209 (10.0)	22 (0.41)
12.8 (32.5)	44330 (197)	30.5	1.56 (0.48)	271 (187)	251 (12.0)	20 (0.38)
12.4 (31.5)	48303 (215)	21.6	0.98 (0.30)	314 (216)	273 (13.1)	22 (0.41)
15.6 (39.6)	77945 (347)	30.9	1.26 (0.38)	320 (221)	441 (21.1)	28 (0.53)

Table 10
Distributed Load Test Data
(Frankenstein 1966)

Ice Thickness inches (cm)	Maximum Load pounds (kN)	Time of Failure minutes	Maximum Deflection feet (m)	Ratio of Max. Load and Square of Ice Thickness lbs/in ² (N/cm ²)	Load Contact Pressure lbs/sf (kN/m ²)	Punching shear lbs/in ² (kN/m ²)
11.4 (29.0)	30,968 (138)	9.1	0.76 (0.23)	238 (164)	9,860 (472)	36 (248)
11.0 (27.9)	28,970 (129)	8.6	0.45 (0.14)	240 (165)	9,220 (441)	35 (241)
13.5 (34.3)	34,810 (155)	9.7	0.65 (0.20)	191 (132)	11,080 (531)	34 (234)
15.4 (39.1)	51,339 (228)	16.8	0.71 (0.22)	216 (149)	16,340 (782)	44 (303)
17.8 (45.2)	61,603 (274)	21.2	0.76 (0.23)	194 (134)	19,610 (939)	46 (317)

Table 11
Concentrated Load Test Data
(Frankenstein 1966)

Frankenstein's distributed load tests indicate a fairly narrow range of collapse load contact pressures per unit thickness of ice, i.e. 20 to 28 lbs/sf/in thickness (0.38 to 0.53 kN/m²/cm thickness). The concentrated load tests also give a narrow range for punching shear, i.e. 34 to 46 lbs/sq in (236 to 317 kN/m²). The ratios of collapse loads to the squares of the ice thicknesses varied in the range of 320 to 604 lbs/in² (221 to 416 N/cm²) for distributed loads and 191 to 240 lbs/in² (132 to 165 N/cm²) for concentrated loads.

In the next section we will consider safe loadings for ice sheets that could be developed during wintertime construction of a small craft harbor. Quick intense loads causing breakthrough and long term viscoelastic loadings are not dealt with here. (Refer to Kerr, 1976 and Nevel, 1976.)

Safe Loads on Ice Sheets

Nevel (1977) has developed a pocket calculator program to predict safe loads based upon an elastic first crack analysis. His analysis and the program are included in Appendix III. Circular and rectangular loads or combinations of loads can be handled.

For our purposes we have solved his general equations for the simple case of one concentrated load. The computed maximum "safe load" can be used for estimating single construction loads on ice sheets; provided the ice is sound and free of discontinuities. The load cannot be placed near free edges of the sheet or in the vicinity of walls or shores where cracks behave as a free edge condition. To be out of the direct influence of these edge conditions the load should be away a distance equal to two or more flexural rigidity lengths. The expression for the maximum safe load P with Poisson's Ratio assumed to be 1/3 is:

$$P = 1.396 \sigma h^2 \frac{(a/l)}{kei'(a/l)}$$

where σ is the allowable stress

h is the ice thickness

a is the radius of the load distribution

l is the flexural rigidity length

kei' is the first derivative of the Kelvin function kei

The expression for the maximum deflection w which will occur directly under the load is

$$w = \frac{(P) [(a/l)ker'(a/l) + l]}{(a/l)^2 k l^2 \pi}$$

where ker' is the first derivative of the Kelvin function ker

k is the weight density of water

Kelvin functions and their derivatives are tabulated in mathematical handbooks. They are difficult to work with for small values of argument (a/l) due to the sensitivity of the functions' values with changes in (a/l). Included in Appendix IV are tables of Kelvin functions and derivatives from Nevel (1959) for arguments ranging between 0.000 and 0.500. Also the appended pocket calculator program has a Kelvin function subroutine that can be used for these or other arguments.

For small values of (a/l) the following approximation for the maximum deflection w is useful.

$$w = \frac{P}{8kl^2}$$

Figure 5 is a plot of the maximum safe load for ice with a flexural strength σ of 100 psi (689 kN/m²) and a modulus of elasticity E of 750 ksi (5168 MN/m²). The maximum safe load is linearly proportional to the flexural strength. For this type of ice loading problem, design flexural strengths would range between 50 and 100 psi (345 and 689 kN/m²) for fair to good ice. Loadings beyond this stress level are not recommended for usual construction procedures. Of course care is necessary in placing loads on any thin ice or placing very large loads regardless of the ice thickness or the analysis. Figure 5 simply gives recommended maximum values that should not be exceeded and that should be used with caution.

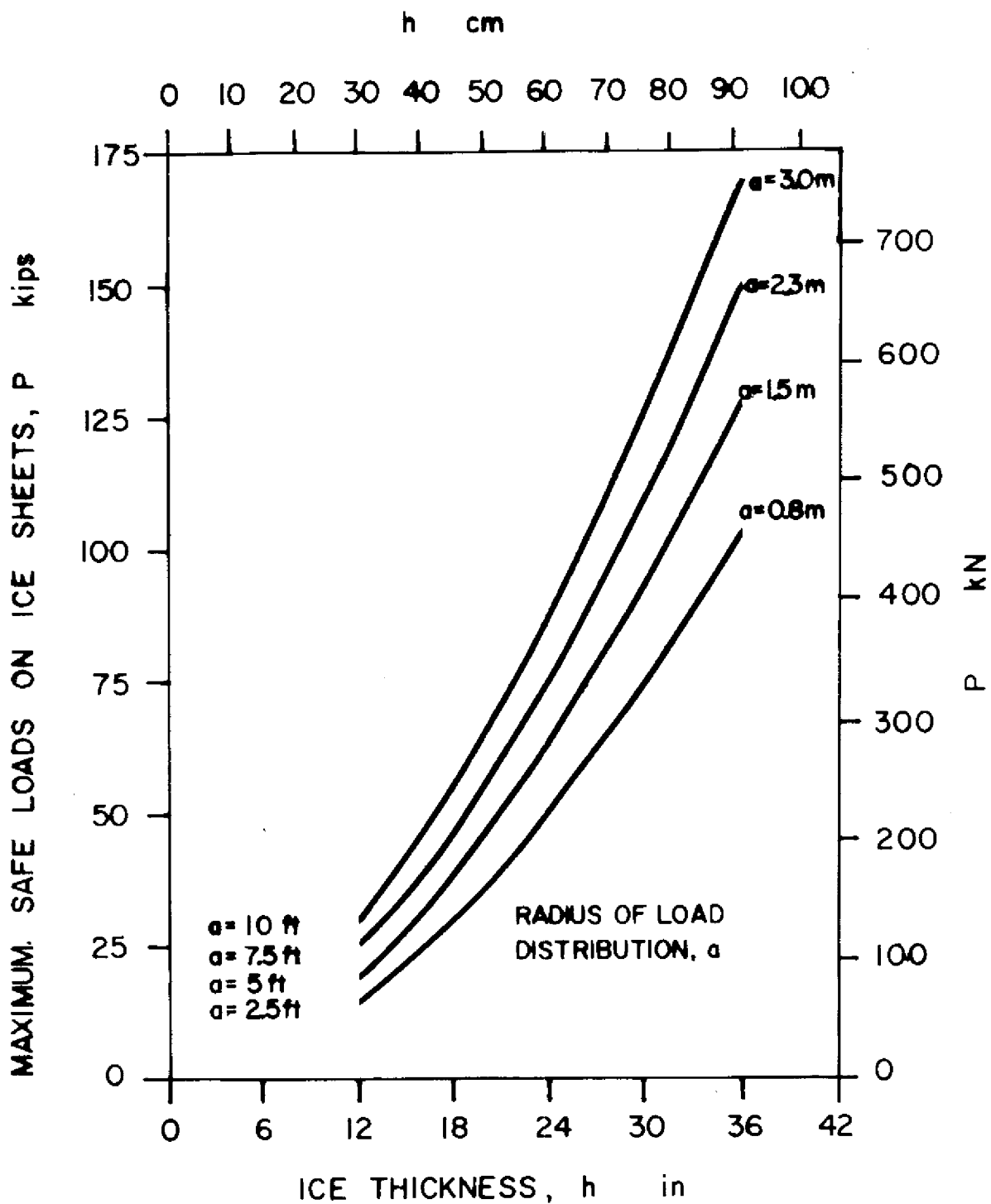


Figure 5. MAXIMUM SAFE LOADS ON ICE SHEETS (after Nevel, 1977)

To illustrate the use of Figure 5 and the equations let us assume we want to place a 20 kip (89 kN) load on a 5 ft by 8 ft (1.5 m by 2.4 m) area. We have 15 inches (38 cm) of sound ice. Through area ratios we will convert the rectangular area to an equivalent circular area.

$$a = \left[\frac{5 \text{ ft} \times 8 \text{ ft}}{\pi} \right]^{\frac{1}{2}} = 3.6 \text{ ft (1.1 m)}$$

From Figure 5 at 15 inches (38 cm) and 3.6 feet (1.1 m) we find the maximum safe load to be 23 kips (102 kN) which is greater than the specified 20 kips (89 kN).

If we have weaker ice, because of warm temperatures or previous damage from construction we would want to reduce the load. The flexural strength may be only 50 psi (345 kN/m²) and for this case the safe load would be halved. In this example we should also consider the contact pressure and the deflection.

$$\text{contact pressure} = \frac{20,000 \text{ lbs}}{5 \text{ ft} \times 8 \text{ ft}} = 500 \text{ psf (23.9 kN/m}^2\text{)}$$

This pressure is high for this relatively small loading area and it would be well to use a larger area for the 20 kip (89 kN) load. But assuming the given loading condition we can compute the deflection of the ice sheet from the formula

$$w = \frac{(P) \left[\frac{(a/l) \ker' (a/l) + 1}{(a/l)^2 k l^2 \pi} \right]}{(a/l)^2 k l^2 \pi}$$

$$\text{where } a/l = 3.6/27.0 = 0.1333 \\ \text{(1 interpolated from Table 9)}$$

$$k = 62.4 \text{ lbs/ft}^3 \text{ (1000 kg/m}^3\text{)}$$

$$w = \frac{(20,000 \text{ lbs}) \left[(0.1333) (-7.4501) + 1 \right]}{(0.1333)^2 (62.4 \text{ lbs ft}^{-3}) (27.0^2 \text{ ft}^2) \pi} \\ = .054 \text{ ft or 0.65 in (1.6 cm)}$$

$$\text{or } w = \frac{P}{8kl^2} = \frac{(20,000 \text{ lbs})}{(8) (62.4 \text{ lbs ft}^3) (27.0^2 \text{ ft}^2)} = 0.55 \text{ ft (1.7 cm) approx.}$$

One criterion for allowable deflection is that the deflection be less than 0.08 times the ice thickness, i.e. the ice sheet will not be submerged. For our 15 inch (38 cm) sheet the allowable deflection criterion is equal to 1.2 inches (3 cm).

If the freeboard of the ice is exceeded water can flood the surface through cracks and other openings. This warms the ice and weakens it and also adds further loads. Loadings on ice less than 18 inches (46 cm) in thickness should be checked for possible submergence. Ice thicker than this will not submerge under the recommended maximum loads.

Figure 5 should be of assistance in estimating construction loads on small craft harbor ice covers. Special precautions are necessary however if moving loads across frozen bodies of water is planned. Moving loads create dynamic effects in the ice cover and water. Unfortunately the natural critical velocity is easily achieved on many lakes. At this velocity, the deflections and stresses are amplified. It is necessary to go at a slow speed or very fast. The technical literature should be reviewed by those planning moving loads across frozen lakes.

Thickening and Strengthening Ice Covers

In using ice for bearing capacity, actual thicknesses should be measured. Dates when a natural ice sheet will be thick enough to support a specified load are of interest and can be estimated from past observations and rules of thumb. One rule is that the thickness is directly proportional to the square root of the Freezing Index (previously defined in Part I). Using α as a proportionality factor we can write the following rule of thumb expression:

$$h = \alpha \sqrt{FI}$$

where h is ice thickness in inches

FI is Freezing Index, Fahrenheit

α is a locality factor ranging between 0.5 for snow covered lakes and 1.0 for lakes without snow.

Assume we have had 45 days of weather where it has generally been below freezing. The Freezing Index would be calculated by summing algebraically the plus and minus departures of the daily mean temperatures from the freezing temperature. The Freezing Index in our example will be assumed to be 750 Fahrenheit degree-days and our locality factor equal to 0.8.

$$\begin{aligned} h &= 0.8 \sqrt{750} \\ &= 22 \text{ inches (56 cm)} \end{aligned}$$

The locality factor α can be historically established by several years' measurements of ambient temperatures and ice thicknesses. It can be used for estimating when sufficient thicknesses of ice might naturally become available. Ice can also be intentionally thickened and strengthened to aid nature.

Hoffman (1967) describes surface flooding techniques for improving natural ice areas. These techniques have been developed by the U.S. Naval Civil Engineering Laboratory. Among their recommendations are the following items.

The maximum mean daily temperature at which ice flooding can be performed satisfactorily is considered to be about $+15^{\circ}\text{F}$ (-9°C). At temperatures much above this point, freezing rates are slow and long periods are required between applications.

The depth of water applied to any point should not be greater than that which will freeze through in 24 hours. At temperatures from 0°F to -10°F (-18°C to -23°C) with little wind, this is about 4 inches (10 cm) of water.

A cooling period equal to the freezing period should be allowed before an ice area is reflooded. Such cooling is necessary for restoration of ice temperature and recovery of ice strength and resistance to creep.

Additional water should not be applied until all areas of the previous flood have frozen solid. The premature reflooding of an unfrozen area is very undesirable since the freezing time increases exponentially with depth.

Air bubbles which form in the flooded ice surface should be broken before reflooding.

Duff (1958) describes in general terms the thinking of logging operators on the strengthening of ice sheets. Ice landings are constructed and maintained by flooding on top of existing ice and rolling any snow that falls.

Where snow is lying on an ice sheet it is, if at all possible, compacted by rolling before flooding. Slush always seems to form after a snowfall. The weight of the snow cover depresses the ice sheet and free water comes up through cracks or the insulating blanket of snow allows a current, probably a thermal in lakes, to weaken the ice sheet from below. Rolling immediately after a snowfall, or during a storm if it is a severe one, improves frost penetration and lessens the slush problem.

Rose and Silversides (1958) describe the merits of surface flooding for increasing the speed at which ice thickens. Starting with a layer of ice 12 inches (30 cm) thick and -20°F (-29°C) weather, if 5 inches (13 cm) of water are added on the surface it will take approximately 15 hours for it to freeze and give a total thickness of 17 inches (43 cm) of ice. If the ice surface is bared and ice is to be formed on the under-surface of the 12 inch (30 cm) ice sheet, it will take 60 hours to add an additional 5 inches (13 cm). This is 4 times as long.

Ohstrom and Denhartog (1976) have reported on a series of cantilever beam tests designed to determine the efficacy of adding reinforcement to an ice cover. Tests were run using 1 inch (2.5 cm) diameter tree branches, 3/16 inch (5 mm) diameter wire rope and 9/16 inch (14 mm) half-round wood dowels as reinforcement. A definite advantage was noted from using reinforcement, even when poorly placed. The reinforced ice carries a load

even after it cracks. Thus, after the initial cracks there is time to remove people and equipment before final breakthrough. Disadvantages to the reinforcement are that the darker types absorb radiation and thereby cause weakening of the ice cover. Also, in many cases, the time and effort required to place reinforcement may exceed those required to achieve equal strength by additional thickening of the ice sheet.

The reinforcing process consists of laying reinforcement material on the ice, then flooding the area and allowing the reinforcement to freeze into the ice. For optimum strength, the reinforcement should be added to the side of the ice that carries the tensile forces. Initial cracking of the ice sheet is caused by tensile stresses near the bottom surface of the ice, but final breakthrough is caused by tensile stresses near the top surface.

PART V

VERTICAL ICE FORCES AND OTHER FORCES

One of the most significant and damaging ice forces results from changes in water levels. These changes cause the ice sheet to move up and down tearing and pulling structures built in small craft harbors.

In Part IV we considered the capacity of an ice sheet to support construction loads. Necessarily we used a conservative value for the strength of the ice. In estimating the uplift forces from ice we will assume stronger ice as it will probably exist sometime during the winter. Computing uplift loads is complicated because we do not know which of several failure criteria best represents the uplift force. We have selected a "first crack" analysis to predict the minimum uplift for which we should design. The maximum uplift force for design still remains a matter of engineering judgment and site circumstances.

This part begins with a discussion of lake level changes. Ranges of uplift loads are then presented together with some ways to attenuate these loads. The section concludes with some comments on buckling of ice sheets and other loads.

Water Level Fluctuations

Water levels, and hence ice levels, in the Great Lakes vary seasonally. The small craft harbor designer must anticipate and estimate these seasonal variations when planning fixed harbor structures, such as docks and piers, launching ramps and bulkheads. To a lesser extent, water level variations affect floating structures. They are of concern, however, e.g. in connection with anchorage and gangways.

To illustrate the importance of water levels on design, consider a fixed height dock specified to be a desired freeboard above normal summer water levels. Should levels prove otherwise, due to larger natural variations or inaccurate estimates, such a dock can end up well above the water or too close to the water. It becomes barely usable by the intended boats. Also, during wind storms over water, severe water level changes can occur. At Buffalo, New York the lake has risen to as much as 8 feet (2.4 m) above the normal water level.

Problems can result with winter ice levels also. Individual pilings supporting a fixed dock may be protected (deiced) with a compressed air bubbler system. Normally the number of pilings would be kept to a minimum to reduce the amount of air required. By doing this, dock members tend to have greater depths because of their longer spans. Should the ice become higher than estimated, the lower elements of the dock members (which are not deiced) may come in contact with the ice sheet or be shoved by broken ice pieces that are frequently found on top of an ice cover.

Local experience can aid the designer in estimating water and ice levels. If severe water level changes can be anticipated, a floating or adjustable height design would be called for. The following publications will also help the designer.

Monthly Bulletin of Lake Levels for the Great Lakes, Department of the Army, Detroit District, Corps of Engineers, P. O. Box 1027, Detroit, Michigan 48231. (Bulletin lists maximum, minimum, and expected levels.)

Hydrograph of Monthly Mean Levels of the Great Lakes, U. S. Department of Commerce, NOAA, National Ocean Survey, C3314, 6001 Executive Boulevard, Rockville, Maryland 20852. (Lists monthly mean lake levels from 1860 to date.)

In addition to seasonal lake level variations, there is an unusual water level phenomenon known as a seiche (pronounced sash). It is a standing wave oscillation of an enclosed or semi-enclosed water body that continues, pendulum fashion, after the cessation of the originating force. It is a short-term rise and fall of the water level and is caused by either persistent, strong winds piling up the water at one end of a basin, or changes in barometric pressure over the lake, and sometimes a combination of both. Although seiches are unnoticeable on small lakes, they are quite noticeable on the Great Lakes and in bays and harbors. The period of a seiche is a few minutes in a bay or harbor and about ten hours for a Great Lake.

Hodek and Doud (1975) measured an almost constant fluctuation of the winter water level in the Ontonagon, Michigan harbor. The amplitude had an observed maximum of 0.8 feet (0.24 m). The major period varied from 5 minutes to more than 10 hours. Higher frequency water oscillations also were observed and a change in the water level of 3 inches (8 cm) in 10 minutes was observed.

Seiches are easily observed in a marina in the summertime by noting a drop in the water surface with respect to some fixed object like a sloping launching ramp or a piling. In fact, severe seiches have been observed where the water level fluctuated three feet (1 m) and more in a few hours.

As a result of seiche action, an ice plate in a harbor moves up and down exerting large forces on structures penetrating the ice sheet. In the next section we will estimate the minimum level of these forces.

Minimum Ice Sheet Uplift Loads

In a manner similar to that used in computing safe loads on ice sheets, we can estimate minimum uplift loads to be expected. The analysis is an elastic one and is compatible with the rapidity with which water levels change under seiche action. The analysis is also a thin plate analysis which is not strictly correct for ice sheets thicker than the embedded pile diameter. For this case the stresses computed are too high in the vicinity of the load. However this is acceptable because it is conservative.

We will assume a round pile frozen into (rather than setting upon) an ice plate and determine the force when the plate first cracks. This will be the minimum force we can expect when a pile or structure is frozen into the ice.

The differential equation formulating this problem has been solved. We have evaluated the solution for the following boundary conditions. At a distance from the center of the concentrated load equal to the radius of the load (distance a), the slope of the deflected ice plate is zero; and at distance a the total load is carried by the stress on the failure surface which is the thickness of the ice plate times $2\pi a$. The crack that forms at failure is a circumferential crack located a distance a out from the center of the load. This crack is consistent with what is seen in the field when an ice sheet pulls upward on a strong well-embedded piling and eventually cracks. The distance a is not the radius of the piling, but is larger. This is due to the failure occurring by cracking in the ice rather than slippage at the ice-pile interface, and because immediately adjacent to the pile the ice is thicker than the rest of the sheet. (An ice collar forms in this area.) This thickening phenomenon results from heat transfer through metal piling (and to some extent through wood piling) increasing the ice thickness in this area. Also as the winter goes on and the crack has formed and refrozen many times, the piling experiences a kind of dipping action in the cold water, (somewhat like dipping a candle wick in wax to form a candle).

The equation for the minimum ice sheet uplift load, based upon this first circumferential crack is as follows:

$$P = \frac{(1/3) \pi \sigma h^2 (a/l)}{\left[\frac{\text{kei}(a/l) \text{kei}'(a/l) + \text{ker}(a/l) \text{ker}'(a/l)}{\text{kei}'(a/l) \text{kei}'(a/l) + \text{ker}'(a/l) \text{ker}'(a/l)} \right]}$$

where σ is the allowable stress

h is the ice thickness

a is the radius of the load distribution

l is the flexural rigidity length

kei and ker are Kelvin functions

kei' and ker' are first derivatives

Figure 6 is a plot of the minimum ice sheet uplift load for ice with a flexural strength σ of 200 psi (1378 kN/m²) and a modulus of elasticity E of 750 ksi (5168 MN/m²). The minimum uplift load is linearly proportioned to the flexural strength, which could be greater than the assumed value of 200 psi (1378 kN/m²). Also, as we will show later, making different assumptions for the failure criterion will result in larger loads.

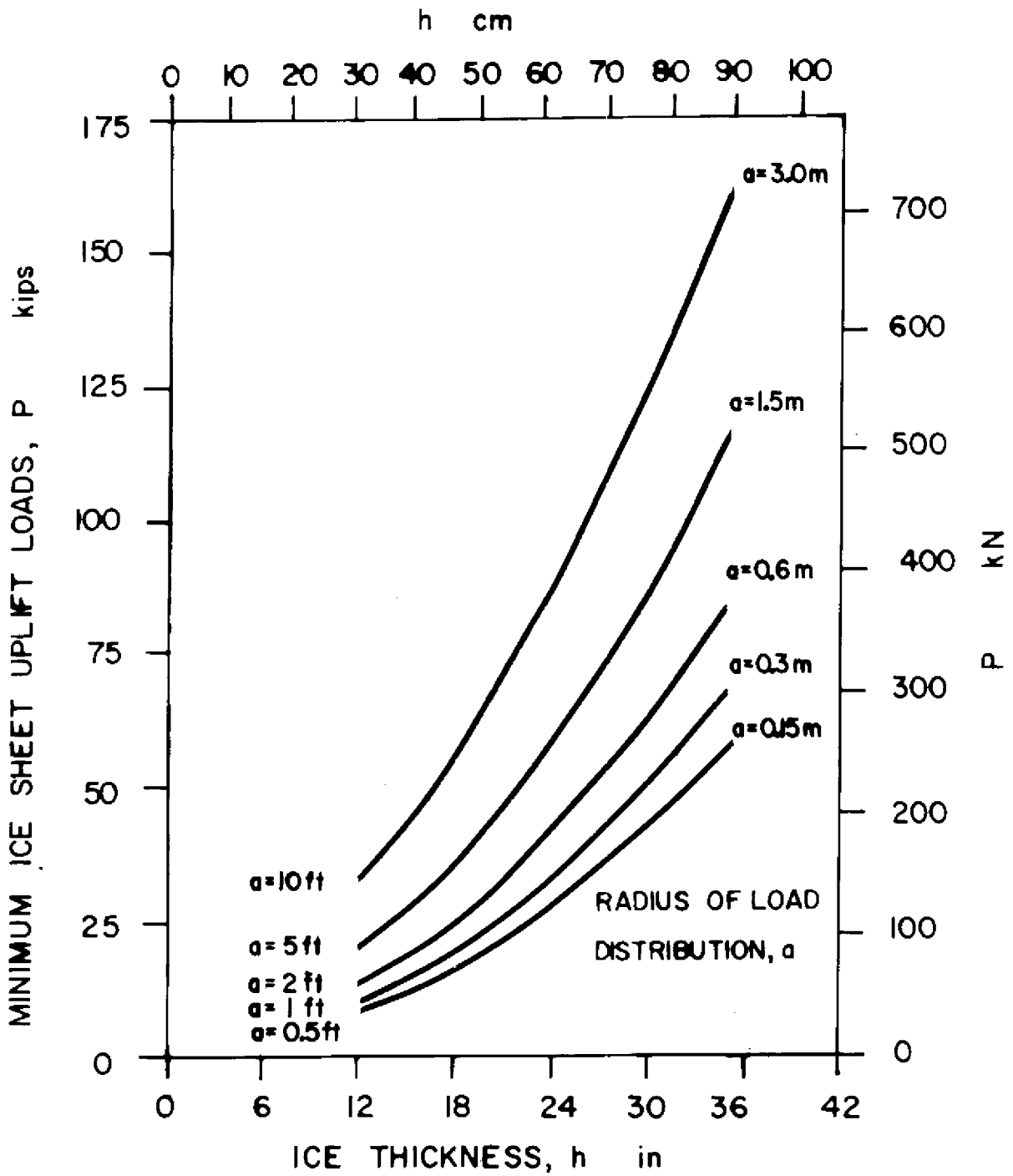


Figure 6. MINIMUM ICE SHEET UPLIFT LOADS

To illustrate the use of Figure 6, let us compute the minimum uplift for a 12 inch (30 cm) round steel pile in 24 inches (61 cm) of ice. As stated above the radius a will be greater than one half pile diameter. For the usual steel pile shapes, the radius of the ice collar will be about six inches (15 cm) greater than the pile radius. (For wood, a value of about half this much has been observed.) From Figure 6 at $h = 24$ inches (61 cm) and $a = 1$ foot (0.3 m), we find the minimum uplift load is 33 kips (147 kN). This estimated load is the least that we should design for with a 12 inch (30 cm) pile in 24 inches (61 cm) of sound cold ice (σ assumed = 200 psi, 1378 kN/m²). We do not know precisely what the maximum load could be, but it could be several times as much. The ice does not fail on the ice-pile interface, but fails in the strength of the ice sheet itself.

The uplift on a square construction could be reasonably approximated by an inscribed circle of radius a equal to $\frac{1}{2}$ of the length of the side. This would be conservative since the angles of a square would tend to cause stress-concentrations in the ice.

Nevel (1972) has formulated a more severe failure criterion for the ice pile uplift problem. It is a criterion which gives a near, if not the maximum, upper bound to the problem. It is assumed that radial cracks form and then a circumferential crack forms connecting the ends of the radials. This cracking pattern forms a series of truncated wedges whose tips are supporting the load and whose bases are failure planes when the circumferential crack develops. If we neglect any side interaction between the wedges, and assume that six wedges have formed the Nevel (1972) solution for the maximum load becomes:

$$P = 1.154 \sigma h^2 \left[1.05 + 2.00 (a/l) + 0.50 (a/l)^3 \right]$$

where the bracketed term is an approximation to an exact solution.

For our example we can compute the maximum load P as follows:

$$a = 1.0 \text{ feet (30 cm)}$$

$$I = 33.8 \text{ ft (10.3 m) at } E = 750 \text{ ksi (5168 kN/m}^2)$$

$$a/l = .0296$$

$$[] = 1.109$$

$$P = (1.154) (200 \text{ lbs in}^{-2}) (24^2 \text{ in}^2) (1.109)$$

$$P = 147,400 \text{ lbs or 147 kips (654 kN)}$$

This truncated wedges load estimate is $4\frac{1}{2}$ times the estimate based upon the first crack analysis. For smaller values of a the loads are 6 times as great and for larger values of a , 3 times as great.

The proper values to use for design are matters of engineering judgment and experience. The values should lie within the ranges presented and an uplift of not less than the minimums indicated on Figure 6 should be used for design with appropriate safety factors. If for example a minimum load is estimated to be 25 kips (111 kN), then the ultimate resistance of the soil foundation system preventing uplift, or the dead weight of the structure, should be greater than 25 kips (111 kN) by perhaps a factor of 2 or 3. In selecting a design criteria for a particular small craft harbor, other factors will enter in; such as whether some damage will be tolerable, the ease with which pullout resistance can be developed, or the location of the pile and its relationships with other piles or dock members.

Ice can also exert down-drag loads when the water level drops and leaves the ice hanging on the dock piles. The ice can easily span across between piles and develop the full dead weight of the ice sheet. Large drops in levels have occurred and it is believed that the ice sheet is capable of losing all its buoyancy. The down load situation is aggravated by a tendency to have thicker ice under shady dock areas than in the more exposed aisle or fairway areas.

There is limited field data on forces on full size piles but several direct observations have been made. Hodek and Doud (1975) and Hodek (1976) have measured vertical loads of 18 kips (80 kN) compression and $11\frac{1}{2}$ kips (51 kN) tension or uplift on a 15 inch (38 cm) instrumented sleeve placed around a dock pile. The thickness of the ice was about 16 inches (41 cm). The loads were those actually felt by force transducers on the instrumented pile sleeve.

Muschell (1976) jacked against an ice cover to pull frozen-in piles. Loads up to 25 kips (111 kN) were recorded. The loading rate was 0.5 psi per second ($3.4 \text{ kN/m}^2/\text{s}$). Ice adhesion to steel was computed by dividing the pullout load by the actual ice thickness and area of ice contact to steel on HP 8 x 36 and HP 10 x 42 piles. The ice adhesion values ranged between 12 and 24 psi (83 and 165 kN/m^2).

In January 1977, Muschell (unpublished) recorded a value of 68 psi (469 kN/m^2) for ice adhesion to an 8-inch (20-cm) pipe pile in a comparable field test.

The lifting force per unit of length of circumference of a structure frozen into an ice sheet becomes less as the size of the structure increases. The lifting force per unit of length will approach the values for long straight walls. Lofquist (1951) and Michel (1970) have estimated the vertical forces exerted by ice rigidly attached to walls. The estimates are based upon an elastic analysis and rapid rises in water levels.

$$p = \frac{\sqrt{2} \sigma h^2}{6 l}$$

$$\Delta = \frac{p}{\sqrt{2} k l}$$

where p is the lifting force per unit length

Δ is the rise in water level

Assume we have 24 inches (61 cm) of ice with a strength of 200 psi (1378 kN/m²) and a modulus $E = 750$ ksi (5168 MN/m²). The uplift force per unit length and the water level rise are computed as follows:

$$p = \frac{(\sqrt{2}) (200 \text{ lb in}^{-2}) (24^2 \text{ in}^2)}{(6) (33.8 \text{ ft})}$$

$$= 803 \text{ lbs/ft (11.7 kN/m)}$$

$$\Delta = \frac{(803 \text{ lbs ft}^{-1})}{(\sqrt{2}) (62.4 \text{ lbs ft}^{-3}) (33.8 \text{ ft})}$$

$$= .27 \text{ ft or } 3\frac{1}{4} \text{ inches (8}\frac{1}{4} \text{ cm)}$$

Assuming a different strength value for the ice will change the uplift load in a linear manner. However the loads computed at σ equal 200 psi (1378 kN/m²) are believed to be adequate since the method of analysis is conservative. There normally is cracking parallel to a wall or long crib structure and this reduces the uplift from that assumed for rigid attachment. Walls and long cribs seem to experience little damage due to ice uplift. Occasionally, however, the top of a crib will be pulled off because it is inadequately secured to the rest of the crib.

The next section presents some suggestions for reducing and eliminating uplift forces.

Reducing Ice Sheet Uplift Loads

In Part III we discussed ways to suppress ice and reduce its thickness. This is the most positive way at this time to reduce ice uplift on small craft harbor structures. A number of other techniques have been tried and are being tested now. The projections are optimistic that reliable and economical ways will be developed to reduce ice uplift forces.

Ice adheres tenaciously to most construction materials. There is no comprehensive treatise on ice adhesion; only technical and research papers.

Representative adhesion values for ice to various materials and coatings determined by Freiburger and Lacks (1961) are presented in Table 12. The results are based on experiments for artificial ice loaded at the rate of 5 psi/s (34 kN/m²/s), and depend strongly on the rate.

	<u>Ice Adhesion Range of Values</u>	
	<u>psi</u>	<u>kN/m²</u>
Metals	85-120	586-827
Woods	45-80	310-551
Plastics	25-40	172-276
Glass	20-150	138-1034
Paints	80-100	551-689
Resin Films	30-130	207-896

Table 12 Ice Adhesion
(after Freiburger and Lacks, 1961)

Jellinek (1957) performed shear experiments with snow-ice sandwiched between two stainless steel plates. The results of his work on small samples indicated the adhesive strength to be independent of thickness of the ice layer and cross-sectional area. He found the adhesive strength to be a linear function of the temperature until it becomes larger than the cohesive strength of ice at about 9°F (-13°C), where a very sharp transition from adhesive to cohesive breaks takes place. Representative values are as follows: 28°F (-2°C)--30.4 psi (209 kN/m²), 7°F (-14°C)--236 psi (1626 kN/m²), and -4°F (-20°C)--233 psi (1605 kN/m²).

Michel (1970) has observed that there is very little available data on strength of adhesion of ice to structures and, there is a lot of scatter in the experimental results because of insufficient control of the uniformity of the structure of the ice and other relevant factors. Michel notes that

in most cases the strength of adhesion of ice to construction materials is as high as the shear strength of the river or lake ice itself, which is usually taken to be from 80 to 150 psi (551 to 1034 kN/m²).

And as previously stated, Muschell (1976 and unpublished) found values ranging up to 68 psi (469 kN/m²).

For our purposes we can say that slippage between ice and the piling material will probably not naturally occur at loads less than the calculated minimums. Therefore in order to reduce uplift effects we must cause the ice to slip at loads less than these minimums.

Field and laboratory experiments have shown that wrapping a pile with various smooth materials doesn't work very well because the materials become unattached after a number of cycles of uplift. Materials that have been tried include tetrafluorethylene polymer wrap (teflon-like) and thin polyethylene sheets. Both materials were torn loose and worked their way up and out of the ice. A three ply wrap with polyethylene sheets was unsuccessful too. The three ply system was tested to see whether the outer layers of polyethylene, which would be assumed stuck to the ice and to the pile, would slide on the inner sheet sandwiched between the two. All layers worked their way out of the ice.

Laboratory studies and field tests are in progress now (1977) to evaluate protective jackets and coatings that could be installed or applied on existing piles or specified for new piles. US CRREL is undertaking this work and reports on their results are expected in 1978. One system of jacketing uses existing fiberglass products and methods for repairing damaged underwater piling. Preliminary laboratory test results show about a 4 fold reduction in the maximum force recorded on a test pile frozen into an ice sheet and displaced up and down in a simulated cyclic seiche action. Work is also underway to evaluate navigation lock wall epoxy and co-polymer coating systems described by Frankenstein et al (1976). Large reductions in adhesion values have been demonstrated but work on coating life and methods of application are needed.

Ice uplift loads can be reduced by causing the ice to crack so that large loads are not transmitted to structures. Group action is frequently effective in accomplishing this cracking. For example, several piles lashed together to act as a single dolphin, are effective in resisting uplift. A series of piles spaced 5 feet (1.5 m) on centers under a pier supporting a boat hoist machine have resisted uplift because of the group action. Also a T-head pier with pairs of pilings spaced about 25 feet (8 m) on centers has been found to act as a unit. A crack forms following the outline of the pier and completely encircling it. This crack demonstrates the group action of the entire piling system.

The piles toward the center of a marina and the piles at the ends of finger piers are more prone to pulling than those closer to shore. This is apparently due to the plate action and boundary conditions on the plate subjected to hydrostatic uplift. The ice sheet may also be frozen fast to the shoreline. This phenomenon suggests designing the outer piles for large

uplift forces and thereby cause the ice to fail about them. If this happens the piles closer in should feel little if any uplift force.

Another system that has been successfully used to eliminate uplift forces on marina pilings is the sleeved pile system (U.S. Patent No. 3,543,523). It allows vertical motion of a pile. It consists of a round hollow steel pile driven (with a follower) so that the top of the pile is 2 feet (0.6 m) below the bottom surface of the ice. A slightly larger diameter hollow round steel pile piece (the sleeve) fits over the top of the driven pile. The driven pile has a cap plate, and welded inside the sleeve about 4 ft (1.2 m) from its lower end is a round bearing plate. When the sleeve is dropped over the pile, the round plate bears on the cap plate. On top of the sleeve is another cap plate for bearing of dock beams. As ice freezes to the sleeve, the sleeve moves up and down over the lower, stationary pile (analogous to a stationary piston in a moving cylinder). The sleeve works well, allowing vertical motion. However horizontal ice forces may still be acting on the piles. Also dockage systems using sleeved piles are more complicated and costly to build because differential vertical motions must be provided for in the dock members and supported utilities that may be on the docks.

Other Ice Forces and Actions

In Part II we reviewed thermally induced thrusts, and in this part have considered uplift. Ice exerts other forces. For example, ice is very abrasive and causes damage to structures, particularly wood structures whose life in ice may be only twenty years, Striegl (1952). Cladding wood structures is necessary to achieve longer service lives. Unprotected concrete is subject to abrasion and freeze-thaw spalling.

Sheltered small craft harbors can experience damage from chunks of ice being driven into the harbor and against the docks during Spring breakup, and during periods when ice goes out of a harbor during Winter storms.

In addition to thermally induced horizontal forces, wind and currents can produce dynamic forces. Specific design recommendations are not now available but in general, marina dockage should be located in protected areas away from dynamic ice forces. However, those wishing information on dynamic effects should refer to the Neill (1976) comprehensive review and assessment of dynamic ice forces on piers and piles. Analytical approaches, design formulas, and full-scale and small-scale laboratory investigations are considered.

Ice under horizontal loadings may buckle before it crushes. Sodhi and Hamza (1977), using the finite element method, have performed a buckling analysis of a semi-infinite plate on an elastic foundation. The analysis determines the effective pressure which will cause the plate to buckle. If the crushing strength of ice is greater than this effective pressure, the plate will buckle; if less, a crushing failure will occur before buckling. Nevel (unpublished) has developed a useful expression based upon the Sodhi and Hamza (1977) finite element analysis.

$$P = k l^3 \left[\frac{b}{l} + \frac{3.32}{1.0 + 0.25 \frac{b}{l}} \right]$$

where P is the buckling load

b is the structure width

l is the flexural rigidity length

k is the weight density of water

To illustrate, let us assume we have 6 inches (15 cm) of ice pushing against a wall 100 feet (30 m) long. The flexural rigidity length l, assuming E equal 750 ksi (5168 MN/m²), is 11.9 feet (3.6 m). The ratio b/l is 100 feet/11.9 feet or 8.40.

$$P = (62.4 \text{ lbs ft}^{-3}) (11.9^3 \text{ ft}^3) \left[8.40 + \frac{3.32}{1.0 + 0.25 (8.40)} \right]$$

$$= 996,000 \text{ lbs or } 996 \text{ kips (4430 kN)}$$

We next compute the effective pressure as follows:

$$\text{Effective Pressure} = \frac{P}{b h}$$

$$= \frac{996,000 \text{ lbs}}{(100 \text{ ft}) (0.5 \text{ ft}) (144 \text{ in}^2 \text{ ft}^{-2})}$$

$$= 138 \text{ lbs in}^{-2} (951 \text{ kN/m}^2)$$

If the crushing strength of ice is greater than this pressure, buckling will occur. The maximum crushing strength may be on the order of 300 psi (2067 kN/m²). In general, for small structures the ice crushes before buckling, except in the presence of thick ice where crushing always takes place.

There is little or no experimental data, especially from full scale structures, to assist in the design of piles for horizontal focus. The American Association of State Highway and Transportation Officials (AASHTO) recommends that highway bridges be designed with the following provisions:

All piers and other portions of structures which are subject to the force of flowing water, floating ice, or drift shall be designed to resist the maximum stresses induced thereby.

The pressure of ice on piers shall be calculated at 400 psi (2756 kN/m²). The thickness of ice and height at which it applies shall be determined by investigation at the site of the structure.

The shortcoming of the AASHTO provision for 400 psi (2756 kN/m²) ice pressure is that it is representative of an impact loading for strong ice failing in compression. The effects of pile shape and orientation, e.g. sloping piles where ice would fail in bending, are not considered. The maximum measured effective ice pressure on a bridge pier to date has been less than 200 psi (1378 kN/m²).

In a marina where Spring ice movements occur the effective ice pressure is probably less than 200 psi (1378 kN/m²). Spring ice in a moving field has very low internal strength.

There is a tendency of ice to squeeze objects placed in it. How this happens is not understood and no methods of analyses are known. When a pontoon is placed in water (ice) it will either be squeezed up and finally rest on the ice, or be squeezed down and drawn further into the ice. The result of this action may be damage to the dock framing members connecting the pontoon units together; or sometimes rupturing of the pontoon material itself.

One hypothesis of the squeezing action is that it is the result of re-freezing water. A small amount of ice adjacent to the pontoon melts during the day's warming sun. At night an ice cover forms over the melt water. This encloses the melt water which subsequently freezes in a partially confined space. This refreezing exerts a squeezing force which either ruptures or moves the pontoon.

A field study to investigate the action of pontoon units frozen in lake ice is scheduled for the winter of 1977-1978.



APPENDIX I--LITERATURE CITED

- Ashton, G. D. 1974. "Air Bubbler Systems to Suppress Ice". Special Report 210. Cold Regions Research and Engineering Laboratory, Hanover, New Hampshire.
- Ashton, G. D. 1975. "Experimental Evaluation of Bubbler Induced Heat Transfer Coefficients". Proceedings of Third International Symposium on Ice Problems. International Association of Hydraulic Research, Hanover, New Hampshire. 133-142.
- Ashton, G. D. 1977. "Numerical Simulation of Air Bubbler Systems". Paper presented at the Third Canadian Hydrotechnical Conference. Quebec, P.Q., Canada. May 26-27, 1977.
- Aune, C. A., Beaudin, L. A., and Borrowman, J. K. 1957. "Effects of Ice on Inland Navigation". Section 1, Communication 3, Permanent International Association of Navigation Congresses, XIX Congress, London: pp. 71-94.
- Drouin, M. and Michel, B. 1974. "Pressure of Thermal Origin Exerted by Ice Sheets upon Hydraulic Structures". CRREL Draft Translation 427. Cold Regions Research and Engineering Laboratory, Hanover, New Hampshire.
- Duff, C. H. 1958. "Ice Landings". Conference on the Bearing Strength of Ice, NRC, Ottawa. Transactions of the Engineering Institute of Canada. 2:3:99-100.
- Dumble, J. H. 1858. "Ice Phenomena, from Observations on Rice Lake". Canadian Journal of Industry, Science and Art, New Series, 3:414-422.
- Frankenstein, G. E. 1966. "Strength of Ice Sheets". Proceedings of Ice Pressures Against Structures Conference, Laval University, Quebec, Nov. 1966. Technical Memorandum No. 92, National Research Council, NRC No. 9851, Ottawa, March 1968, 79-87.

- Frankenstein, G. E. et al. 1976. "Ice Removal from the Walls of Navigation Locks". Proceedings of the Symposium on Inland Waters for Navigation, Flood Control & Water Diversions, Colorado State University, Aug. 10-12, 1976. American Society of Civil Engineers, New York.
- Freiberger, A. and Lacks, H. 1961. "Ice-phobic Coatings for Deicing Naval Vessels". Proceedings of the Fifth Naval Sciences Symposium. p. 234-237.
- Glen, J. W. 1974. "The Physics of Ice". Cold Regions Science and Engineering Monograph II-C2a. Cold Regions Research and Engineering Laboratory, Hanover, New Hampshire.
- Glen, J. W. 1975. "The Mechanics of Ice". Cold Regions Science and Engineering Monograph II-C2b. Cold Regions Research and Engineering Laboratory, Hanover, New Hampshire.
- Gold, L. W. 1973. "Ice--A Challenge to the Engineer". Proceedings of Fourth Canadian Congress of Applied Mechanics, Montreal, 1973, pp. G19-G36. National Research Council of Canada, Technical Paper No. 395, NRC 13436.
- Gow, A. J. and Langston, D. 1977. "Growth History of Lake Ice in Relation to its Stratigraphic, Crystalline and Mechanical Structure". CRREL Report 77-1. Cold Regions Research and Engineering Laboratory, Hanover, New Hampshire.
- Hobbs, P. V. 1974. Ice Physics. Clarendon Press, Oxford.
- Hodek, R. J. and Doud, J. O. 1975. "Instrumented Piles for the Measurement of Ice-Uplift Forces". Proceedings of Third International Symposium on Ice Problems, International Association of Hydraulic Research, Hanover, New Hampshire. 409-417.
- Hodek, R. J. 1976. "A Field Study of Ice-Pile Interaction 1975-1976 Season". Unpublished research report submitted to US Cold Regions Research and Engineering Laboratory under Contract No. DACA 89-76-C-0007. December 1976.
- Hoffman, C. R. 1967. "Ice Construction--Method of Surface Flooding". Naval Facilities Engineering Command Technical Report R511. U.S. Naval Engineering Laboratory, Port Hueneme, California.
- Jellinek, H. H. G. 1957. "Adhesive Properties of Ice". Research Report 38. Cold Regions Research and Engineering Laboratory, Hanover, New Hampshire.
- Kerr, A. D. 1976. "The Bearing Capacity of Floating Ice Plates Subjected to Static or Quasi-Static Loads". Journal of Glaciology. 17:76:229-268.

- Korzhasin, K. N. 1971. "Action of Ice on Engineering Structures". CRREL Draft Translation 260. Original 1962. Cold Regions Research and Engineering Laboratory, Hanover, New Hampshire.
- Lavrov, V. V. 1969. "Deformation and Strength of Ice". Main Administration of the Hydrometeorological Service of the Council of Ministers of the USSR, Arctic and Antarctic Scientific Research Institute, Leningrad. Translated from Russian, Israel Program for Scientific Translations, Jerusalem, 1971.
- Lofquist, B. 1951. "Lifting Force and Bearing Capacity of an Ice Sheet". National Research Council of Canada Technical Translation No. 164. Original 1944.
- Mellor, M. 1964. "Properties of Snow". Cold Regions Science and Engineering Monograph III-A1. Cold Regions Research and Engineering Laboratory, Hanover, New Hampshire.
- Metge, M. 1976. "Thermal Cracks in Ice". Doctoral Thesis. Department of Civil Engineering. Queen's University, Kingston, Ontario.
- Michel, B. and Ramseier, R. O. 1969. "Classification of River and Lake Ice Based Upon Its Genesis, Structure and Texture". Report S-15. Departement de Genie Civil, Section Mecanique des Glaces, Universite Laval.
- Michel, B. 1970. "Ice Pressure on Engineering Structures". Cold Regions Science and Engineering Monograph III-B1b. Cold Regions Research and Engineering Laboratory, Hanover, New Hampshire.
- Michel, B. 1971. "Winter Regime of Rivers and Lakes". Cold Regions Science and Engineering Monograph III-B1a. Cold Regions Research and Engineering Laboratory, Hanover, New Hampshire.
- Muschell, J. E. 1976. "Design, Specifications, and Construction of Pilings for Small Craft Harbors". Unpublished paper presented at Docks and Marinas Institute, University of Wisconsin-Extension, Department of Engineering, May 4-5, 1976. James E. Muschell, President, United Marine Associates, 111 North Main, Cheboygan, Michigan 49721.
- Neill, C. R. 1976. "Dynamic Ice Forces on Piers and Piles. An Assessment of Design Guidelines in the Light of Recent Research". Canadian Journal of Civil Engineering. Vol. 3:305-341.
- Nevel, D. E. 1959. "Tables of Kelvin Functions and Their Derivatives". U.S. Army Snow, Ice and Permafrost Research Establishment (SIPRE) Technical Report 67. SIPRE is now the U.S. Cold Regions Research and Engineering Laboratory, Hanover, New Hampshire.

- Nevel, D. E. 1972. "The Ultimate Failure of a Floating Ice Sheet". Proceedings of the Ice Symposium, 1972. International Association of Hydraulic Research, Leningrad. 1-5.
- Nevel, D. E. 1976. "Creep Theory for a Floating Ice Sheet". CRREL Special Report 76-4. Cold Regions Research and Engineering Laboratory, Hanover, New Hampshire.
- Nevel, D. E. 1977. "Safe Ice Loads Computed with a Pocket Calculator". Unpublished. U.S. Cold Regions Research and Engineering Laboratory, Hanover, New Hampshire.
- Ohstrom, E. G. and DenHartog, S. L. 1976. "Cantilever Beam Tests on Reinforced Ice". CRREL Report 76-7. Cold Regions Research and Engineering Laboratory, Hanover, New Hampshire.
- Petrunichev, N. N. 1954. "On the Static Pressure of Ice", (O staticheskom davlenii l'da). Ice Thermal Problems in Hydraulic Engineering. Leningrad.
- Pounder, E. R. 1965. Physics of Ice. Pergamon Press, Ltd., London.
- Rose, L. B. and Silversides, C. R. 1958. "The Preparation of Ice Landings by Pulp and Paper Companies in Eastern Canada". Conference on the Bearing Strength of Ice, NRC, Ottawa. Transactions of the Engineering Institute of Canada. 2:3:101-105.
- Runnels, L. K. 1966. "Ice". Scientific American, 215:118-124.
- Sodhi, D. S. and Hamza, H. E. 1977. "Buckling Analysis of a Semi-Infinite Ice Sheet". Fourth International Conference on Port and Ocean Engineering Under Arctic Conditions. St. John's, Newfoundland. September 26-30, 1977.
- Striegl, A. R. 1952. "Ice on the Great Lakes and Its Engineering Problems". Paper presented at Joint Meeting of American Meteorological Society and Geophysical Union. September 11, 1952, Chicago.
- Williams, G. P. 1966. "Freeze-Up and Break-Up of Fresh-Water Lakes". Proceedings of Ice Pressures Against Structures Conference, Laval University, Quebec, November 1966. Technical Memorandum No. 92, National Research Council, NRC No. 9851, Ottawa, March 1968, 203-215.
- Zarling, J. P. 1974. "Ice Engineering in Small Craft Marinas: An Annotated Bibliography". Advisory Report No. 8. University of Wisconsin Sea Grant College Program, University of Wisconsin-Madison.

Behavior of Ice Under Load

Whatever the type of static load acting on ice (compression, tension, bending, shear) slip plays a decisive role in the overall deformation pattern. Slip in ice begins simultaneously with the load application. It is most intensive at the beginning, and then decreases according to a power law. The widely held view that at the beginning the deformation is purely elastic, and that the above-mentioned processes take place only after some time, is erroneous. The elastic limit of ice is small, less than 7 psi (50kN/m²).

The fraction of the elastic deformation in the total deformation at the beginning of a short-time load action is less than later, i.e., ice is not a linearly elastic material and does not obey Hooke's law. This basic peculiarity of ice distinguishes it from other materials, in particular metals.

The linearity of some parts of the deformation diagrams for compression and bending do not indicate that ice obeys Hooke's law in its usual meaning, since Young's modulus E in the expression "stress equals E times strain" must be replaced by another proportionality factor. This is the strain modulus which is not constant but depends on the duration of the load application.

The failure mechanism of ice varies with the test conditions (temperature, duration of load action, and direction of force), and is in the final analysis determined by the extent to which slip takes place both inside and between the crystals.

None of the existing models simulating the mechanical properties of a body is fully applicable to ice, because one of its constituent elements, the "dashpot" (considered as plunger moving in a liquid according to Newton's law of viscosity) must be replaced by a more complicated structure, by means of which not only the permanent set but also the elastic lag is allowed for. Studies carried out during recent years have shown that ice does not obey the law of viscosity since the relationship between the stress and the strain rate is not linear for it. It is at present impossible to express the stress-strain relationship analytically by allowing for all the laws mentioned above, which govern the behavior of ice under load.

The Dependence of the Properties of Ice on the Conditions of its Formation and Growth

It is well known that the quality of ice (including the mechanical properties of the crystals) depends on the conditions of its growth. The mechanical strength of the crystals vary directly with the time taken for the ice to grow. A number of defects in the crystal structure is small when the ice grows slowly, since the build-up of new lattice layers proceeds in small steps; these new layers are connected more regularly to the already finished planes. Furthermore, impurities are able to diffuse from the growing faces into the solution.

Other conditions being equal, the upper layers grow faster than the lower ones, so that the quality of the upper layers is worse.

APPENDIX II--DEFORMATION AND STRENGTH OF ICE, LAVROV

This appendix contains an abbreviated summary of a monograph prepared by Lavrov (1949). It is based on experimental studies on structurally simulated ice whose small-scale crystal structure is similar to that of an ice cover. This very important requirement is not fulfilled in small samples cut from a natural ice cover. The laws of deformation and strength presented are for forces acting on ice for short periods, i.e. from a few seconds to a few minutes. Problems with very long-term strength and creep of ice are not dealt with.

Three peculiarities distinguish ice from other materials. First, it exists at a temperature within a few degrees (a difference of tens of Celsius degrees being rare) of its melting point, ice therefore usually contains some liquid water between crystals. The water acts like a lubricant, reducing the sliding resistance between crystals. Secondly, ice does not react chemically with impurities and forms no solid solutions with them. The impurities accumulate gradually and form many pores, cavities, etc. in the ice. The third peculiarity is the comparatively large size of ice crystals. Their transverse dimensions vary between about a tenth of an inch (a few mm) and an inch (several cm). In metals these dimensions come out to small fractions of a few hundredths of an inch (a mm). These peculiarities cause ice to be a material which in its totality appears to consist of plastic hinges, so that it sharply reacts to static loads.

The Ratio of Transverse and Longitudinal Strains (Poisson's Ratio)

Poisson's ratio plays an important role in the laws governing the behavior of ice under load. Poisson's ratio for ice is usually determined dynamically from the difference between the propagation velocities of the transverse and longitudinal elastic waves. Its average value at temperatures below 32°F (0°C) is 0.53. Experimental values range from 0 to more than 2.5. Poisson's ratio depends upon stress, in some cases exceeds the theoretically possible maximum, and is different for tension and for compression. The results obtained can be explained only on the basis of the actual behavior of the ice under load, i.e., by allowing for its plasticity.

The quality of ice depends on the rate of its growth, so the strength of an ice cover formed at low temperatures is less than that of an ice cover of equal thickness, formed during milder weather.

The presence of snow on ice retards the removal of the latent heat of crystallization from the lower boundary of the ice, so that its growth rate decreases. The thickness and strength of natural ice cover therefore fluctuates.

The Modulus of Elasticity and the Shear Modulus

Natural ice, particularly when its crystals are small, has various orientations of the crystal axes; the crystals are separated by intercrystalline layers containing impurities and liquid phase. In addition, air bubbles are distributed over the bulk of the ice. The moduli of elasticity for the ice cover are therefore smaller than the elastic constants of monocrystals, and vary with the structure of the ice.

The elastic properties of ice are most accurately determined by means of dynamical methods, i.e., by measuring the propagation velocity of elastic (sound) waves in ice. Ultrasonic waves and the method of resonance vibrations yield the local values of the moduli of elasticity, while seismic methods yield averaged values for an area.

General shortcomings of all dynamical methods of determining the elastic properties is the approximatness of the theory, which results from considering the ice as an isotropic body.

Allowing for the peculiarities of the various dynamical methods of determining the moduli of elasticity, it appears that the latter differ significantly for fresh-water ice of different origin and from different water bodies.

Young's modulus E and the shear modulus G vary with temperature and method by which determined. Approximate average values are 1200 ksi (8300 MH/m^2) and 400 ksi (2800 MH/m^2) respectively.

The Strain Moduli (Uniaxial Compression, Tension, Bending, and Slip and Shear)

In studying the behavior of ice under static load it is useful to introduce the concept of the strain modulus. The reason is that the stress-strain diagrams have considerable linear parts.

In contrast to the modulus of elasticity the strain modulus is computed from the total, i.e., the elastic, the recovered, and the remanent, strain. It therefore depends not only on the temperature and structure of the ice but also on the magnitude of the load and the time during which it acts. The strain modulus may therefore have many values for each kind of deformation.

If only the properties of the samples are considered, all values of the strain modulus should be assumed to be equally probable, taking into account the dependence of the strain modulus on the above-mentioned factors. The scatter of its values indicates only that the test conditions or the structure

of the ice in some tests differed from those in others. The data found in the various sources on the mechanical properties of ice should, therefore, be grouped according to their similar features. This, however, is not always possible due to the lack of information on the test conditions. The strain modulus must in any case be selected according to the test conditions. The less time the load acts on the ice, the larger should be the value of the strain modulus.

When information on the properties of the ice cover is required, and the question arises of which value of the strain modulus should be given preference, there is, strictly speaking, no possibility of solving this problem by using the results of tests of samples having an arbitrary structure. Far more accurate data on the mechanical properties will then be provided by samples of structurally simulated ice.

The results of strain moduli in uniaxial compression, tension, bending, and slip and shear are presented in Table II-1.

	ksi	Strain Modulus Range
		MH/m^2
Uniaxial Compression	71- 768	490- 5296
Tension	17- 71	118- 490
Bending	135-1707	932-11768
Slip and Shear	6- 36	41- 245

Table II-1 Strain Moduli Structurally Simulated Ice (after Lavrov, 1969)

The strain moduli in compression and tension increase under repeated load applications.

The large differences in the strain modulus in bending are due not only to differences in the ice structure and temperature but also to the influence of the sample dimensions. This last factor was not considered important until recently, although it plays an important role in bending tests. The clear dependence of the strain modulus in bending on the ratio of the distance between supports to the sample height is due to the proximity of the ice temperature to the melting point and to the appearance of stress concentrations and microcracks at the corners of cavities. This causes irreversible and slowly reversible deformations which take place in the ice practically as soon as the load is applied.

The strain modulus in bending decreases when the load is increased and increases when a load is applied again unless the stress is very high.

The strain modulus in shear depends on the temperature, the concentration of impurities, the stress system, the dimensions of the shear surface, and the duration of the load application.

Ultimate Compressive Strength

The ultimate compressive strength of ice is, like that of other materials, usually established from the results of tests of samples (cubes) subjected to forces acting on one side. The sample is under these conditions deformed in the direction of compression but is free to expand in the transverse direction. The quality of work done in preparing the sample has a considerable influence on the test results.

Carefully prepared samples of structurally simulated fresh-water ice gave the following range of results: ultimate compressive strength with the direction of force perpendicular to the ice surface 730-1270 psi (5031-8414 kg/m^2) and for the direction of the force parallel to the ice surface 156-614 psi (1075-4236 kg/m^2).

Tensile Strength

The tensile strength of ice has been little investigated, like its shear strength. This may be due to the lack of examples in which ice is under real conditions subjected to tension.

Lavrov reports on the research of several other people. They found that tensile strengths lay in the range of 7) to 199 psi (490 to 1373 kg/m^2).

Lavrov's tests on structurally simulated ice show lower strengths than natural ice. This may be due to the different dimensions of the crystals and to differences in the development of the intercrystalline layers.

The Differences in the Properties of Ice Under Tension and Compression

As noted, the tensile strength and strain modulus in tension are considerably less than the corresponding magnitudes in compression. Lavrov carried out special investigations on homogeneous structurally simulated ice. He found the compressive strength of this type of ice to be 9 times higher than its tensile strength. This is due to the structure of the ice. Part of the vertical cross-sectional area of ice consists of intercrystalline layers and cavities filled with impurities and air. During tension the force is counteracted by the cohesive strength of the material connecting adjacent grains. Only part of the cross-section thus takes up the force. The crystal layers bonding the cavities can move freely in opposite directions, thus altering the shape of the cavities and increasing their size.

During compression the cavities become filled and the entire cross-section of the sample thereafter takes up the force.

On the basis of the experimentally established differences in the ultimate strength (1:9) it may be assumed that in fresh-water ice not subjected to any external force about 90% of the cross-sectional area is taken up by intercrystalline layers and cavities, with only 10% of it formed by direct bonds between adjacent crystals. However, this area ratio is not always observed since the quality of the ice (including the extent to which intercrystalline layers have developed in it) depends on the conditions of its formation and its growth rate. Furthermore, the microstructure of the ice changes with the lapse of time, due to recrystallization and other factors. There are thus cases in practice where the differences in the tensile and compressive strength of ice are less than 1:9. On the other hand, in thawing ice these differences are greater than 1:9.

Shear Strength

The results of Lavrov's tests carried out on structurally simulated ice gave a shear strength range of 63 to 422 psi (471 to 2913 kg/m^2). The shear strength depends on the sample size (scale factor), the duration of the load action, and the temperature when shear occurs along a circular surface in the center of an ice sheet. The direction of the force during the tests was perpendicular to the ice surface (along the vertical axes of the crystallites).

Bending Strength

Lavrov determined an average bending strength of 316 psi (2177 kg/m^2) for structurally simulated ice. The direction of the force was perpendicular to the ice surface and the duration of the load action was 4 seconds.

The bending strength was computed by means of the usual formulas of the strength of materials, which are suitable for determining the stresses only when the elastic strains are small. In the case of failure the strains are comparatively large and irreversible. Furthermore, the behavior of the ice at the beginning of the load action considerably differs from that assumed in the theory of elasticity. Hence, the bending strength, determined from the formula for a freely supported beam, cannot be considered as the true maximum tensile stress, but is an arbitrary magnitude. The computed bending strength therefore exceeds the computed tensile strength.

Lavrov determined an average bending strength of 161 psi (1108 kg/m^2) for structurally simulated ice in cantilever bending. The tensile strength and bending strength are of similar magnitude when cantilever beams are tested.

The Freezing Strength of Ice

Lavrov reports the research results of several others. In one case the average value of the normal freezing strength of ice to different surfaces at 27°F (-3°C) was about 294 psi (1961 kg/m^2). Surfaces included were ice to copper, ice to iron, and ice to glass. Tests on ice to polystyrene gave values about one-tenth as much.

Researchers have concluded that the strength with which water and other liquids freeze to solid surfaces does not depend upon whether the latter are

Summary of Strength Properties Reported by Lavrov

A summary of strength properties reported by Lavrov is presented in Table II-2. The summarized values are qualified on one or more variables such as strain rate, temperature or sample size. They are applicable only for forces acting on ice for short periods, i.e., from a few seconds to a few minutes.

Property	Average Value or Range of Values
Poisson's Ratio	0.33
Elastic Limit	less than 7 psi (50 kN/m ²)
Young's Modulus	1200 ksi (8300 MN/m ²)
Shear Modulus	400 ksi (2800 MN/m ²)
Uniaxial Compression Strain Modulus	71-768 ksi (490-5296 kN/m ²)
Tension Strain Modulus	17-71 ksi (118-490 MN/m ²)
Bending Strain Modulus	135-1707 ksi (932-11768 kN/m ²)
Slip and Shear Strain Modulus	6-36 ksi (41-245 MN/m ²)
Ultimate Compressive Strength (force perpendicular to surface)	730-1220 psi (5031-8414 kN/m ²)
Ultimate Compressive Strength (force parallel to surface)	156-614 psi (1079-4236 kN/m ²)
Tensile Strength	71-199 psi (490 to 1373 kN/m ²)
Shear Strength	68-422 psi (471 to 2913 kN/m ²)
Freely Supported Beam Bending Strength (force perpendicular to surface)	316 psi (2177 kN/m ²)
Cantilever Beam Bending Strength (force perpendicular to surface and applied from above)	161 psi (1108 kN/m ²)
Freezing Strength to Metals	71-284 psi (490-1961 kN/m ²)
Freezing Strength to Plastics and Varnishes	about one-tenth that of metals

Table II-2 Strength Properties (after Lavrov, 1969)

wetted by the liquid considered or not. They state further: "The strength with which ice freezes to plastics and varnishes is approximately one-tenth of that with which it freezes to glass or metals".

Other tests have given freezing strengths of fresh-water ice lower values, in the range of 71 to 142 psi (490 to 980 kN/m²).

The Friction Coefficient

The friction coefficient was determined as the ratio of the towing force to the weight of the sample together with an additional load. The static friction coefficient was determined by starting the sample, while the dynamic friction coefficient was determined during steady motion of the sample.

An ice surface almost always carries a thin liquid film consisting of water molecules. The frictional force thus is the sum of two components, namely dry friction and boundary friction with water lubrication. This is supported by the increase in the friction coefficient when the temperature of the ice surface is lowered.

It was found by experiment that steel skids are better than wooden ones at temperatures down to -22° F (-30° C), since the coefficient of boundary friction of steel is less than that of wood. Skids made of a material which is a poor heat conductor are better at temperatures below -31° F (-35° C), since part of the heat developed by friction is lost to the surroundings via heat-conducting skids; this interferes with the formation of a watery film, so that friction increases.

Researchers found that the static friction coefficient of ice on non-rusty steel is 0.15 to 0.25 and 0.30 to 0.35 on painted red lead.

Tests on Lake Ladoga were performed in an area cleared of snow. The ice surface was smooth and without cracks, but was uniformly covered by several hundredths to a tenth of an inch (1 to 3 mm) prominences. The lower surface of the ice was smooth.

The average friction coefficients of ice on steel and steel on ice were at 30° F (2° C) as follows: static friction coefficient ranged from 0.49 to 0.91 and the dynamic friction coefficient ranged from 0.08 to 0.15. The field results differed considerably from those obtained in the laboratory, perhaps due to scale effects.

APPENDIX III

SAFE ICE LOADS COMPUTED WITH A POCKET CALCULATOR

by

D. E. Nevel

U.S. Army Cold Regions Research and Engineering Laboratory
Hanover, NH 03755

April 1977

INTRODUCTION

When a load is placed on a floating ice sheet, the ice sheet is bent downward creating stresses within the ice. The downward deflection increases the water pressure on the bottom of the ice which in turn supports the load. If the maximum tensile stress within the ice exceeds the tensile strength of the ice, the ice will crack. Although the ice sheet can still carry more load before breakthrough occurs, the first crack is generally used to predict safe bearing capacity. In some cases flooding of the ice sheet may create operational difficulties, and a limiting deflection is used rather than first crack.

Previously the computations for the deflection and stresses of a floating ice sheet have been obtained by computers or programmable desktop calculators. Recently programmable pocket calculators have become powerful enough to perform these computations. Although they are slower, they do provide a means for computation in the field which has been non-existent before.

The purpose of this report is to provide a program to calculate the deflection and stresses for a floating ice sheet on the Hewlett-Packard model 67 pocket calculator. CREEL does not necessarily endorse the HP-67 since there are other programmable pocket calculators that may also perform the same computations.

The user of the program must select appropriate values for the mechanical properties of the ice in order to compute reliable deflection and stresses. Engineering judgement must be used in selecting the allowable ice strength and when dealing with non-ideal situations.

REQUIRED INFORMATION

A rectangular coordinate system must be defined on the ice sheet for locating the loads relative to each other. For each load, the coordinates of the center of the load, the magnitude of the load, and the distribution of the load must be known. The load may be assumed to be uniformly distributed over a circular area or a rectangular area whose dimensions and orientation are known. The load from a pneumatic tire can be assumed to be uniformly distributed over a circular area whose radius can be determined from the air pressure in the tire.

Young's modulus, Poisson's ratio, and the ice thickness must be specified for the ice sheet, as well as the density of supporting water.

The coordinates where the deflection and stresses are to be computed must be specified. For safe bearing capacity prediction, one should choose the coordinates that will give the largest stress within the ice sheet. When the loads are sufficiently far apart, the largest stress will occur directly under the center of the heaviest load. When two loads of equal magnitude are extremely close together the largest stress may occur between the loads. A few trial computations may be necessary to find where the stresses are the largest.

THEORETICAL APPROXIMATIONS AND LIMITATIONS

The calculator program uses the elastic thin plate theory to represent a floating ice sheet of uniform thickness, and considers a

load applied uniformly to a circular or rectangular area. Previously the rectangular area solution has been expressed by a Fourier series which frequently is slowly convergent. This program uses a new solution expressed by a power series which is more rapidly convergent. In order to further reduce the space and time requirements, the deflection is calculated from four concentrated loads, one at each corner of the rectangular area. This is a good approximation because the deflection does not depend significantly upon the distribution of the load.

Even with these simplifications, the rectangular area solution requires much more time than the circular area solution. Further time-savings can be obtained by noting that the stresses become less dependent on the load's distribution as the calculation point moves further away from the load. Hence, at a sufficiently large distance from the load, an equivalent circular area or concentrated load may be substituted for the rectangular area. For distances greater than five times the flexural rigidity length l , the deflection and stresses are nearly zero for either the circular or rectangular area solution and the calculation may be omitted.

The elastic thin plate theory is adequate except for calculating the stresses in the vicinity of a relatively concentrated load. For this situation, the three-dimensional theory of elasticity should be used. For this theory solutions exist for both rectangular and circular load distributions, but they are expressed inconveniently for numerical computation. In practice, loads distributed over a circular area (e.g. a pneumatic tire) tend to be more concentrated than loads distributed

over a rectangular area (e.g. a crawler track). The program uses a method proposed by Westergaard when the stresses are evaluated directly under the center of a circular area. The method replaces the radius a of the load distribution circle with $\sqrt{1.6 a^2 + b^2}$ $-0.675 b$, when the radius a is less than 1.742 times the ice thickness b . Using this new radius in the thin plate theory gives the same stress as the three-dimensional theory of elasticity.

EQUATIONS

The most convenient form of the solution for a load uniformly distributed over a circular area has been given by Max Wyman. The symbols are defined as follows:

- E is Young's modulus of the ice,
- ν is Poisson's ratio of the ice,
- h is the thickness of the ice,
- k is the weight density of the water,
- l is $[(Eh^3/12k(1-\nu^2))]^{1/4}$, the flexural rigidity length,
- P is the total load,
- r and θ are polar coordinates from the center of the load,
- R is r/h , the non-dimensional radial coordinate,
- a is the radius of the load's distribution,
- A is a/h , the non-dimensional load radius,
- v is the deflection of the ice sheet,
- σ_r is the radial stress at the bottom of the ice sheet.
- σ_θ is the tangential stress at the bottom of the ice sheet.

When $R > A$, the equations are:

$$\frac{(\sigma_r - \sigma_\theta) h^2 \pi}{2P(1-\nu) 3} = \frac{2}{R} [-D \operatorname{ker}'R + C \operatorname{ker}''R] + \frac{(\sigma_r + \sigma_\theta) h^2 \pi}{2P(1+\nu) 3},$$

$$\frac{(\sigma_r + \sigma_\theta) h^2 \pi}{2P(1+\nu) 3} = C \operatorname{ker} R + D \operatorname{ker} R,$$

$$\frac{Wk \ell^2 \pi}{P} = -D \operatorname{ker} R + C \operatorname{ker} R,$$

where $C = \frac{\operatorname{ker}'A}{A}$ and $D = \frac{\operatorname{ber}'A}{A}$. When $A = 0$, $C = 0$ and $D = 1/2$.

When $A > R$, the equations are:

$$\frac{(\sigma_r - \sigma_\theta) h^2 \pi}{2P(1-\nu) 3} = \frac{2}{R} [-D \operatorname{ber}'R + C \operatorname{ber}''R] + \frac{(\sigma_r + \sigma_\theta) h^2 \pi}{2P(1+\nu) 3},$$

$$\frac{(\sigma_r + \sigma_\theta) h^2 \pi}{2P(1+\nu) 3} = C \operatorname{ber} R + D \operatorname{ber} R,$$

$$\frac{Wk \ell^2 \pi}{P} = -D \operatorname{ber} R + C \operatorname{ber} R + \frac{1}{A^2},$$

where $C = \frac{\operatorname{ker}'A}{A}$ and $D = \frac{\operatorname{ker}''A}{A}$. When $R = 0$, $\sigma_r - \sigma_\theta = 0$.

The stresses must be determined relative to the x, y coordinate system in order to add to the stresses from other loads. The equations for this are

$$\frac{\sigma_x + \sigma_y}{2} = \frac{\sigma_r + \sigma_\theta}{2}$$

$$\frac{\sigma_x - \sigma_y}{2} = \frac{\sigma_r - \sigma_\theta}{2} \cos 2\theta$$

$$\sigma_{xy} = \frac{\sigma_r - \sigma_\theta}{2} \sin 2\theta$$

Consider a load uniformly distributed over a rectangular area as shown in Figure 1. The symbols are defined by:

x and y are coordinates which define the center of the load,

x_0 and y_0 are coordinates where the stresses are evaluated,

x_r and y_r are coordinates where the stresses are evaluated in a coordinate system whose origin is at the center of the load

and is parallel to the sides of the rectangle,

θ is the angle of the x_r axis measured from the x axis in a counterclockwise direction,

X is x_r/k and Y is y_r/k , non-dimensional coordinates,

a is one half the length of the load in the x_r direction,

b is one half the length of the load in the y_r direction,

A is a/k and B is b/k , non-dimensional length of the load, and

E, ν, h, k, ℓ, P and w are defined as before.

The equations to determine the x_r and y_r coordinates are:

$$x_r = (x_0 - x) \cos \theta + (y_0 - y) \sin \theta$$

$$y_r = -(x_0 - x) \sin \theta + (y_0 - y) \cos \theta$$

The equations to determine the stresses at the bottom of the ice sheet relative to the X, Y coordinate system are:

$$\frac{(\sigma_x + \sigma_y)h^2}{2P(1+\nu)} = \frac{3}{4\pi AB} [I(X+A, Y+B) - I(X+A, Y-B) + I(X-A, Y-B) - I(X-A, Y+B)]$$

$$\pm \frac{3}{4\pi AB} [I(Y+B, X+A) - I(Y-B, X+A) + I(Y-B, X-A) - I(Y+B, X-A)]$$

$$\frac{\sigma_{XY} h^2}{P(1-\nu)} = \frac{3}{4\pi AB} [kei \sqrt{(X+A)^2 + (Y+B)^2} - kei \sqrt{(X+A)^2 + (Y-B)^2} + kei \sqrt{(X-A)^2 + (Y-B)^2} - kei \sqrt{(X-A)^2 + (Y+B)^2}]$$

where

$$I(x, y) = \left(\frac{x}{2}\right)^2 \sum_{n=1,3}^{\infty} \frac{(-1)^n}{n! (n+1)!} \frac{2n}{(x/2)^{2n}} \left(-\frac{y}{x}\right)^n \sum_{k=0,1}^n \frac{n! (y/x)^k}{k! (n-k)!} \frac{1}{2k+1}$$

$$+\left(\frac{y}{2}\right)^2 \sum_{n=0,2}^{\infty} \frac{(-1)^{n/2}}{n! (n+1)!} \frac{2n}{(x/2)^{2n}} [-\gamma - \text{Ln} \frac{\sqrt{x^2 + y^2}}{2} + \phi(n) + \frac{(-1)^{n/2}}{n+1}] \sum_{k=0,1}^n \frac{n! (y/x)^k}{k! (n-k)!} \frac{1}{2k+1}$$

$$+\left(\frac{x}{2}\right)^2 \sum_{n=0,2}^{\infty} \frac{(-1)^{n/2}}{n! (n+1)!} \frac{2n}{(x/2)^{2n}} \sum_{k=0,1}^n \frac{(-1)^k}{k! (n-k)!} \frac{1}{2k+1} \left\{ -\frac{\arctan(y/x)}{(y/x)} \right.$$

$$\left. + \sum_{r=0,1}^k \frac{(-1)^r (y/x)^{2r}}{2r+1} \right\}$$

where γ is Euler's number and $\phi(n) = \frac{1}{1} \cdot \frac{1}{2} \cdot \frac{1}{3} \cdots \frac{1}{n}$. The equations to determine the stresses relative to the x, y coordinate system are:

$$\frac{\sigma_x + \sigma_y}{2} = \frac{\sigma_x + \sigma_y}{2}$$

$$\frac{\sigma_x - \sigma_y}{2} = \left(\frac{\sigma_x - \sigma_y}{2}\right) \cos 2\theta - \sigma_{XY} \sin 2\theta$$

$$\sigma_{xy} = \left(\frac{\sigma_x - \sigma_y}{2}\right) \sin 2\theta + \sigma_{XY} \cos 2\theta$$

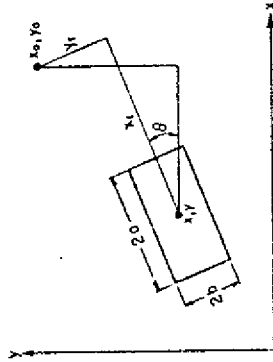


Figure 1. Rectangular load distribution.

GENERAL PROCEDURE

Turn on the calculator and set the other switch to run. The

program to compute the deflection and the stresses for a load uniformly distributed over a circular area is divided into two parts which are labeled 1 and 2. The program to compute the deflection and stresses for a load uniformly distributed over a rectangular area is divided into two parts which are labeled 3 and 4. The results of either program 2 or 4 are:

REG 0	Identification #		
REG 6	deflection	w	(inches)
REG 7	stress sum	$(\sigma_x + \sigma_y)/2$	(psi)
REG 8	stress difference	$(\sigma_x - \sigma_y)/2$	(psi)
REG 9	shearing stress	σ_{xy}	(psi)

Program 5 adds the deflection and stresses from either program 2 or 4 to the respective sums which are in registers 1 through 4. From these new sums it determines and stores the maximum stress in register A and the angle from the x axis of the crack in register B. Between computation of each load, the sums are saved on a magnetic card referred to as the sum card. Side 2 of the program 5 magnetic card is not used, and can be used for the sum card.

INPUT DATA

1. For a load uniformly distributed over a rectangular area (Fig. 1), the following data should be keyed into memory. Neither the length a or b of the rectangle may be equal to zero.

REGISTER	DATA (units)	DEFINITION
0	ID#	a load identification number
1	x (inches)	coordinate of the load's center
2	y (inches)	coordinate of the load's center
3	P (pounds)	magnitude of the load
4	a (inches)	rectangle half-length along x_r
5	b (inches)	rectangle half-length along y_r

6	θ (degrees)	the angle of x_r from x
7	E (psi)	Young's modulus of ice
8	ν	Poisson's ratio of ice
9	h (inches)	thickness of ice
A	k (lb/in ³)	weight density of water
B	x_o (inches)	coordinate of computations
C	y_o (inches)	coordinate of computations

2. For a load uniformly distributed over a circular area, the input is the same except for the distribution of the load in registers 4, 5 and 6. Registers 5 and 6 are not used, while register 4 contains the radius a (inches) of the circular area. This radius may be equal to zero.

3. To store data into a register, key the data into the display register, press STO followed by the register symbol. For example to store 1 for the ID#, press 1, STO, 0. To display data from a register in order to check the input, press RCL followed by the register symbol.

4. The operator may find it time consuming to repeatedly key in all the data for each load. For each load the ice and water data as well as the place of computation do not change. The operator may find it convenient to record the input data for the first load on a magnetic card. Then for succeeding loads, this card may be read into memory and only data which are different need be keyed into memory.

When the computation is to be repeated for a different ice thickness or other parameter change, the operator may find it convenient to record the input for each load on a magnetic card. Then for succeeding computations, each card can be read into memory, and only the appropriate parameter need be keyed.

If the input data is to be recorded on a magnetic card, the secondary registers should be clear since this allows memory to be recorded on one side of a magnetic card rather than on two sides. Consult the HP manual for ways to clear these registers.

To record the memory registers on a magnetic card, press f, W/DATA and insert the card. To read the registers from a magnetic card into memory, just insert the card.

5. The units of the input data are pounds, inches and degrees. A different force and length unit may be used for input which will give the deflection and stress expressed in these same units.

Programs 1 and 2

Program 1 is for a load uniformly distributed over a circular area. Program 2 is a continuation of program 1 and assumes that the results of program 1 are still in memory. The operating instructions are:

1. Read program 1 by inserting side 1 of the 1 magnetic card (side 2 is not used).
2. Store input data in memory.
3. Press A to start the program. After about 5 seconds, the calculator stops and displays 2, the next required program.

4. Read program 2 by inserting side 1 of the 2 magnetic card followed by side 2.

5. Press A to start the program. After about 30 seconds the program stops and displays 5, the next required program.

6. Proceed to program 5.

Program 3 and 4

Program 3 is for a load uniformly distributed over a rectangular area. Program 4 is a continuation of program 3 and assumes that the results of program 3 are still in memory. The operating instructions are:

1. Read program 3 by inserting side 1 of the 3 magnetic card followed by side 2.

2. Store input data in memory.

3. Press A to start the program. After about 60 seconds, the calculator stops and displays 4, the next required program.

4. Read program 4 by inserting side 1 of the 4 magnetic card followed by side 2.

5. Press A to start the program. After about 300 seconds, the calculator stops and displays 5, the next required program.

6. Proceed to program 5.

Program 5

Program 5 is a continuation of program 3 or 4. Program 5 assumes that the results of program 3 or 4 are still in memory. The operating instructions are:

1. Read program 5 into memory by inserting side 1 of the 5 magnetic card. Side 2 is not used by program 5.

3. For a succeeding load (any load except the beginning load of a computation), press A to start the program. The program pauses for about one second and displays the ID#. During this pause, insert the sum card, and the sums will be read. If the sum card is not inserted during the pause, the program will repeat until it is inserted.

For the BEGINNING load of a computation ONLY, press B to start the program. This zeros the sum and eliminates the reading of the sum card.

3. When the program stops, CRD is displayed. Insert the sum card, and memory will be recorded.

4. The angle of the crack is stored in register B and the maximum stress is stored in register A as well as being displayed. If this was not the last load of a computation, process any additional load by either program 1 or 3.

Subroutines

The subroutines Kelvin (z) and I (x,y) may be of use in other programs. The following is a brief description of these subroutines that will allow their use for this purpose.

The Kelvin (z) subroutine is stored in steps 102 through 213 of program 2. This subroutine uses registers A, B, I, and O through 9. The subroutine also uses Euler's number $Y = 0.5772156649$ which is assumed to be in register E. Therefore, be sure that register E contains Y. To execute the subroutines, place the argument z in the x register and

press E. The subroutine will compute $ker(z)$, $ber(z)$, $ker'(z)$, $ber'(z)$, $kei(z)$, $bei(z)$, $kei'(z)$, $bei'(z)$ in registers 1 through 8 respectively. The argument z will be in register A. The method of computation is from Don Kevel, Tables of Kelvin functions and their derivatives, CRREL Technical Report 67, June 1959. The series is truncated when the last term becomes less than 10^{-6} . The exponent 6 is stored in step 159 and may be changed to obtain other accuracies.

The subroutine I (x,y) is stored in steps 61 through 220 of program 4. This subroutine uses registers A, B, I, and O through

19. The subroutine also uses Euler's number $Y = 0.5772156649$ which is assumed to be in register E. Therefore, be sure register E contains Y. To execute the subroutine, place the argument y in register Y, the argument x in register X, and press E. The subroutine will give I (x,y) in register X. The series is truncated when the last term becomes less than 10^{-6} . The exponent 6 is stored in step 135 and may be changed to obtain other accuracies.

Examples

The following numerical examples are provided for the purpose of checking and debugging the programs. For the Kelvin (z) subroutine with the accuracy set at 10^{-6} , the results for z=1 are:

REG 1	2.867062088 -01	REG 5	-4.949946366 -01
REG 2	9.843817812 -01	REG 6	2.495660400 -01
REG 3	-6.946038910 -01	REG 7	3.523699135 -01
REG 4	-6.244575218 -02	REG 8	4.973965115 -01

For programs (1) and (2) there are various options which should be checked.

For R>A, A may or may not be zero. For A>R, R may or may not be zero.

For A>R and R>O, Westergaard's substitution may or may not be made. The following examples cover all cases.

The input data for program (1) are:

REG	R>A=0	A>R=0	Westergaard A>R=0
1	100	100	0
2	100	100	0
3	10000	10000	10000
4	0	20	5
7	10 ⁶	10 ⁶	10 ⁶
8	1/3	1/3	1/3
9	10	10	10
A	62.4/1728	62.4/1728	62.4/1728
B	170	100	0
C	170	100	0

The output data from program (2) are:

REG	R>A=0	A>R=0	Westergaard A>R=0
6	5.9282837411 -01	6.761493320 -01	6.790823603 -01
7	6.216841289 +01	1.935510530 +02	2.807218953 +02
8	0	0	0
9	-1.534340994 +01	0	0

The next two options can also be used to check program 5. The input data are:

REG	R>A=0	A>R=0
0	1	2
1	0	63
2	0	63
3	10000	10000
4	20	20
7	10 ⁶	10 ⁶
8	1/3	1/3
9	10	10
A	62.4/1728	62.4/1728
B	70	70
C	70	70

The output data from program (2) are:

REG	R>A=0	A>R=0
6	5.974546370 -01	6.748975099 -01
7	6.221160230 +01	1.857763777 +02
8	0	0
9	-1.501987756 +01	-1.943671630 +00

The results of program 5 are:

REG	Input	Output
1	1.272352147 +00	ZW
2	2.479879800 +02	$E(\sigma_x + \sigma_y)/2$
3	0	$E(\sigma_x - \sigma_y)/2$
4	-1.696354919 +01	$E\sigma_{xy}$
A	2.619515292 +02	maximum stress
B	4.500000000 +01	crack angle (degrees)

For the I (x,y) subroutine with the accuracy set at 10^{-6} , the result is $I(1,1,5) = 6.407935381 -02$.

The example to check program 3 and 1 is:

REG	Input	Output
1	0	
2	0	
3	10000	
4	30	
5	5	
6	30	6.068974047 -01
7	10^6	6.566463303 +01
8	1/3	7.014794041 +00
9	10	-1.337575308 +01
A	62.4/1729	
B	50	
C	80	

MEMORY REGISTER USE

EXCEPT FOR INPUT AND OUTPUT

REG	Input	Output
0	ID#	$I(x,y)$
1	R	$x_p, X+A$
2	Z0	$y_p, Y+B$
3	A	$3P(1+v)/4\pi ABh^2$
4	A	$X - A$
5		$Y - B$
6	$P/\pi k_1^2$	$\pi k_1^2/P$
7	$3P(1+v)/\pi h^2$	$(x/2)^2$
8	$3P(1-v)/\pi h^2$	$(y/x)^2$
9		
A		$z/2 - z$
B		PT
C	C	
D	D	Z0
E	Y	$3P(1-v)/4\pi ABh^2$
I	Z	Y
10		Index
11		n
12		ker z
13		ber z
14		ker'z
15		ber'z
16		kei z
17		bei z
18		kei'z
19		bei'z
		ϕ

PROGRAM 1

PROGRAM 1

Line	Label	Operation	Register	Value/Expression	Line	Label	Operation	Register	Value/Expression
1	LBL A				57	T			
2	RCL 7				58	4			1.74
3	RCL 9				59	RCL 4			a
4	STO X 9				60	X ²			a ²
5	RCL 9				61	1			
6	X				62	.			
7	X				63	6			1.6
8	RCL A				64	X			1.6 a ²
9	1/X				65	RCL 9			h ²
10	STO 6				66	+			1.6 a ² /h ²
11	X				67	1			1
12	1				68	+			1.6 a ² /h ² +1
13	RCL 8				69	√			√(1.6 a ² /h ² +1)
14	X ²				70	.			
15	-				71	6			
16	+				72	7			
17	1				73	5			.675
18	2				74	-			new a/h
19	+				75	X > Y			a/h > 1.74
20	√				76	CTO 1			
21	STO 6				77	RCL 9			b ²
22	√				78	√			h
23	STI				79	X			new a
24	RCL C				80	STO 4			new a
25	RCL 2				81	LBL 1			
26	-				82	RCL 4			a
27	RCL B				83	RCL			l
28	RCL 1				84	+			A
29	-	X ₀ -X							
30	+ P	polar							
31	RCL	l							
32	+	R							
33	STO 1	R							
34	R +	θ							
35	2	2							
36	X	2θ							
37	STO 2	2θ							
38	RCL 3	P							
39	π	π							
40	+	P/π							
41	STO X 6	P/πk ²							
42	RCL 9	h ²							
43	+	P/πh ²							
44	3	3							
45	X	3P/πh ²							
46	STO 7	3P/πh ²							
47	STO X 8	3vP/πh ²							
48	RCL 8	3vP/πh ²							
49	STO + 7	3(1+v)P/πh ²							
50	-	3(1-v)P/πh ²							
51	STO 8	3(1-v)P/πh ²							
52	RCL 1	R							
53	X ≠ 0	R ≠ 0							
54	CTO 1								
55	1								
56	.								

PROGRAM 2

113	STO 7	ker'z	141 +	1/n	141 X
114	STO 8	ber'z	142 STO + 9	φ	170 STO - 7
115	STO 9	φ	143 LBL 4		171 RCL B
116	1	1	144 RCL A	z/2	172 RCL 6
117	STO B	PT	145 RCL 0	n	173 X
118	STO 2	ber z	146 +	z/2n	174 STO - 5
119	RCL A	z/2	147 RCL B	PT	175 RCL B
120	X ≠ 0	z ≠ 0	148 X	PT z/2n	176 RCL 4
121	STO 2		149 STO B	PT	177 X
122	π	π	150 STO + (1)	I	178 STO - 3
123	4	4	151 DSZ		179 RCL B
124	+	π/4	152 RCL 9	φ	180 RCL 2
125	STO - 5	ker'z	153 X		181 X
126	RTH		154 STO + (1)	I	182 STO - 1
127	LBL 2		155 DSZ		183 π
128	8	8	156 RTH		184 4
129	STI	Index	157 ABS	ABS (φ PT)	185 +
130	GSB 3	n, φ, PT, I	158 EXX		186 STO B
131	GSB 4	PT, I	159 6		187 RCL 4
132	RCL B	PT	160 CHS	10 ⁻⁶	188 X
133	CHS	-PT	161 X < Y	10 ⁻⁶ < φ PT	189 STO - 7
134	STO B	PT	162 GTO 2		190 RCL B
135	GSB 3	n, φ, PT, I	163 RCL A	z/2	191 RCL 2
136	GTO 4	PT, I	164 LN	LN(z/2)	192 X
137	LBL 3		165 RCL E	Y	193 STO - 5
138	1	1	166 +	Y+LN(z/2)	194 RCL B
139	STO + 0	n	167 STO B	Y + LN (z/2)	195 RCL 8
140	RCL 0	n	168 RCL 8	ber'z	196 X

PROGRAM 2

169	X	ker'z	170 STO - 7	ker'z	197 STO + 3
170	STO - 7	ker'z	171 RCL B	Y+LN(z/2)	198 RCL B
171	RCL B	Y+LN(z/2)	172 RCL 6	ber'z	199 RCL 6
172	RCL 6	ber'z	173 X	π/4 ber'z	200 X
173	X		174 STO - 5	ker z	201 STO + 1
174	STO - 5	ker'z	175 RCL B	Y+LN(z/2)	202 RCL 6
175	RCL B	Y+LN(z/2)	176 RCL 4	ber'z	203 RCL A
176	RCL 4	ber'z	177 X	z	204 2
177	X		178 STO - 3	ker'z	205 X
178	STO - 3	ker'z	179 RCL B	Y+LN(z/2)	206 STO A
179	RCL B	Y+LN(z/2)	180 RCL 2	ber z	207 +
180	RCL 2	ber z	181 X	ker z	208 STO - 7
181	X		182 STO - 1	ker z	209 RCL 2
182	STO - 1	ker z	183 π	π	210 RCL A
183	π	π	184 4	4	211 +
184	4	4	185 +	π/4	212 STO - 3
185	+	π/4	186 STO B	π/4	213 RTH
186	STO B	π/4	187 RCL 4	ber'z	
187	RCL 4	ber'z	188 X	π/4 ber'z	
188	X	π/4 ber'z	189 STO - 7	ker'z	
189	STO - 7	ker'z	190 RCL B	π/4	
190	RCL B	π/4	191 RCL 2	ber z	
191	RCL 2	ber z	192 X	π/4 ber z	
192	X	π/4 ber z	193 STO - 5	ker'z	
193	STO - 5	ker'z	194 RCL B	π/4	
194	RCL B	π/4	195 RCL 8	ber'z	
195	RCL 8	ber'z	196 X	π/4 ber'z	

PROGRAM 3

1 DEL A
 2 RCL 7
 3 RCL 9
 4 STO X 9
 5 RCL 9
 6 X
 7 X
 8 RCL A
 9 STO 7
 10 +
 11 1
 12 RCL 8
 13 X²
 14 -
 15 +
 16 1
 17 2
 18 +
 19 $\sqrt{\quad}$
 20 STO X 7
 21 $\sqrt{\quad}$
 22 STI
 23 RCL B
 24 STO - 1
 25 RCL C
 26 STO - 2
 27 RCL 6
 28 RCL 2

29 RCL 6
 30 RCL 1
 31 R +
 32 CHS
 33 STO 1
 34 R +
 35 STO 2
 36 R +
 37 R +
 38 STO - 2
 39 R +
 40 STO - 1
 41 RCL 6
 42 2
 43 X
 44 STO C
 45 RCI
 46 STO + 1
 47 STO + 2
 48 STO + 4
 49 STO + 5
 50 RCL 3
 51 π
 52 +
 53 STO + 7
 54 RCL 4
 55 RCL 5
 56 X

57 RCL 9
 58 X
 59 +
 60 *
 61 7
 62 5
 63 X
 64 STO 3
 65 STO X 3
 66 RCL 8
 67 STO + 2
 68 -
 69 STO D
 70 *
 71 5
 72 7
 73 7
 74 2
 75 1
 76 5
 77 6
 78 6
 79 4
 80 9
 81 STO E
 82 CLX
 83 STO 6
 84 RCL 1

85 h²
 86 ABh²
 87 P/ π ABh²
 88 3/4
 89 3P/ 4π ABh²
 90 3P/ 4π ABh²
 91 3Pv/ 4π ABh²
 92 3Pv/ 4π ABh²
 93 3P(1+v)/ 4π ABh²
 94 3P(1-v)/ 4π ABh²
 95 3P(1-v)/ 4π ABh²
 96 3P(1-v)/ 4π ABh²
 97 3P(1-v)/ 4π ABh²
 98 h²
 99 ABh²
 100 P/ π ABh²
 101 3/4
 102 3P/ 4π ABh²
 103 3P/ 4π ABh²
 104 3Pv/ 4π ABh²
 105 3Pv/ 4π ABh²
 106 3P(1+v)/ 4π ABh²
 107 3P(1-v)/ 4π ABh²
 108 3P(1-v)/ 4π ABh²
 109 3P(1-v)/ 4π ABh²
 110 3P(1-v)/ 4π ABh²
 111 π k²/P
 112 8

PROGRAM 3

A
 X + A
 X - A
 X - A
 Y
 B
 Y + B
 Y - B
 Y - B
 X - A
 ke1 $\sqrt{X^2+Y^2}$
 cXY
 Y + B
 X - A
 ke1 $\sqrt{X^2+Y^2}$
 cXY
 Y - B
 X + A
 ke1 $\sqrt{X^2+Y^2}$
 cXY
 Y + B
 X + A
 ke1 $\sqrt{X^2+Y^2}$
 cXY
 3P(1-v)/ 4π ABh²
 cXY
 π k²/P
 8

113 X $8\pi k^2/P$
 114 STO + 6 W
 115 4
 116 RTN
 117 LBL E kei (z)
 118 + P polar
 119 P \rightarrow S
 120 2
 121 + z/2
 122 STO A z/2
 123 CLX 0
 124 STO 0 n
 125 STO 1 ker z
 126 STO 3 ker'z
 127 STO 4 ber'z
 128 STO 5 kei z
 129 STO 6 bei z
 130 STO 7 kei'z
 131 STO 8 bei'z
 132 STO 9 ϕ
 133 1
 134 STO B PT
 135 STO 2 ber z
 136 RCL A z/2
 137 X \neq 0 z \neq 0
 138 GTO 2
 139 π
 140 4

141 + $\pi/4$
 142 CHS $-\pi/4$
 143 GTO 5
 144 LBL 2
 145 8
 146 STI index
 147 GSB 3 n, ϕ , PT, E
 148 GSB 4 PT, E
 149 RCL B PT
 150 CHS -PT
 151 STO B PT
 152 GSB 3 n, ϕ , PT, E
 153 GTO 4 PT, E
 154 LBL 3
 155 1
 156 STO + 0 n
 157 RCL 0 n
 158 + 1/n
 159 STO + 9 ϕ
 160 LBL 4
 161 RCL A z/2
 162 RCL 0 n
 163 + z/2n
 164 RCL B PT
 165 X PT z/2n
 166 STO B PT
 167 STO + (i) bei'z
 168 DSZ W

169 RCL 9 ϕ
 170 X ϕ PT
 171 STO + (i) kei'z
 172 DSZ
 173 RTN
 174 ABS ABS(ϕ PT)
 175 EEX
 176 6
 177 CHS 10^{-6}
 178 X < Y $10^{-6} < |\phi$ PT|
 179 GTO 2
 180 RCL A z/2
 181 LN LN(z/2)
 182 RCL E Y
 183 + Y + LN(z/2)
 184 RCL 6 bei z
 185 X
 186 STO - 5 kei z
 187 π
 188 4
 189 + $\pi/4$
 190 RCL 2 ber z
 191 X
 192 STO - 5 kei z
 193 RCL 5 kei'z
 194 LBL 5
 195 P \rightarrow S
 196 STO - 6 W

PROGRAM 11

PROGRAM 12

113	RCL 9	-φ	141	RTN	169	F7 0	197	STO 7	I _r
114	-	φ+5/(n+1)	142	LBL 3	170	OTO 7	198	1	1
115	X		143	RCL A	171	RCL B	199	STO 8	P _r
116	STO + 1		144	1	172	X	200	LBL 8	(y/x) ²
117	SF 0		145	STO + 0	173	STO X 5	201	RCL B	-(y/x) ²
118	GSE 4		146	RCL 0	174	RCL 5	202	CHS	P _r
119	STO + 1		147	+	175	LBL 6	203	STO X 8	P _r
120	LBL 1		148	+	176	RCL 6	204	RCL 8	P _r
121	RCL 2		149	RCL 0	177	RCL 6	205	1	1
122	CHS	-P	150	1/X	178	X	206	STO + 6	r
123	STO 2	P	151	STO - 9	179	1	207	RCL 6	r
124	CF 0		152	X	180	+	208	2	2
125	GSB 3		153	STO x 2	181	+	209	x	2r
126	π	π	154	LBL 4	182	STO + 4	210	+	2r+1
127	X		155	CLX	183	RCL 0	211	+	P _r /(2r+1)
128	4	4	156	STI	184	RCL 0	212	STO + 7	1
129	+		157	1	185	X > Y	213	RCL 6	r
130	STO - 1	1	158	STO 5	186	OTO 5	214	RCL 6	k
131	RCL 1	1	159	F7 0	187	RCL 4	215	X > Y	k > r
132	+		160	RCL 3	188	RCL 2	216	OTO 8	I _r
133	ABS		161	STO 4	189	X	217	RCL 7	P _r
134	FEX		162	LBL 5	190	RTN	218	RCL 5	P _r
135	6		163	RCL 0	191	LBL 7	219	X	P _r
136	CHS	10 ⁻⁶	164	RCL 0	192	CHS	220	OTO 6	P _k
137	X < Y		165	-	193	STO X 5			P _k
138	OTO 2		166	ISZ	194	CLX			0
139	RCL 1	1	167	RCL 1	195	STO 6			r
140	P + 5		168	+	196	RCL 3			Q

PROGRAM 5

1	LBL A				
2	4				
3	STI				
4	CF 3				
5	RCL 0				
6	MERGE				
7	PAUSE				
8	F? 3				
9	GTO 1				
10	GTO A				
11	LBL 1				
12	STO 0	ID#			
13	RCL 6	V			
14	STO + 1	V			
15	RCL 7	$(\sigma_x + \sigma_y)/2$			
16	STO + 2	$I(\sigma_x + \sigma_y)/2$			
17	RCL 8	$(\sigma_x - \sigma_y)/2$			
18	STO + 3	$I(\sigma_x - \sigma_y)/2$			
19	RCL 9	σ_{xy}			
20	STO + 4	$I \sigma_{xy}$			
21	P + S				
22	CL REG				
23	P + S				
24	3				
25	6				
26	0	360			
27	RCL 4	$I \sigma_{xy}$			
28	RCL 3	$I(\sigma_x - \sigma_y)/2$			
29	+ P				
30	RCL 2	Polar			
31	+	$I(\sigma_x + \sigma_y)/2$			
32	STO A	σ			
33	R +	σ			
34	X < 0	angle < 0			
35	+				
36	2	2			
37	+				
38	9				
39	0	90			
40	-	angle			
41	STO B	angle			
42	RCL A	σ			
43	W/DATA				
44	RTN				
45	LBL B	Begin Load			
46	CLX	0			
47	STO 1	$I \sigma_{xy}$			
48	STO 2	$I(\sigma_x + \sigma_y)/2$			
49	STO 3	$I(\sigma_x - \sigma_y)/2$			
50	STO 4	$I \sigma_{xy}$			
51	STO 5				
52	RCL 0	ID#			
53	GTO 1				



APPENDIX: IV

Technical Report 67

JUNE, 1959

Tables of Kelvin Functions and their Derivatives

by D. E. Nevel

U. S. ARMY SNOW ICE AND PERMAFROST
RESEARCH ESTABLISHMENT

Corps of Engineers
Wilmette, Illinois

TABLES OF KELVIN FUNCTIONS AND THEIR DERIVATIVES

by

D. E. Nevel

The bearing capacity of a floating ice sheet can be computed by considering it a plate on an elastic foundation. The differential equation describing this is

$$\nabla_{\chi}^4 w + w = \frac{q}{k} \quad \text{where the operator}$$

$$\nabla_{\chi}^2 = \frac{d^2}{d\chi^2} + \frac{1}{\chi^2} \frac{d^2}{d\theta^2} + \frac{1}{\chi} \frac{d}{d\chi}.$$

Assuming that the boundary conditions are symmetrical with respect to the origin, the differential equation becomes

$$\frac{d^4 w}{d\chi^4} + \frac{1}{\chi} \frac{d^3 w}{d\chi^3} - \frac{2}{\chi^2} \frac{d^2 w}{d\chi^2} + \frac{2}{\chi^3} \frac{dw}{d\chi} + w = \frac{q}{k}$$

where

q = uniform distributed load

k = foundation modulus

w = deflection

x, θ = polar coordinates

$\chi = x/\ell$

$\ell = \sqrt[4]{\frac{Eh^3}{12k(1-\mu^2)}} = \text{characteristic length}$

E = modulus of elasticity

h = thickness of the plate

μ = Poisson's ratio.

The solution of this differential equation is given in terms of Kelvin functions as (Wyman, 1950):

$$w = A \operatorname{ber}(\chi) + B \operatorname{bei}(\chi) + C \operatorname{ker}(\chi) + D \operatorname{kei}(\chi) + \frac{q}{k}.$$

These Kelvin functions are also important in other physical problems, for instance in the fields of electrical engineering, heat flow, and shell analysis. Because of the wide application of Kelvin functions, there is a need for a detailed accurate table presently unavailable.

The formulas for these functions and their first derivatives are:

$$\operatorname{ber}(\chi) = \sum_{n=0, 2, 4, 6}^{\infty} \frac{(-1)^{\frac{n}{2}} \left(\frac{\chi}{2}\right)^{2n}}{n! n!}$$

$$\operatorname{ber}_{\phi}(\chi) = \sum_{n=2, 4, 6}^{\infty} \frac{(-1)^{\frac{n}{2}} \left(\frac{\chi}{2}\right)^{2n}}{n! n!} \phi(n)$$

TABLES OF KELVIN FUNCTIONS AND THEIR DERIVATIVES

$$\text{ber}'(\chi) = \sum_{n=2,4,6}^{\infty} \frac{(-1)^{\frac{n}{2}} \left(\frac{\chi}{2}\right)^{2n-1}}{(n-1)! n!}$$

$$\text{ber}'_{\phi}(\chi) = \sum_{n=2,4,6}^{\infty} \frac{(-1)^{\frac{n}{2}} \left(\frac{\chi}{2}\right)^{2n-1}}{(n-1)! n!} \phi(n)$$

$$\text{bei}(\chi) = \sum_{n=1,3,5}^{\infty} \frac{(-1)^{\frac{n-1}{2}} \left(\frac{\chi}{2}\right)^{2n}}{n! n!}$$

$$\text{bei}_{\phi}(\chi) = \sum_{n=1,3,5}^{\infty} \frac{(-1)^{\frac{n-1}{2}} \left(\frac{\chi}{2}\right)^{2n}}{n! n!} \phi(n)$$

$$\text{bei}'(\chi) = \sum_{n=1,3,5}^{\infty} \frac{(-1)^{\frac{n-1}{2}} \left(\frac{\chi}{2}\right)^{2n-1}}{(n-1)! n!}$$

$$\text{bei}'_{\phi}(\chi) = \sum_{n=1,3,5}^{\infty} \frac{(-1)^{\frac{n-1}{2}} \left(\frac{\chi}{2}\right)^{2n-1}}{(n-1)! n!} \phi(n)$$

$$\text{ker}(\chi) = \text{ber}_{\phi}(\chi) - \text{ber}(\chi) \ln \frac{\chi}{2} + \frac{\pi}{4} \text{bei}(\chi)$$

$$\text{ker}'(\chi) = \text{ber}'_{\phi}(\chi) - \text{ber}'(\chi) \ln \frac{\chi}{2} + \frac{\pi}{4} \text{bei}'(\chi) - \frac{\text{ber}(\chi)}{\chi}$$

$$\text{kei}(\chi) = \text{bei}_{\phi}(\chi) - \text{bei}(\chi) \ln \frac{\chi}{2} - \frac{\pi}{4} \text{ber}(\chi)$$

$$\text{kei}'(\chi) = \text{bei}'_{\phi}(\chi) - \text{bei}'(\chi) \ln \frac{\chi}{2} - \frac{\pi}{4} \text{ber}'(\chi) - \frac{\text{bei}(\chi)}{\chi}$$

where $\phi(n) = \frac{1}{1} + \frac{1}{2} + \frac{1}{3} + \dots + \frac{1}{n}$

and $\ln \gamma = 0.577215664901533$ (Euler's constant)

Other important derivatives and integrals may be expressed in terms of the functions and first derivatives.

$$\text{ber}''(\chi) = -\text{bei}(\chi) - \frac{\text{ber}'(\chi)}{\chi}$$

$$\text{ber}'''(\chi) = -\text{bei}'(\chi) + \frac{\text{bei}(\chi)}{\chi} + \frac{2\text{ber}'(\chi)}{\chi^2}$$

$$\int \chi \text{ber}(\chi) d\chi = \chi \text{bei}'(\chi)$$

$$\text{bei}''(\chi) = \text{ber}(\chi) - \frac{\text{bei}'(\chi)}{\chi}$$

$$\text{bei}'''(\chi) = \text{ber}'(\chi) - \frac{\text{ber}(\chi)}{\chi} + \frac{2\text{bei}'(\chi)}{\chi^2}$$

$$\int \chi \text{bei}(\chi) d\chi = -\chi \text{ber}'(\chi)$$

$$\text{ker}''(\chi) = -\text{kei}(\chi) - \frac{\text{ker}'(\chi)}{\chi}$$

$$\text{ker}'''(\chi) = -\text{kei}'(\chi) + \frac{\text{kei}(\chi)}{\chi} + \frac{2\text{ker}'(\chi)}{\chi^2}$$

$$\int \chi \text{ker}(\chi) d\chi = \chi \text{kei}'(\chi)$$

TABLES OF KELVIN FUNCTIONS AND THEIR DERIVATIVES

$$\text{kei}''(\chi) = \text{ker}(\chi) - \frac{\text{kei}'(\chi)}{\chi}$$

$$\text{kei}'''(\chi) = \text{ker}'(\chi) - \frac{\text{ker}(\chi)}{\chi} + \frac{2 \text{kei}'(\chi)}{\chi^2}$$

$$\int \chi \text{kei}(\chi) d\chi = -\chi \text{ker}'(\chi)$$

Table I gives the Kelvin functions and their first derivatives. Table II gives $\text{ber}_\phi(\chi)$ and $\text{bei}_\phi(\chi)$ and their first derivatives. These functions were computed by means of a Bendix G-15 D electronic computer.

The tabulated value consists of a sign, followed by two digits representing a floating point exponent p as used in Bendix G-15 D Intercom 1000 D (Bendix Computer Division, 1958), followed by a twelve digit number. The correct value of the function is

$$(\text{sign}) (12 \text{ digit number}) (10)^{p-50}$$

Example: $\text{ker}'(0.050) = -52.199803991221$ in floating point
 or -19.9803991221 in decimal notation.

The computed functions are accurate to the last digit; except that $\text{ker}(\chi)$, $\text{ker}'(\chi)$, $\text{kei}(\chi)$, and $\text{kei}'(\chi)$ are occasionally in error only in the last digit.

The values of the functions are plotted in Figures 1-3.

The appendix gives the method used in computing the functions.

The solution of the symmetrical plate problem is

$$w = A \text{ber}(\chi) + B \text{bei}(\chi) + C \text{ker}(\chi) + D \text{kei}(\chi) + \frac{q}{k}$$

$$\text{radial slope} = \frac{1}{l} \frac{dw}{d\chi}$$

$$\text{radial moment} = -k l^2 \left[\frac{d^2 w}{d\chi^2} + \frac{\mu}{\chi} \frac{dw}{d\chi} \right]$$

$$\text{radial shear} = -k l \left[-A \text{bei}'(\chi) + B \text{ber}'(\chi) - C \text{kei}'(\chi) + D \text{ker}'(\chi) \right]$$

$$\text{tangential slope} = 0$$

$$\text{tangential moment} = -k l^2 \left[\frac{1}{\chi} \frac{dw}{d\chi} + \mu \frac{d^2 w}{d\chi^2} \right]$$

$$\text{tangential shear} = 0$$

$$\text{displaced vol of water} = 2\pi l^2 \int \chi w d\chi.$$

REFERENCES

Bendix Computer Division of Bendix Aviation Corp* (1958) Manual CB-078, Intercom 1000 programming system for the Bendix G-15 computer.

McLachlan, N. W. (1934) Bessel functions for engineers, Oxford University Press.

Wyman, M. (1950) Deflections of an infinite plate, Canadian Journal of Research, A28.293-302.

* 5630 Arbor Vitae Street, Los Angeles 45, California.

TABLES OF KELVIN FUNCTIONS AND THEIR DERIVATIVES

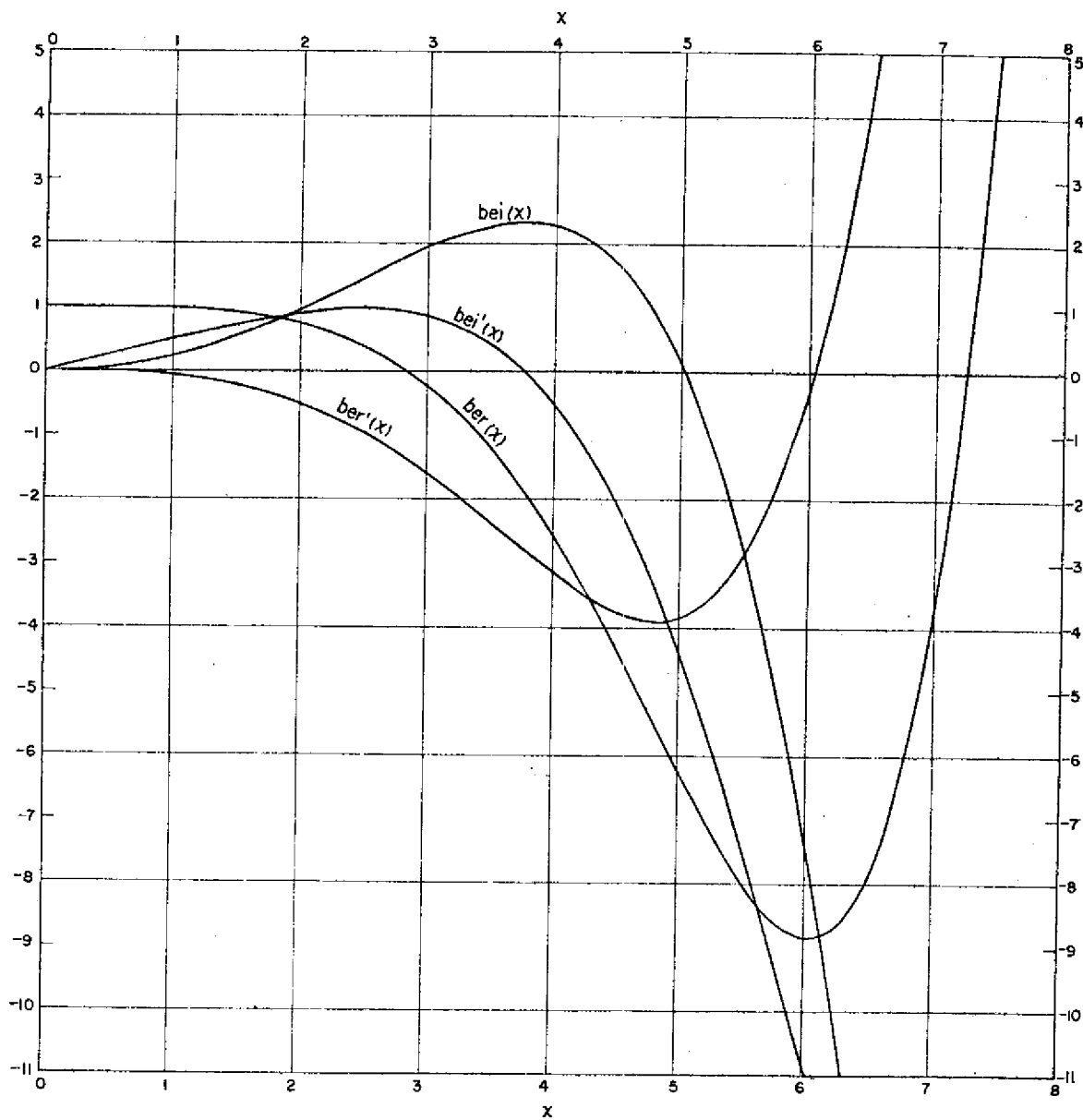


Figure 1.

TABLES OF KELVIN FUNCTIONS AND THEIR DERIVATIVES

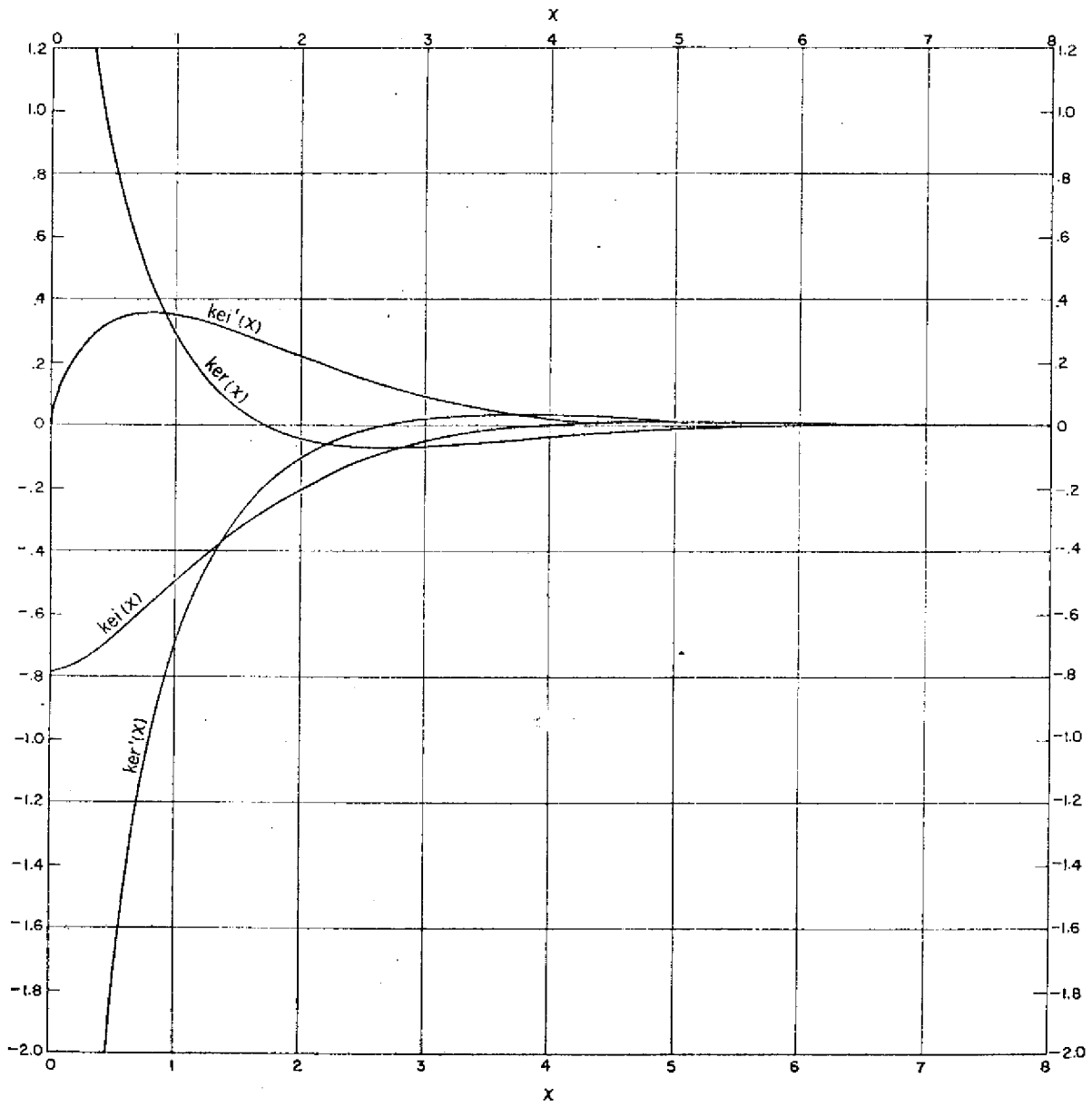


Figure 2.

